X-632-63-111

90p

N63 21251
Code 1

96p

IMP PROGRAMMER

NASA TMX 50427

OTS PRICE

XEROX $ 8.10 ph

MICROFILM $ 2.90 mf

H.D. Moore JUNE 1963 90 p

(NASA TM X-50427; X-632-63-111) OTS: $8.10 ph, 2.90 mf

6621307

NASA

NASA — GODDARD SPACE FLIGHT CENTER —

GREENBELT, MD.

IMP PROGRAMMER

Prepared by:
H. D. Moore

Approved by:
H. J. Peake

Cognizant engineers:
J. C. Schaffert
J. N. Libby
H. D. Moore

FOREWORD

This report presents to the IMP Project personnel a working document explaining the functions of the programmer in detail. Section I is an explanation in general terms of the overall basic relation of the programmer to the payload.

Section II, a documentation of the circuitry used in the IMP programmer, will be of value to those groups interested in a detailed technical description.

Section III is an interface document written specifically for those groups who have an electrical connection to the programmer. This section will also be of benefit to the Systems Integration Branch.

CONTENTS

	Page
1. BASIC RELATION TO PAYLOAD	1
1.1 RELATIVE POSITION IN PAYLOAD	1
1.2 CONTROL OF PAYLOAD	1
1.3 REDUNDANT FEATURES	2
1.4 RELIABILITY	2
1.5 PHYSICAL STRUCTURE	3
2. CIRCUIT FUNCTION AND EXPLANATION	3
2.1 CARD 1	3
2.1.1 Undervoltage Detector	3
2.1.2 Decade Oscillator	9
2.1.3 Magnetic-Core Counter	9
2.2 CARD 2	10
2.2.1 Gas-Cell Thermal Controls	10
2.2.2 Magnetometer Calibrators	17
2.2.2.1 Plus Calibrator	17
2.2.2.2 Minus Calibrator	17
2.2.3 Fluxgate Calibrators	17
2.2 LAMP STARTER	18
2.3 CARD 3	18
2.3.1 Magnetometer Amplifier	23
2.3.2 Magnetometer Search Oscillator and Lockout Amplifier	23

2.3.3 H-1 Current Attenuator and Driver Amplifier 24

2.3.4 Magnetometer Telemetry Filter Amplifier 24

2.3.5 Frequency Analog Converter 25

2.3.6 Magnetometer Clipper Amplifier 25

2.4 CARD 4 25

2.4.1 Reference Frequency Oscillator 975-cps 31

2.4.2 Fourth Sequence Identification Frequency Oscillator 1010-cps 31

2.4.3 Gated Telemetry Mixer-Amplifier 32

2.5 CARD 5 38

2.5.1 Despin Timer 38

2.5.2 Boom Erection 43

2.5.3 Magnetometer Extension 43

2.5.4 Undervoltage Relay 44

2.6 CARD 6 44

3. INTERFACES 49

3.1 CARD 1 49

3.1.1 Input 49

a. Batteries 49

b. Undervoltage Converter 49

c. Turn-on Plug 49

3.1.2 Output 49

a. Undervoltage Relay 49

b. One-Year Timers 49

c. Payload Test Plug 49

3.2 CARD 2 49

3.2.1 Input 49

a. Encoder 49

b. Programmer Converter 50

c. Rubidium Vapor (Rb) Magnetometer 50

d. Programmer Card 3 50

3.2.2 Output 50

a. Rubidium-Vapor (Rb) Magnetometer 50

b. Fluxgate Calibration Coils 51

3.3 CARD 3 51

3.3.1 Input 51

a. Rubidium-Vapor (Rb) Magnetometer 51

b. Programmer-Converter 51

3.3.2 Output 51

a. Rubidium-Vapor (Rb) Magnetometer 51

b. Programmer Card 2 52

c. Programmer Card 4 52

3.4 CARD 4 52

3.4.1 Input 52

a. Encoder 52
b. Programmer Card 3 52
c. Programmer-Converter 52
3.4 OUTPUT TO TRANSMITTER 52
3.5 CARD 5 53
3.5.1 Input (Programmer Functions Only) 53
a. Undervoltage Converter 53
b. Programmer Card 1 53
c. Umbilical Plug 53
d. Fluxgate Boom Microswitch 53
e. Magnetometer (MTM) Extension Microswitch 53
3.5.2 Output 53
a. Despin Squibs 53
b. Boom Squibs 53
c. Magnetometer (MTM) Extension Squibs 53
d. Prime Converter and Batteries 54
3.6 CARD 6 54
3.6.1 Input 54
a. Card 1 54
b. Solar Paddles 54
3.6.2 Output Batteries 54

ILLUSTRATIONS

Figure		Page
1	IG1, Card 1, Undervoltage Systems	5
2	Card 1	7
3	Card 1, Signal Diagram	8
4	Encoder - Programmer Functions	11
5	IG2, Card 2, Magnetometer Gating Circuits	13
6	Card 2	15
7	Card 2, Signal Diagram	16
8	IG3, Card 3, Magnetometer Electronics	19
9	Card 3	21
10	Card 3, Signal Diagram	22
11	H-1 Current Output	24
12	IG4, Card 4, Telemetry Gated-Mixer Amplifier	27
13	Card 4	29
14	Card 4, Signal Diagram	30
15	IG4, Card 4, Oscillator Waveforms	31
16	Gated-Amplifier Signal Diagram	33
17	Encoder Video Waveforms	34
18	Formation of Zero Reference Blank Time	35
19	Video With Blanks Filled In	35
20	Mixing Of Magnetometer Video Encoder Sync Burst	36
21	Formation Of 0-All Channel of Fourth Sequence	37
22	IG5, Card 5, Relay Card	39
23	Card 5	41
24	Card 5, Signal Diagram	42
25	IG6, Card 6, One-Year Timer	45
26	Card 6	47
27	One-Year Timer	48
28-56	Schematics (no captions)	

Figures 30, 35, 44, and 51 appear at end of document.

1. BASIC RELATION TO PAYLOAD

1.1 RELATIVE POSITION IN PAYLOAD

The programmer in a spacecraft is positioned, electrically, between a portion of the time base generator (encoder) functions and certain gated or timed functions within the remainder of the payload. In addition to this position, the IMP programmer is placed between the batteries and the various power converters. It will also provide the only video input to the telemetry transmitter.

1.2 CONTROL OF PAYLOAD

The discussion of the programmer's control of the payload will proceed logically from the batteries to the video input of the telemetry transmitter.

Between the batteries and the payload converters lies the undervoltage detector. It is the function of this unit to determine when the batteries have decayed to an output of 12v. At this point, a major portion of the payload is turned off for a period of 8 hours. At the end of 8 hours, the payload will automatically turn back on. If the batteries are still below 12v, the payload will again be turned off for another period of 8 hours. This cycle continues until the batteries have been charged sufficiently to give an output greater than 12v. At this point, the payload will remain on. This entire circuit is contained within programmer card 1, a detailed description of which may be found in Section 2, paragraph 2.1. This card also supplies a current to an electrolytic timer which will "kill" the payload after operation of 1 year.

The next consideration will be the direct link between the programmer and the various experiments. In IMP there is a connection to two experiments only, the rubidium magnetometer and fluxgate magnetometer experiments.

From the programmer's standpoint, the Rb (rubidium) magnetometer experiment consists of a McKeen coil system (two magnetic field reference coils), a gas cell, and a magnetometer. It is the function of the programmer to supply a plus and a minus calibrating current to each of the two reference coils to produce a reference magnetic field. The gas cell is controlled to a temperature of 42°C by means of a heating coil to which current is supplied by the programmer. The rubidium lamp also receives a 5-second starting pulse if it is not operating at the beginning of the fourth sequence. *

The telemetry gating and mixing amplifier receives video from the encoder and magnetometer-amplifier, conditions it, and passes it to the telemetry transmitter.

The relay section of the programmer acts in response to signals from the undervoltage detector or the blockhouse, turning the payload either on or off. This section also controls the despin, magnetometer extension, boom erection mechanisms.

1.3 REDUNDANT FEATURES

Only those functions vital to the entire payload are made redundant. These functions are the undervoltage, despin, boom erection, MTM extension circuits, and the telemetry-gated mixer-amplifier. Loss of any other circuitry would be detrimental only to certain experiments namely, the R_b experiment and the fluxgate calibration.

If failure of a payload subsystem should cause excessive current drain, the batteries would deteriorate rapidly, causing the loss of the entire payload. The undervoltage circuit protects against this, justifying redundancy.

The telemetry-gated mixer-amplifier is the only video input to the transmitter, thus some protection against failure is needed. Two identical circuits are operated on a time-sharing basis. Each circuit will drive the transmitter 50 percent of the time. The operation of the despin, boom erection and magnetometer extension circuits are also critical to the entire payload and are, therefore, made redundant.

1.4 RELIABILITY

Most of the circuits used in this programmer have been used in spacecraft before and have proven highly reliable. An undervoltage circuit very similar to the one in IMP has been functioning properly in S-51 (Ariel) since July 12, 1962. This same circuit has been used in Explorers XII, XIV, and XV.

---

*See "IMP PFM Encoder" Revision A, Aug. 6, 1963, by H. D. White

All the components used are operated well below their maximum tolerances. Most of the transistors used are purchased on a high reliability program. This, coupled with conservative circuit design, ensures a high degree of circuit reliability.

1.5 PHYSICAL STRUCTURE

The IMP programmer consists of six main cards (mother boards) each containing a number of modules (Figures 2, 6, 9, 13, 23 and 26). Each module is connected to the main card by means of a Micro-D (MD) series Cannon connector. The main card connection to the payload is by means of a "D" series Cannon connector. Each main card is 1 inch in height (with exception of card 6) and of standard IMP peripheral dimensions (Figures 2, 6, 9, 13, 23 and 26). Three of the main cards contain a Micro-D (MD) series Cannon connector next to the payload connector to facilitate monitoring of the programmer functions during integration, test, and evaluation.

2. CIRCUIT FUNCTION AND EXPLANATION

2.1 CARD 1 (Figures 3, 29 and 30)

2.1.1 Undervoltage detector (G11 and G21) (Figure 31)

The battery voltage, applied to pin 3 of this module, is means of R1, C1, R16 and C3. Without the filtering an going transients would appear to the detector as an und dition. R1, R16, R2, R3 and Q4 form a voltage-divide applies a voltage to the base of Q1 proportional to that of the batteries. Transistors Q1 and Q2 form a standard Schmitt circuit. When the input (pin 3) reaches a desired level (+12v) for an undervoltage condition, the Schmitt circuit flips to its other state. Normally Q1 is biased on by the input to its base. In this state Q2 is biased off by R8 and R11 causing its collector to be at 12v. In an undervoltage condition, however, Q2 becomes biased on due to Schmitt action. This causes the voltage at the collector of Q2 to drop. This decrease in voltage biases Q3 on. When Q3 becomes saturated, its collector rises from 0 to +11v. (The loss of about 1v is due to the diode (CR2) drop and the emitter-to-collector drop of Q3.) This rise in voltage of the collector of Q3 develops a positive pulse at pin 9 due to differentiation by C2 and the resistive load to which pin 9 is connected. This pulse starts the decade oscillator.

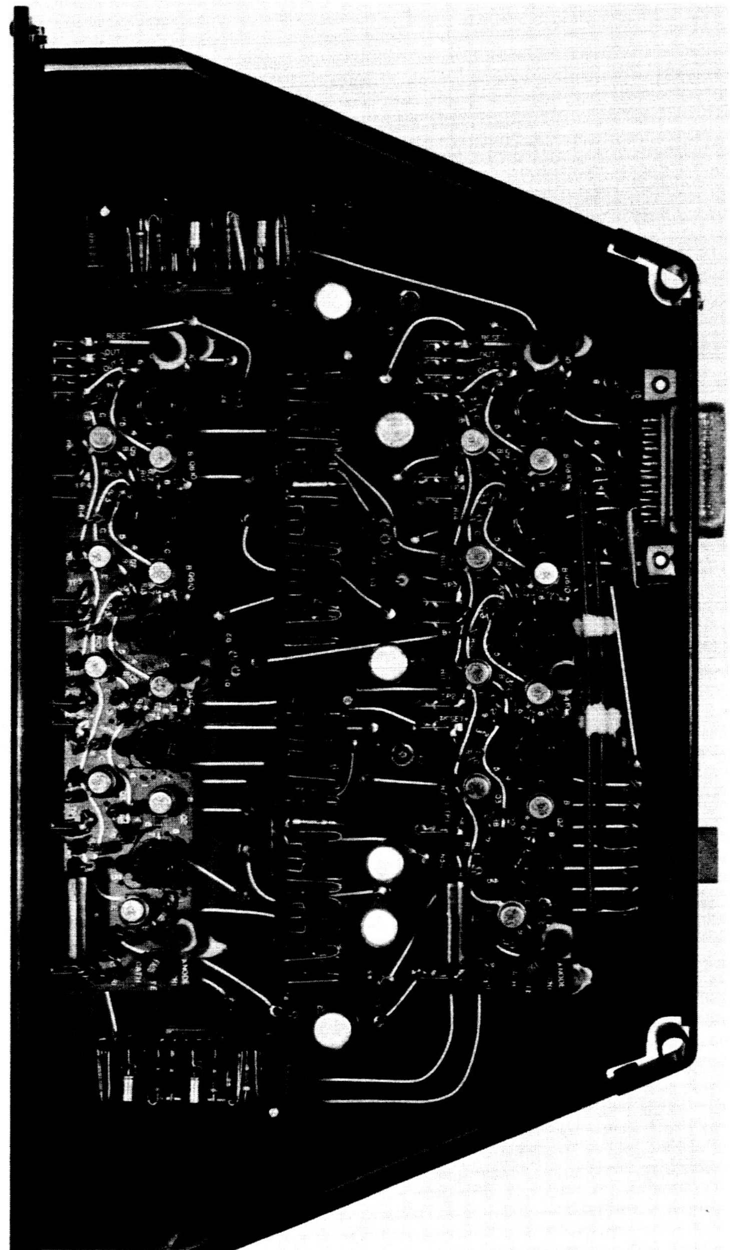

Figure 1 – 1G1, Card 1, Undervoltage System (Top)

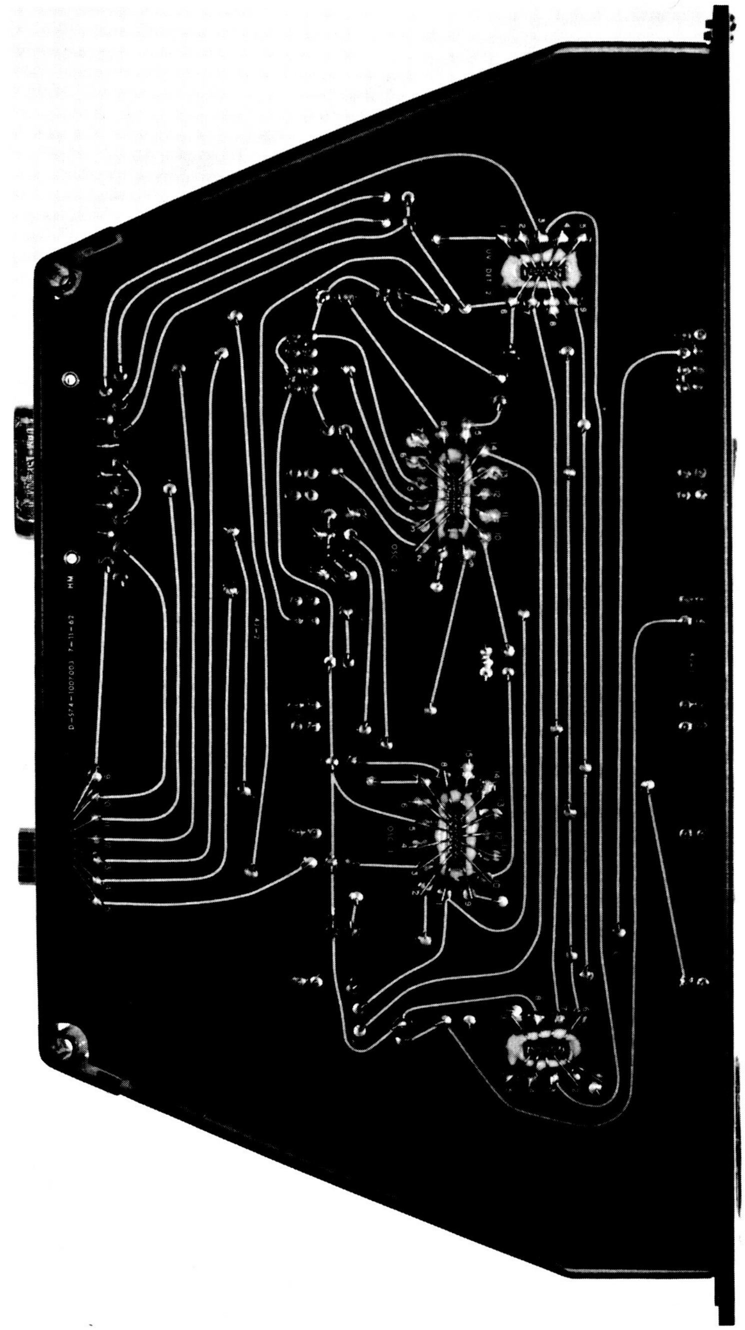

Figure 1 – 1G1, Card 1, Undervoltage System (Bottom)

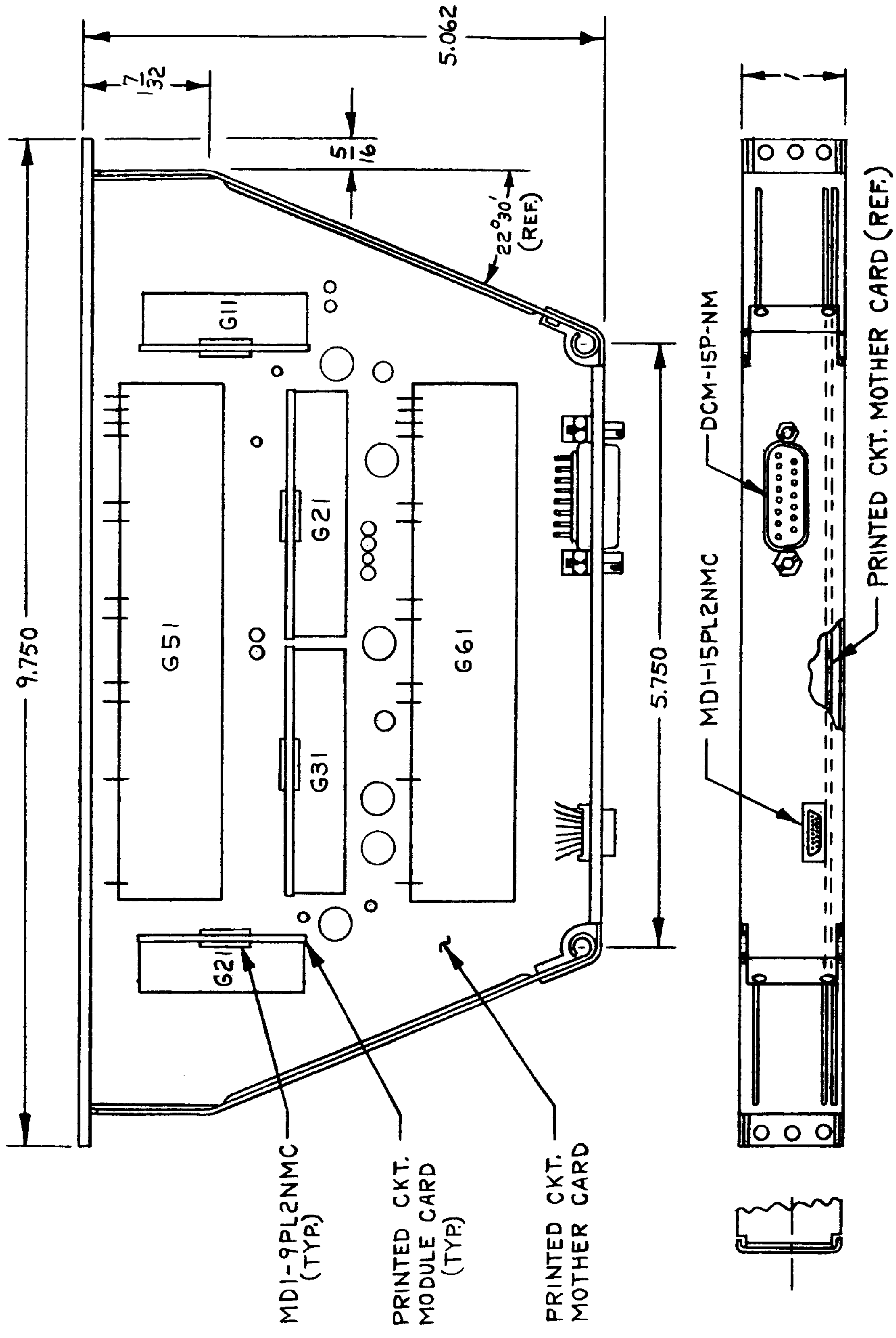

Figure 2 – Card 1

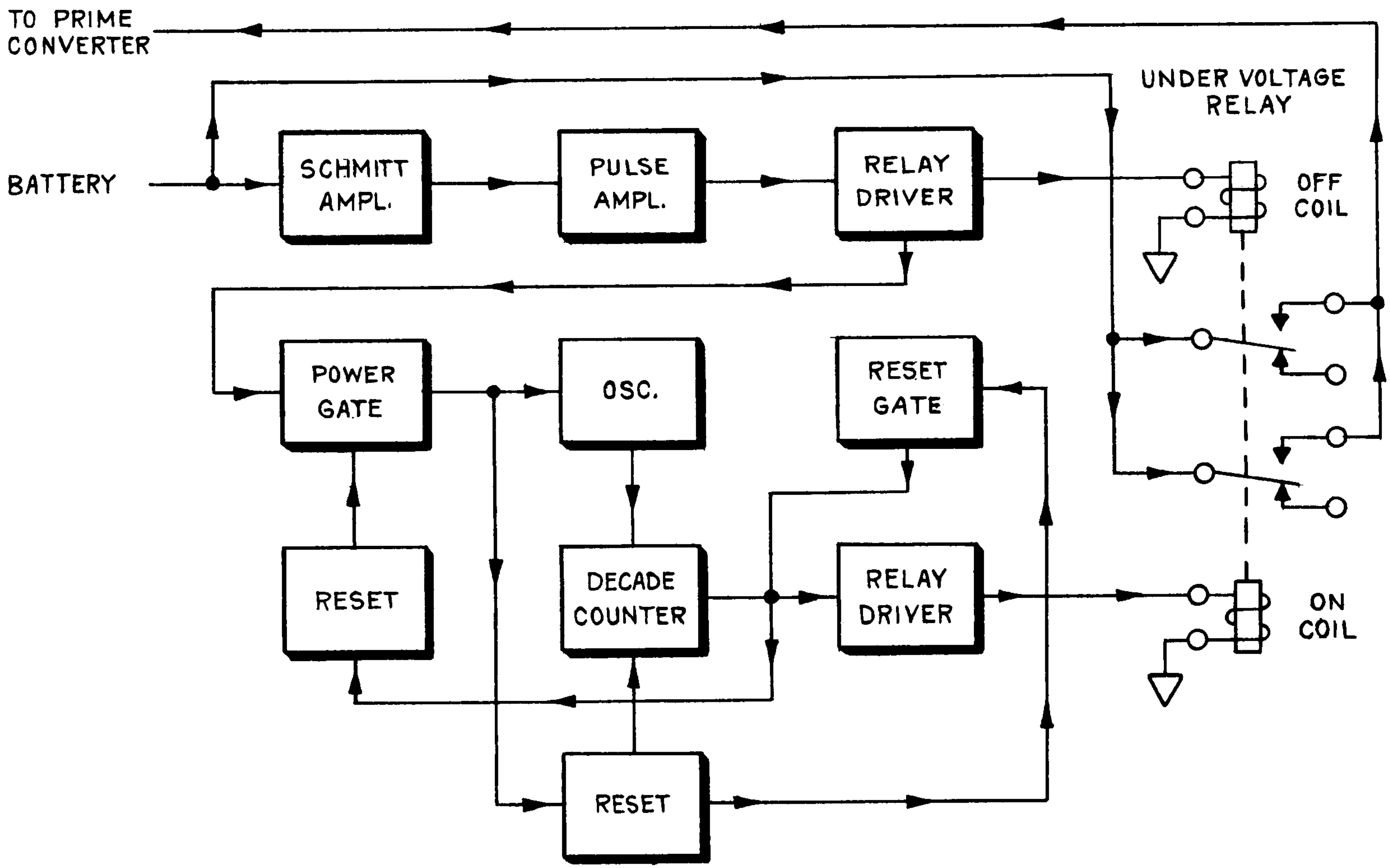

Figure 3 – Card 1, Signal Diagram

2.1.2 Decade oscillator (G31 and G41) (Figure 32)

In addition to a unijunction oscillator, this module contains the various pulse amplifiers required to drive the undervoltage relay and the counter reset function.

The positive pulse from pin 9 of the undervoltage detector enters pin 15 of the decade oscillator turning Q1 on and allowing the "loadoff" capacitor to discharge through its anode-to-cathode path. This discharge develops a pulse at the cathode of Q1 which is coupled to the gate by R2. The diode CR1 isolates the positive pulse developed at the gate of Q1 from the rest of the mother card. The pulse at the cathode of Q1 drives the "off" coil of a latching relay. CR2 eliminates the inductive feedback of the relay coil. This same pulse turns Q2 on. The turn-on of Q2 supplies B+ to the oscillator and turns Q5 on. Q5 allows the discharge of C1 which then performs two functions with the generated positive pulse: resets the magnetic-core counter via pin 9 and drives Q6 to saturation. At this point, an explanation of the function of Q6 is in order. When the core counters are reset, they generate a pulse at pin 2 of the decade oscillator which would turn the payload on again. Q6 clamps this pulse to ground. At the end of the undervoltage time (usually 8 hours), a positive pulse from the magnetic-core counter enters pin 2 of the oscillator module and turns on Q7 which allows the discharge of the "load on" capacitor. The positive pulse generated as a result of this discharge turns the payload on via the on coil of the undervoltage latching relay. This same pulse causes Q3 to become saturated. When saturated, it shorts the gate to the cathode of Q2, turning Q2 off and stopping the oscillator.

2.1.3 Magnetic-core counter* (Figure 33)

The counter used here is a divide by 10,000 unit. The basic principle of operation is as follows. The magnetic core begins in a negatively saturated state and is incrementally stepped toward positive saturation by means of constant volt-second pulses. When positive saturation occurs, one output pulse is generated and the core is reset to its negatively saturated condition. If each core becomes saturated with

*Developed by General Time Corporation, Stamford, Connecticut. Additional theory and explanation of operation may be obtained from J.D. Freeman of General Time Corporation.

10 input pulses, 4 such units may be cascaded to achieve division by 10,000. With the above in mind, consider next the operation of the electronic circuit that accomplishes this function (Figure 33). A positive pulse from the decade oscillator enters pin 7 upon initiation of the counting sequence, causing the cores to be saturated negatively. Winding N1 of T1, R1, C1, and SCR-1 constitute the pulse former of the counter. Its output is a constant volt-second pulse independent of the input or triggering pulse. A positive pulse at pin 5 turns SCR-1 on, thus discharging C1 through N1. The pulse thus developed is transformer-coupled to N2. Because T1 is so wound that each input pulse causes saturation of the core, the blocking oscillator, Q1, is triggered which in turn generates a positive pulse at tap 10 of T1. This is inverted in windings N3 and N4 of T1, presenting a negative pulse at tap 11 which turns Q2 on, coupling the pulse to the next stage. Unlike the windings of T1, the remaining cores are wound so that saturation does not occur until it receives 10 pulses. On the tenth pulse into T2, the blocking oscillator is activated, generating a positive pulse at tap 19. It is again inverted through N3 and N4 of T2. The process continues in a manner similar to that in T1. The positive pulse developed by the blocking oscillator also returns the core to negative saturation. After a count of 10,000, the output from this unit is coupled to pin 9 of the decade oscillator, which turns the decade oscillator off, turns the payload on, and resets the undervoltage detector.

2.2 Card 2 (Figures 34 and 35)

2.2.1 Gas-cell thermal control (Figures 36 and 42)

Q1, Q2 and Q8 operate in response to the Rb on gate.* When this gate is at +6.7v, Q1 is saturated and Q2 is therefore biased beyond cutoff by Vce-saturation of Q1. In this condition, the remainder of the circuit will operate in response to the resistance of the heat sensor (thermistors) connected to pin 7. R4, R5 and the heat sensor form a voltage divider whose output drives a Schmitt circuit (Q3 and Q4). As the resistance of the heat sensor increases, due to a decrease in temperature at the gas cell, the voltage at the base of Q3 increases. When this voltage reaches a certain level, the Schmitt circuit flips. In this condition, Q4 is cut off and the zener breakdown voltage of D1 is exceeded. R11, R12, and C1 act as a transient filter. With the breakdown of the zener, a voltage

*See IMP PFM Encoder, revision A, August 6, 1962, by H.D. White.

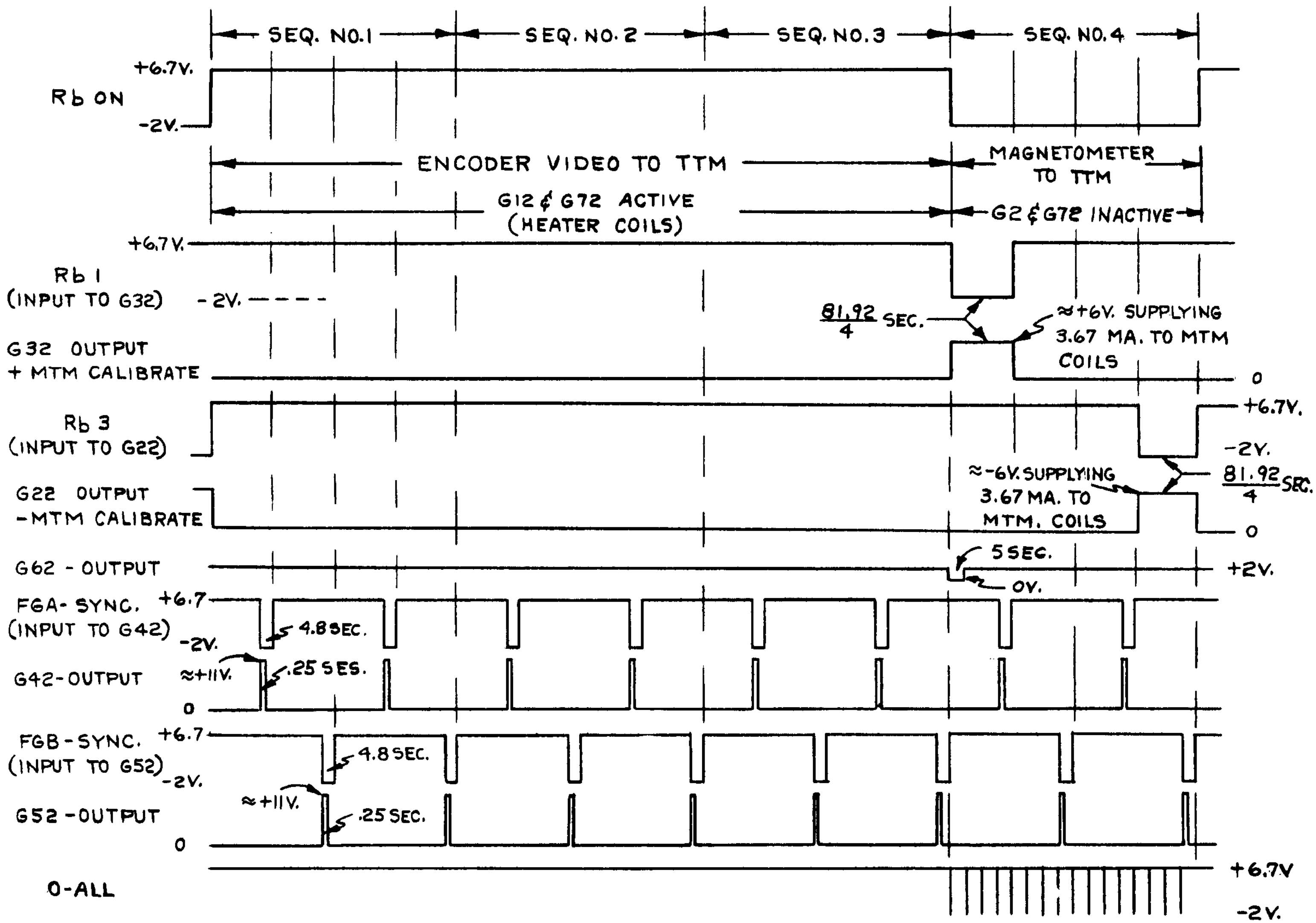

Figure 4 – Encoder Programmer Functions

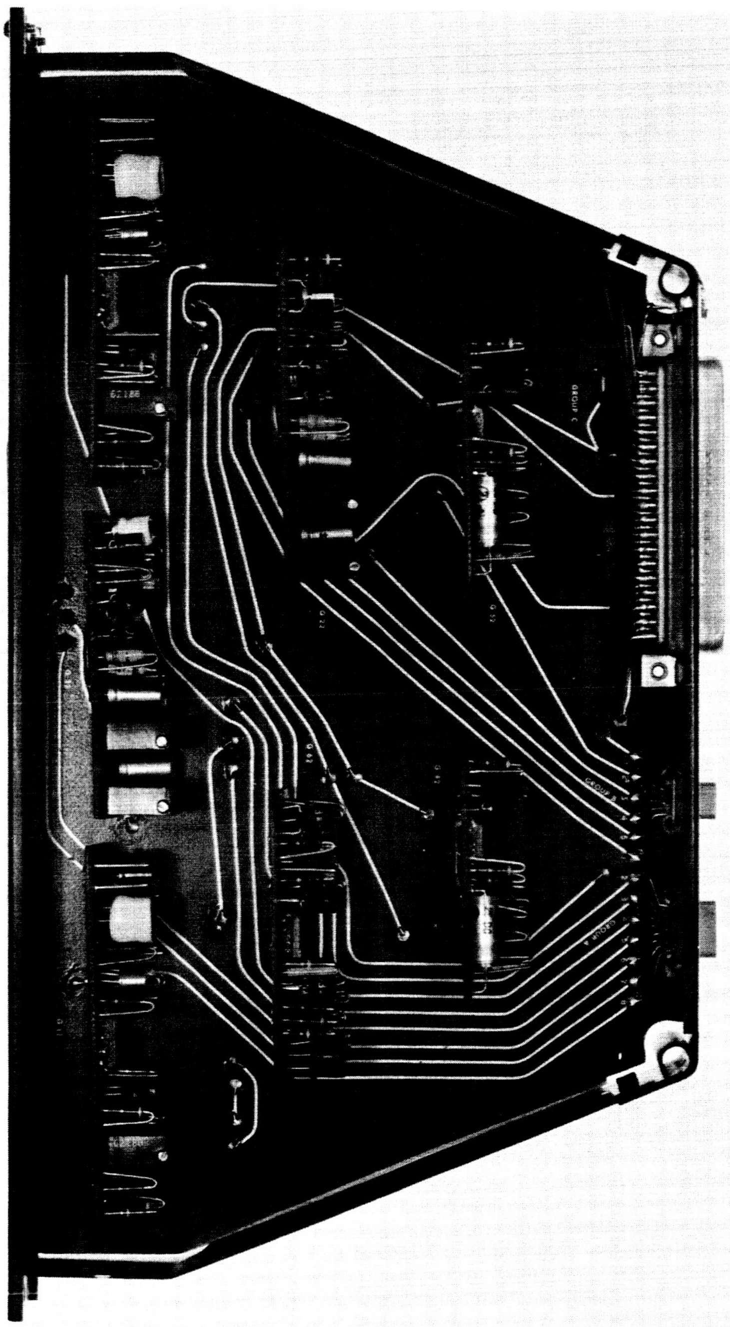

Figure 5 – IG2, Card 2, Magnetometer Gating Circuits (Top)

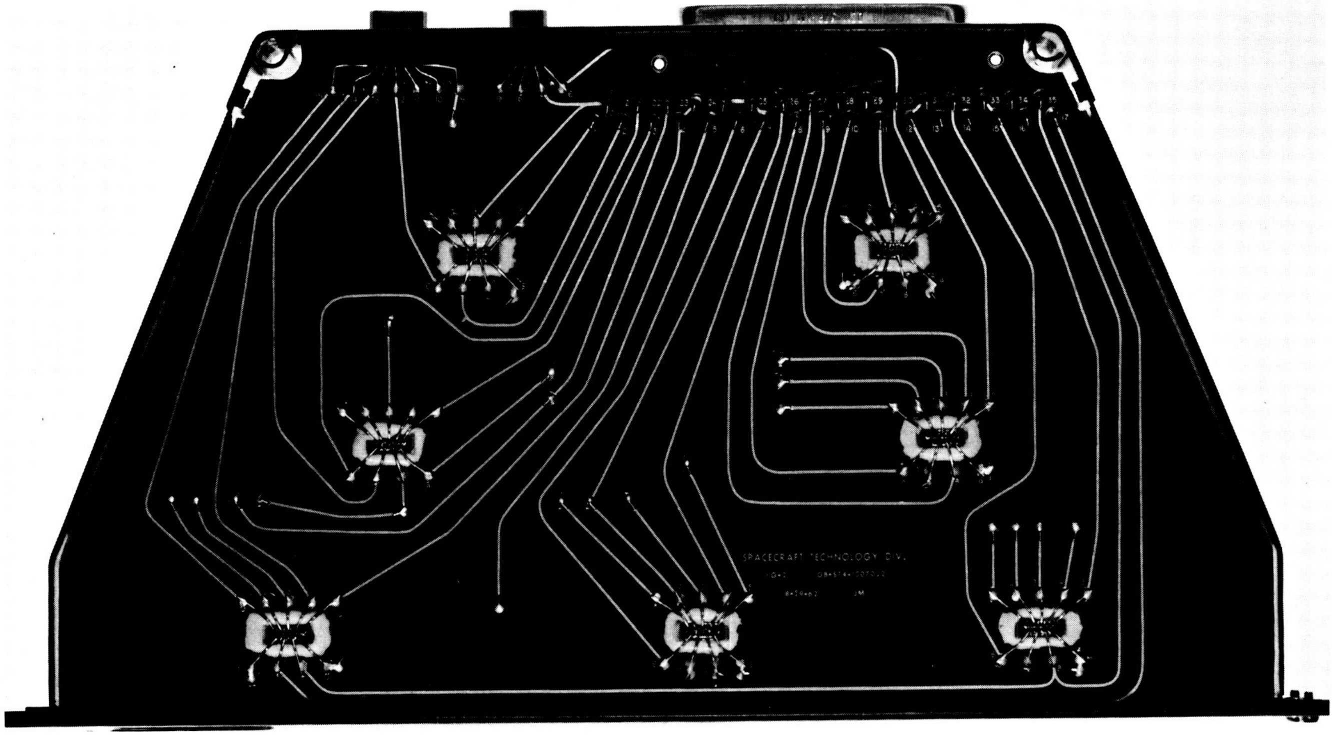

Figure 5 – IG2, Card 2, Magnetometer Gating Circuits (Bottom)

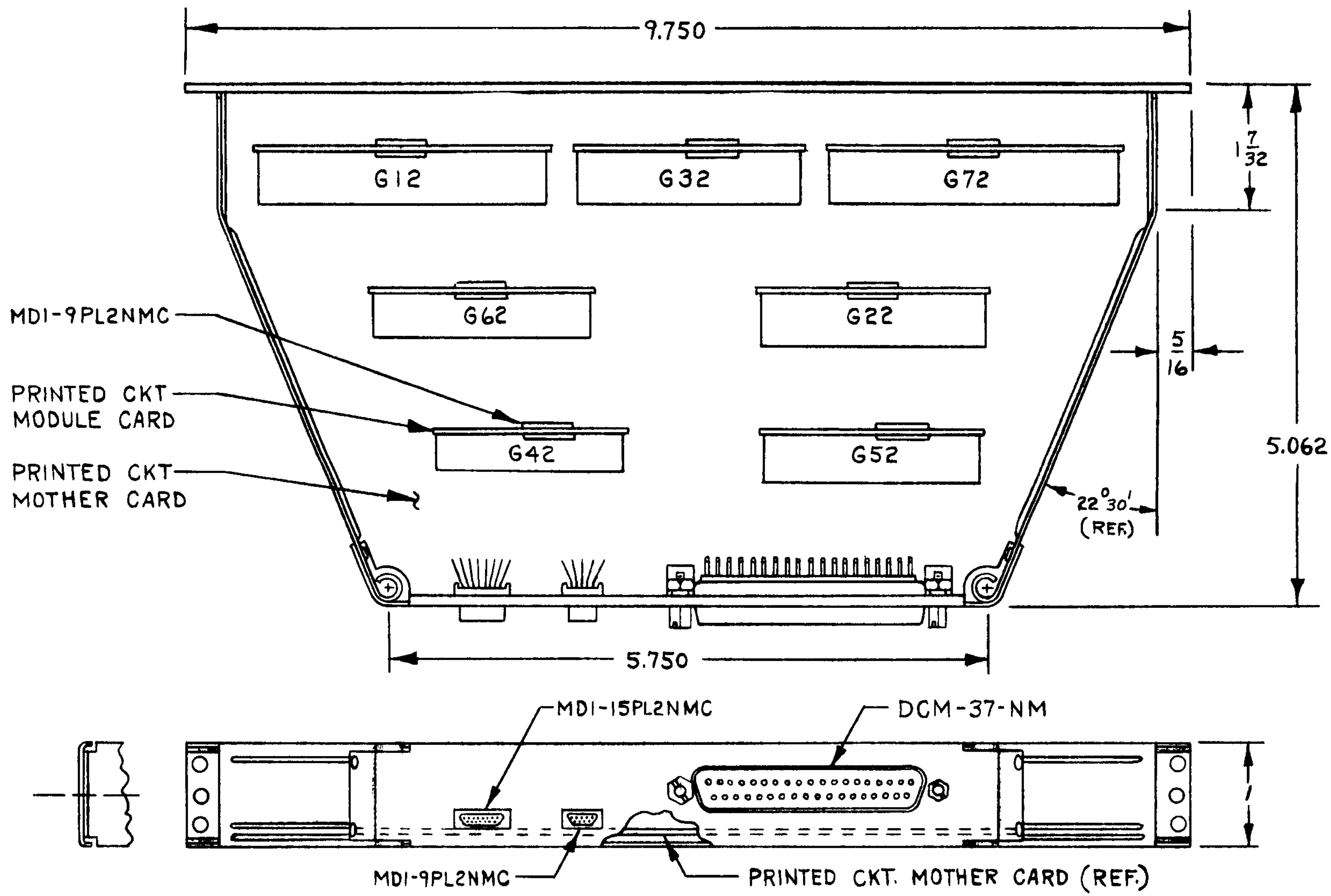

Figure 6 – Card 2

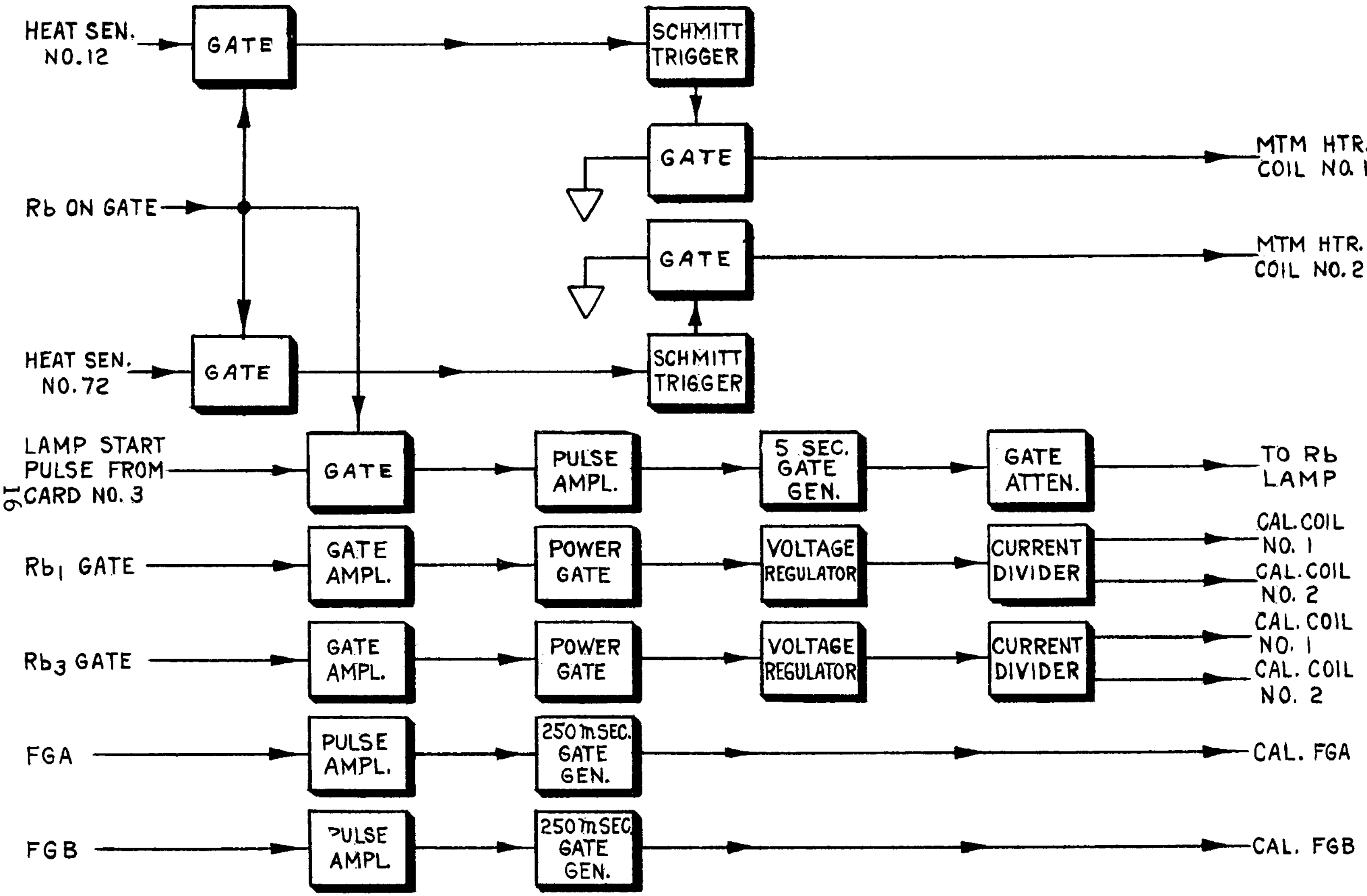

Figure 7 – Card 2, Signal Diagram

is applied to the emitter-follower, Q5, which in turn drives Q6 and Q7 to saturation, completing the circuit to the gas-cell heating coils. When the Rb on gate is a -2v, Q1 is biased beyond cutoff and Q2 is biased on by R2. This simulates a hot condition at the gas cell, opening the circuit to the heating coils.

2.2.2 Magnetometer calibrators

2.2.2.1 Plus calibrator (Figure 38)

The gate (Rb1) which activates this circuit via pin 4 is +6.7v at standby and -2v in the active condition. In the standby condition, the CR1 zener voltage is not exceeded, therefore both Q1 and Q2 are biased off and, hence, there is zero voltage at the collector of Q2. In the active condition, the zener voltage of CR1 is exceeded, driving Q1 and Q2 to saturation. The voltage at the collector of Q2 is now equal to the supply voltage minus Vce-saturation of Q2 or about 11.5v. Q3, Q4, Q5, CR2, CR3, and CR4 form a voltage regulator for the current to be supplied to the McKeen coil system of the magnetometer. The resistors, R13, R14, and R15 determine the proper ratio between the two currents supplied to a ±.1 percent accuracy. R12 adjusts the total current supplied.

2.2.2.2 Minus calibrator (Figure 37)

This unit is activated by the Rb3 gate which is identical to the Rb1 gate, except that it occurs at a different time. In the standby condition, Q1, Q2, and Q3 are biased off, giving 0v output to the regulator circuit (Q3, Q4, Q5, CR2, CR3, and CR4). In the active condition with -2v at pin 4 Q1 acts as an emitter-follower and Q2 becomes saturated. Q3 also becomes saturated at this point due to the biasing of R5, R4, and Q2 (saturation). A minus voltage is now supplied to the regulator. The rest of the circuit is identical to the plus calibrator except that it delivers a minus voltage to the appropriate resistors.

2.2.3 Fluxgate calibrators (A&B) (Figures 39 and 40)

These units are identical except that they are driven by different gates. Each calibrator is activated via pin 5 when its respective fluxgate sync goes from +6.7v to -2v. This step in voltage is differentiated by C1 and R2, resulting in a negative going pulse at the base of Q1. Q1 becomes saturated by this pulse, causing a positive pulse to occur at its collector. C2 couples this pulse to the gate of Q2, turning it on. With the cathode of Q2 now at about 11.5v, the emitter of Q3 begins to rise exponentially to this voltage with a time constant approximately equal to (R7 + R8) (C4). The emitter will rise until breakdown of the unijunction (Q3) occurs. At this time a positive pulse is generated at B1 of Q3. This pulse is applied to the base of Q4 via C3 and D1, saturating it, and thus turning Q2 off. The calibrating current is taken from the 500-millisecond +12v pulse generated at the cathode of Q2.

2.2.4 Lamp starter (Figure 41)

This unit is controlled by two signals, one coming from the magnetometer electronics and the other from the encoder (Rb on). If the Rb lamp requires a starting pulse, a zero volt signal from card 3 will be applied to the base of Q1, turning Q1 off. When the Rb on gate is at -2v, Q8 becomes back-biased and Q2 is off. In effect, Q1 and Q2 form an and gate. With both of them off, their collectors rise to +12v. This rise in voltage is differentiated by C1 and R4, then coupled the gate of Q4 by Q3, C2, and R6. Q4, Q5, and Q7 form a one-shot multivibrator as explained in the description of the fluxgate calibrators. In the case of the lamp starter gate the one-shot generates a 5-second 11.5v pulse at the cathode of Q4, which turns Q6 off. With Q6 off, there is zero voltage at pin 6, the gate required to start oscillations within the lamp.

2.3 Card 3 (Figures 10, 43, and 44)

Before beginning the circuit explanation, it would be advantageous to first understand its function. Consider the signal diagram (Figure 10). The 7 to 15 microvolt signal from the photocell is amplified and conditioned by the magnetometer filter, and saturated amplifiers. The remaining modules form a feedback network which generates a current (H-1) that will cause an oscillatory condition to exist in the magnetometer and its electronics. The frequency of this oscillation is proportional to the ambient magnetic field and is present in the output of the photocell. This output is the basis for the analog data to be telemetered to earth.

Certain circuits within this card were originally designed to have a phase bandwidth from 20 cycles to 70 kc. Since its completion, the bandwidth criterion has been decreased to 20 cycles to 10 kc. Because of this, it would appear that there is considerable overdesign in these circuits.

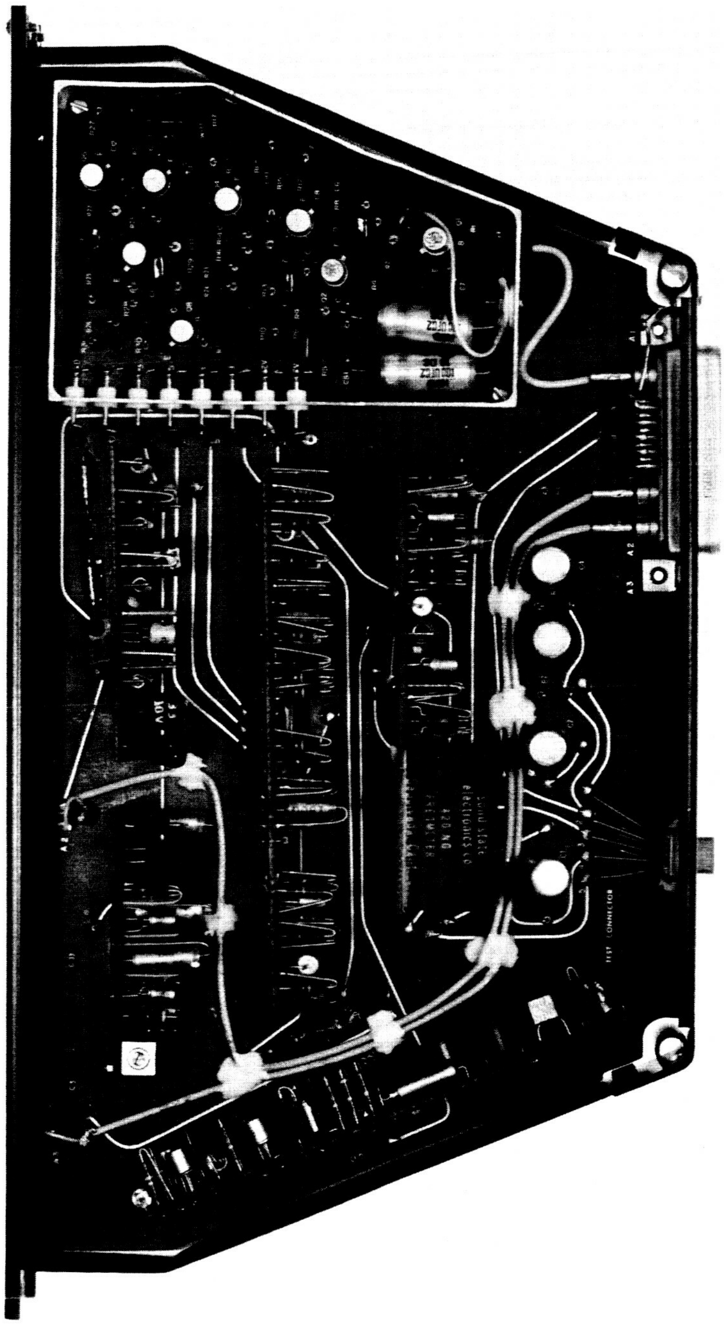

Figure 8 – IG3, Card 3, Magnetometer Electronics (Top)

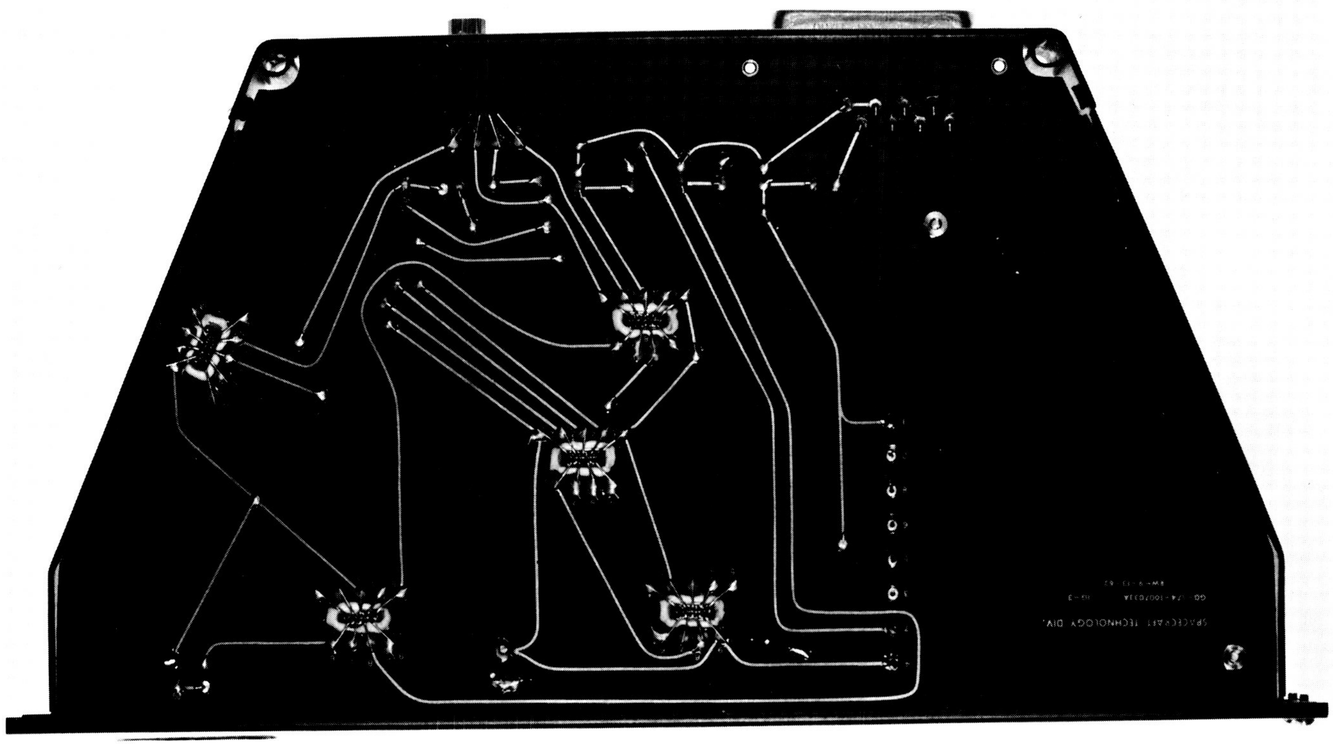

Figure 8 – IG3, Card 3, Magnetometer Electronics (Bottom)

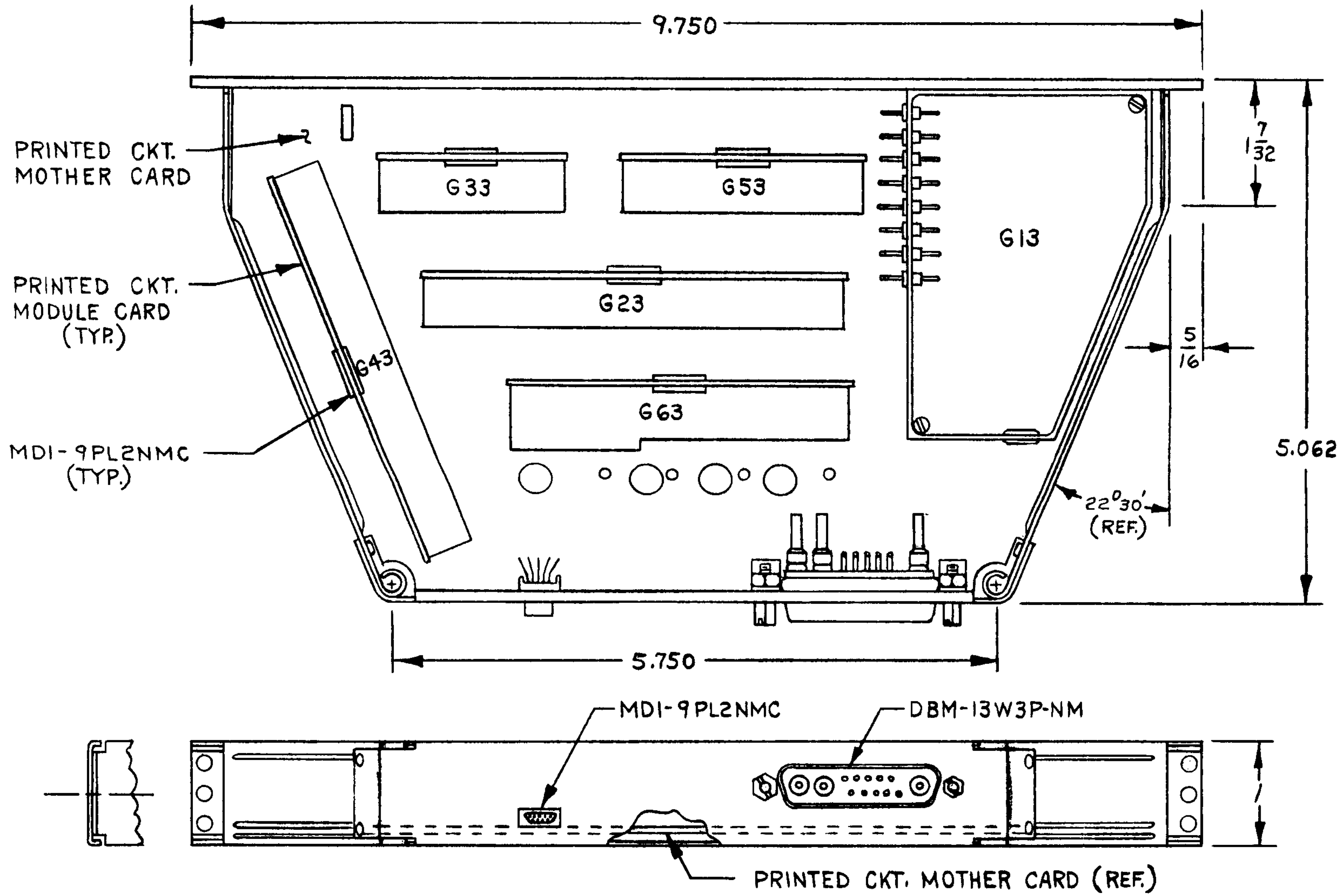

Figure 9 – Card 3

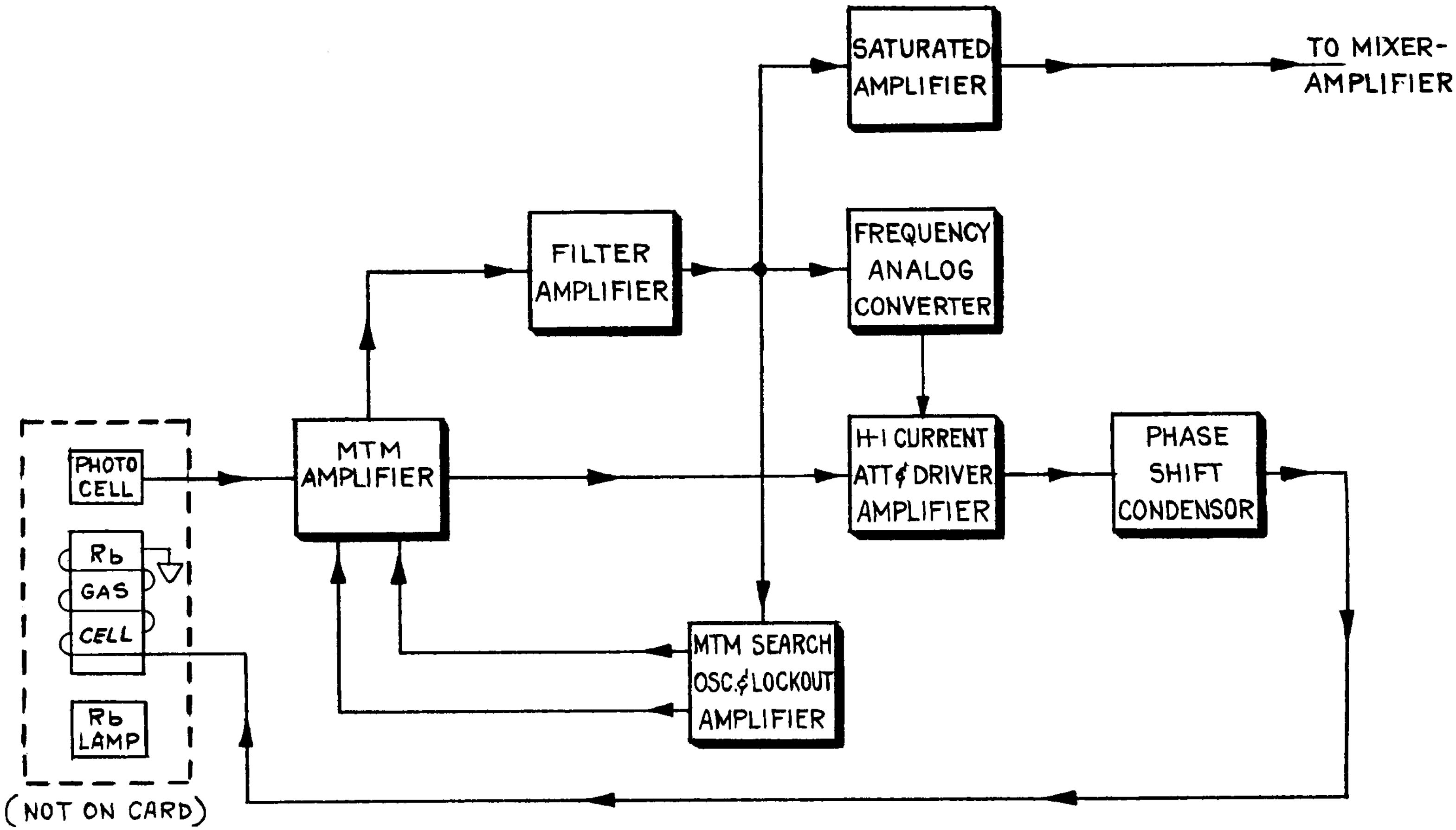

Figure 10 – Card 3, Signal Diagram

2.3.1 Magnetometer-amplifier (Figure 45)

Q1 through Q5 are a series of cascaded Class A amplifiers which have a total gain of 100 db. The input signal is in the order of 10 microvolts. This low-level signal, coupled with the high gain of the amplifier, necessitated the use of an additional B+ filter (R10, C4, and C5) in the first two stages. Q6, acting as a phase splitter, presents the in-phase and 180 degrees out-of-phase signal to the clamping transistors Q7 and Q8, respectively. These clamps are alternately opened and closed at a rate dictated by the magnetometer search oscillator and lockout amplifier (G23). The clamping action allows the output of the amplifier to be alternately either in-phase or 180 degrees out-of-phase with the input signal. This output eventually becomes the H-1 current which is coupled to the H-1 coil through a 90 degree phase shifting capacitor.

2.3.2 Magnetometer search oscillator and lockout amplifier (Figure 46)

This module controls the search rate of clamping transistors Q7 and Q8 of the magnetometer amplifier G13. It also stops the searching when the phase of the photocell signal causes oscillation of the Rb magnetometer and its electronics. Q1, R3, R4, and C1 constitute a 4-cps unijunction oscillator whose output drives Q3 to saturation. Because Q3 is normally biased off, a negative-going pulse is generated at its collector when it becomes saturated. This pulse triggers the flip-flop, Q4 and Q5, via C2, C3, and the steering diodes D1 and D2. The outputs of the flip-flop control search clamps Q7 and Q8 of the magnetometer amplifier G13 (Figure 45). The base of Q6 receives the photocell signal via the magnetometer amplifier and the telemetry filter amplifier. This route was taken to improve the signal-to-noise ratio. If the phase of the H-1 current is such that an oscillatory condition exists, a signal will appear at the base of Q6. The positive half of the signal drives Q8 and Q9 to saturation. The square wave thus developed at the collector of Q9 is filtered to give a dc voltage which turns Q10 on. With Q10 on, Q11 is biased to saturation by R41 and R42. The positive voltage now at the collector of Q11 saturates Q2, thus clamping the output of the search oscillator to ground. With the flip-flop, Q4 and Q5, now in a fixed position, the search clamps within the magnetometer amplifier are fixed to give a constant phase output.

2.3.3 H-1 current attenuator and driver amplifier, G33 (Figure 40)

It is the function of this unit to condition the photocell signal, after amplification by G13, so that it will be suitable for feedback to the H-1 coil. The approximate output is:

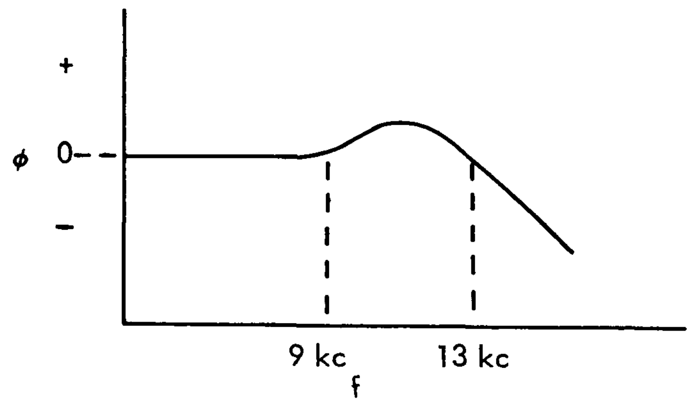

Figure 11 – H-1 Current Output

The leading phase between 9 kc and 13 kc is controlled by R16 and C5 in parallel with R4. The rolloff and subsequent lagging phase is controlled by C6, R15, Q1, and Q2. The impedance of C6 and R15 becomes smaller as the frequency increases, causing an attenuation of the signal at the base of Q5. The B1-B2 junctions of Q1 and Q2 act as variable resistors which are controlled by a dc voltage to their respective emitters. This voltage is supplied by the frequency analog converter (G53). Q3 is used to isolate the attenuator network from the amplifier Q4. Q5 is used in an emitter-follower configuration to drive the low-impedance H-1 coil. Adjustment of the amplitude of the H-1 current is accomplished by R9.

2.3.4 Magnetometer telemetry filter-amplifier, G43 (Figure 48)

This circuit was designed to improve the signal-to-noise ratio by a sharp rolloff beyond 70 kc. The upper end of the bandwidth has since been reduced to 10 kc, but it was not considered practical to change the circuit. The emitter followers Q1 and Q2, isolate the filter (L1, L2, L3, L4, L5, L6, C1, C2, C3, and C5) impedance-wise from the rest of the circuit. Q3 amplifies the signal to its original amplitude before entering the filter.

2.3.5 Frequency analog converter (Figure 49)

This unit provides a dc voltage which is proportional to the photocell signal frequency. The voltage thus developed drives the H-1 current attenuator (G33) so as to compensate for H-1 current amplitude variation due to a change in the impedance of the phase shift capacitor over the frequency range. Q1 provides the needed impedance transformation to drive Q2 as a saturated amplifier. This type of amplifier is needed because the Freqmeter is dependent upon both the amplitude and frequency of the input signal. Q3 and Q4, operating as complementary emitter followers, provide the low-impedance drive source needed. Q5 inverts and amplifies the dc output (yellow lead) of the Freqmeter. Q6 provides the low-impedance drive for the attenuators, Q1 and Q2, of G33 (Figure 47).

2.3.6 Magnetometer clipper amplifier, G63 (Figure 50)

This circuit transforms the output of G43 (Figure 48) to a square wave. CR1 and CR2 clip the signal symmetrically about zero. This clipped signal is amplified by Q2 and Q3 operating as a saturated amplifier. The output is attenuated by R13 and R14 to comply with the peak-to-peak amplitude required by card 4, the gated telemetry amplifier.

2.4 Card 4 (Figures 14, 16, and 51)

It is the function of this card to condition the payload telemetry in accord with a predetermined format* as dictated by the encoder and with the needs of the Tracking and Data Reduction groups.

The encoder format consists of three normal sequences and one rubidium sequence. During the first three (normal) sequences, the encoder video is shaped into a clean square wave and passed to the transmitter. During the fourth (Rb) sequence, the encoder video is gated off and the Rb-magnetometer video is allowed to pass to the transmitter. It was also necessary to allow the encoder sync channel to pass during this sequence. In order to have continuous magnetometer video and at the same time allow the encoder sync frequency to pass, the two are mixed during the 0-all sync channel, with the magnetometer video being attenuated 80 percent. To identify the fourth

*See H. D. White, etc.

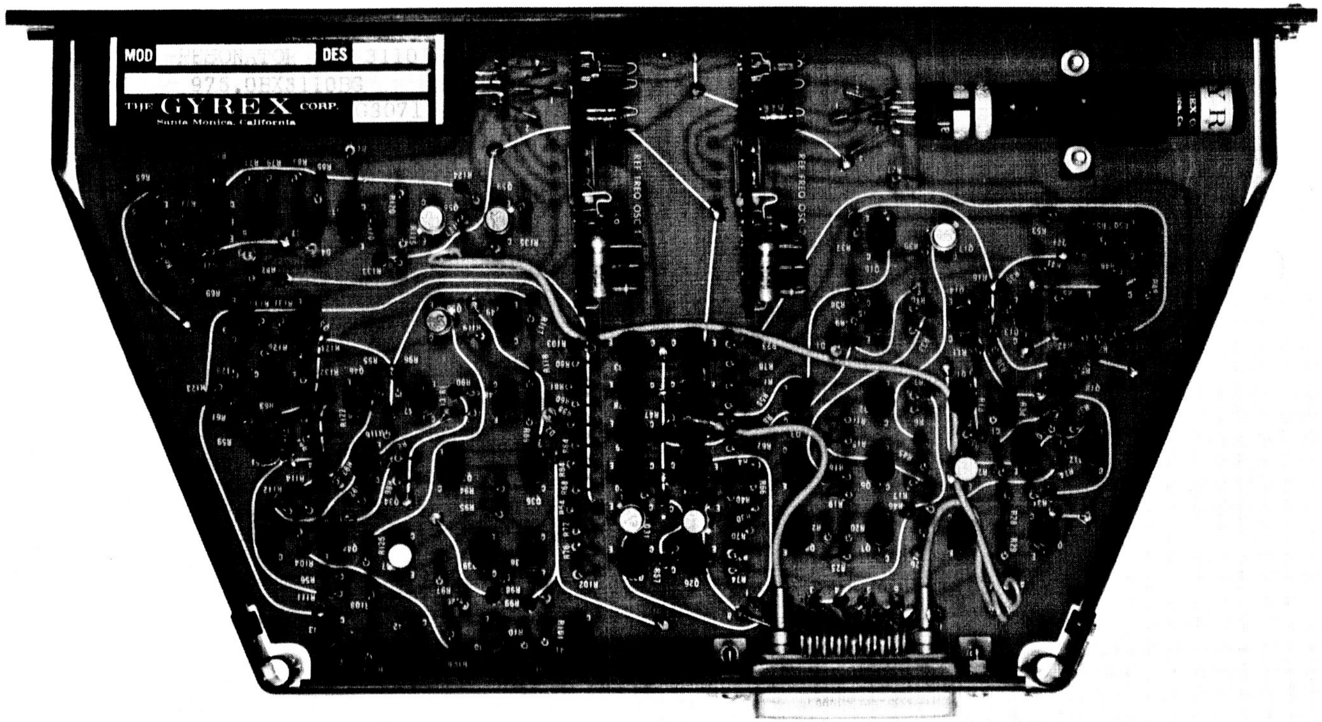

Figure 12 – IG4, Card 4, Telemetry Gated-Mixer Amplifier (Top)

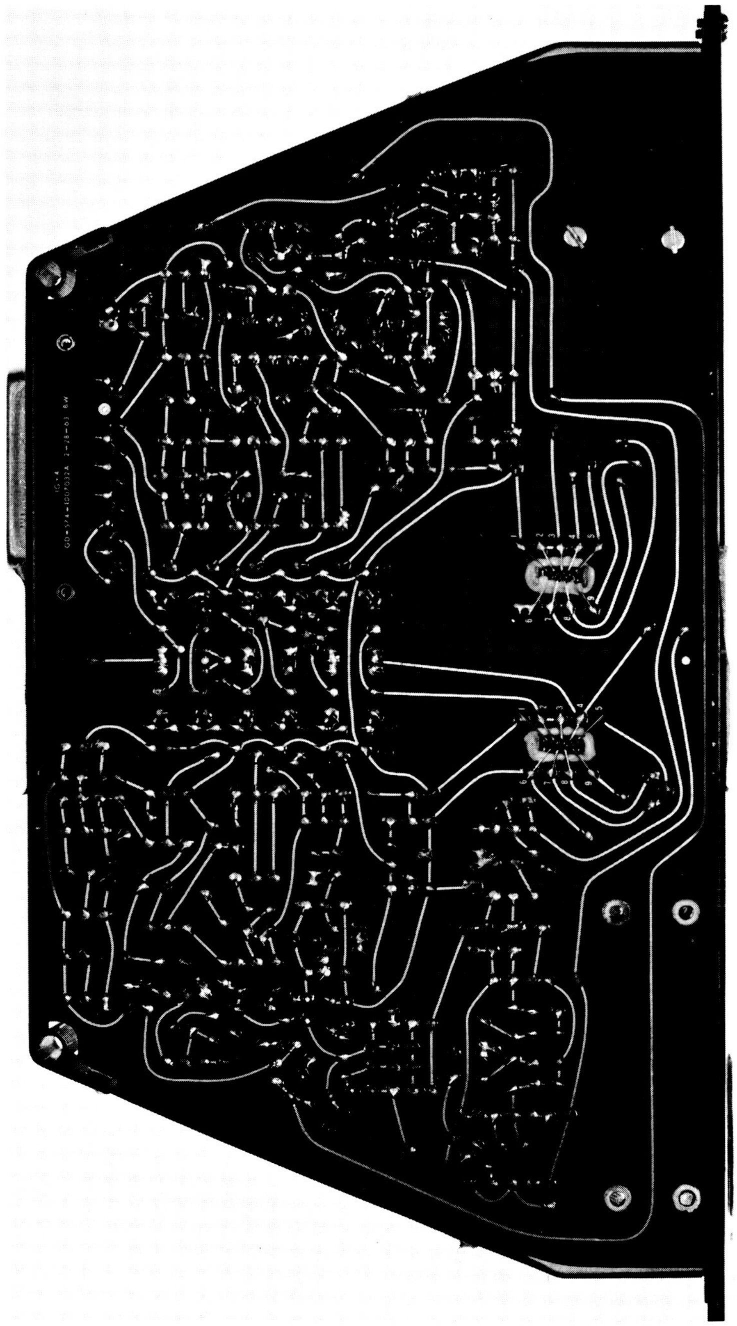

Figure 12 - IG4, Card 4, Telemetry Gated-Mixer Amplifier (Bottom)

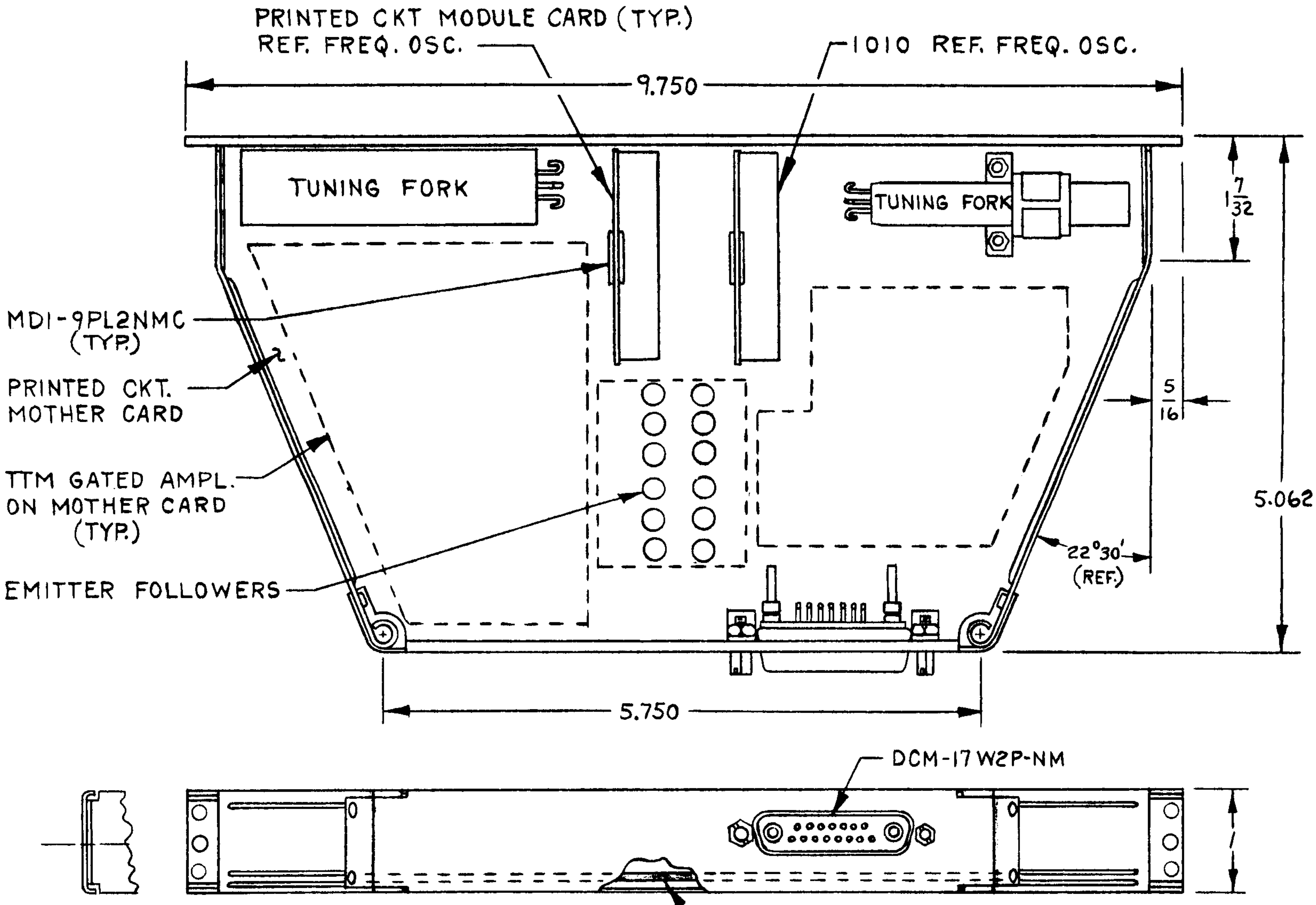

Figure 13 – Card 4

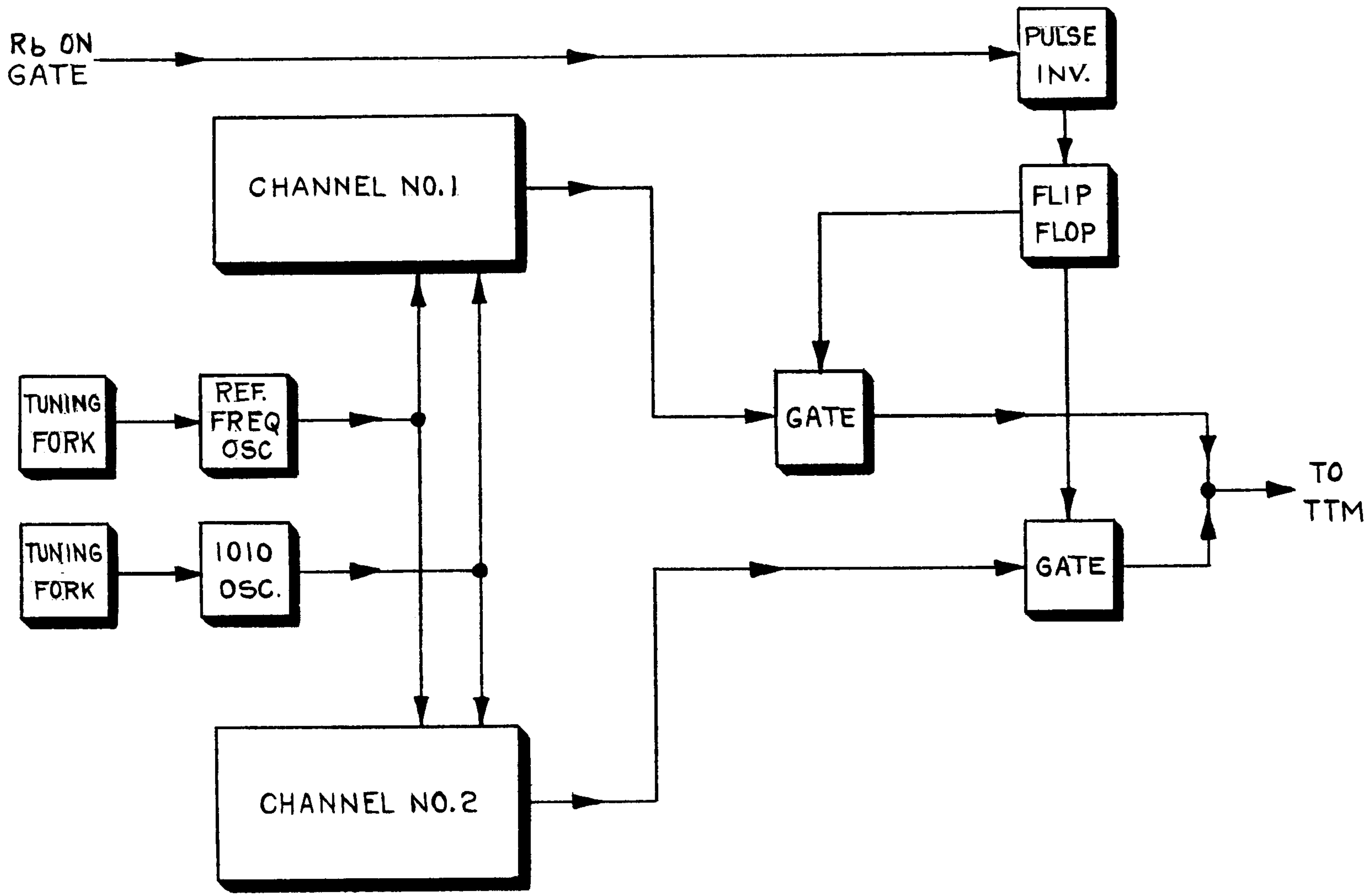

Figure 14 – Card 4, Signal Diagram

sequence through the telemetry, a 1010-cps frequency is injected into the video during the blank time of the 0-all sync channel. During the first three sequences, a 975-cps frequency fills in the blank time of the encoder video.

2.4.1 Reference-frequency oscillator -975 cps ±.1 percent (Figure 52)

(Basically, this is the circuit suggested by Gyrex Corp., for use with their tuning forks). Q1 provides the feedback to the drive coil of the tuning fork. The pickup coil, pins 3 and 4 of the tuning fork, drive Q1 from saturation to beyond cutoff. In the cutoff condition, considerable overshoot occurs at the collector of Q1 due to the windings of T1 and the tuning fork. This overshoot is clipped by D1, acting as a normal diode. Zener action in D1 occurs when Q1 becomes saturated (Figure 15).

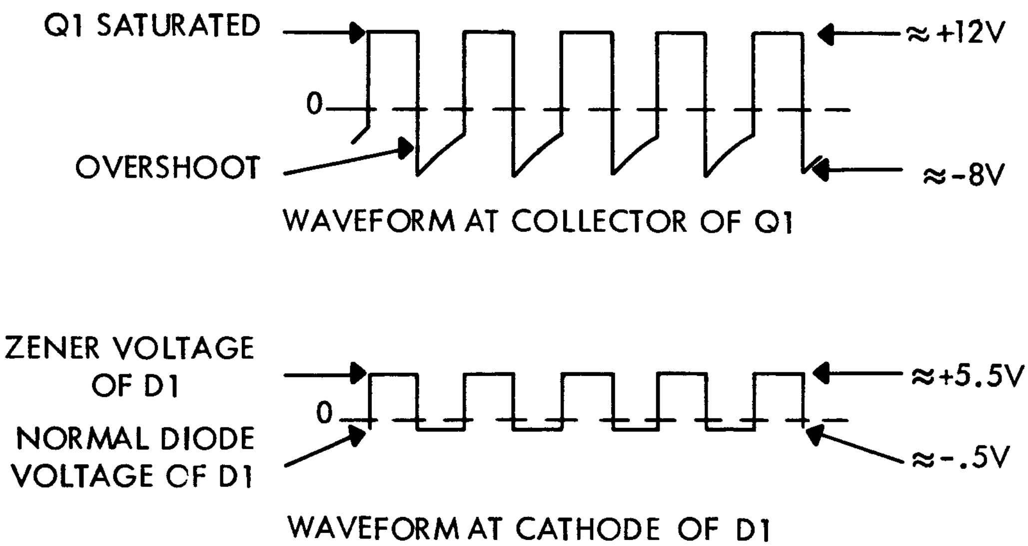

Figure 15 – IG4, Card 4, Oscillator Waveforms

2.4.2 1010 (±.1 percent) cps. Fourth sequence identification frequency oscillator (Figure 52)

This frequency is generated primarily for use as an identification of the fourth sequence through the telemetry. Encoder video, which contains the sequence identification, is not transmitted during the fourth (rubidium) sequence. Except for the frequency generated, the circuits of the reference-frequency oscillator and this unit are identical.

2.4.3 Gated telemetry mixer-amplifer (Figure 51)

Because of the relatively high-impedance output of the encoder, an emitter-follower must be used in series with each of its outputs. Consider the conditioning of the encoder video. It was first necessary to rid the waveform of the counting pulses which appeared on the positive and negative peaks of the square wave. After shifting the D.C. level of the encoder video to zero, the video is amplified via a pseudo-saturated amplifier (Q1, Q2, Q3, and Q4). The 24v p-p square wave thus developed at the collectors of Q1 and Q4 is then attenuated by R12 and R13 (Figure 17).

Driven by the Rb_{on} gate, Q14 clamps the encoder video to ground during the fourth sequence. During the sync channel in the fourth sequence the 0-all gate turns Q14 off, allowing the encoder sync to mix with the magnetometer video. Q13 is biased on by the encoder blank gate during the blank time to give a zero reference to the trailing edge of the video data burst (Figure 18).

The video, conditioned as in Figure 18, is then coupled to the base of Q19, where the blanks are filled in with a 975-cps reference frequency. Consider, next, the gating of the reference frequency. The gating of this signal is controlled by the blank gate from the encoder. Q7 and Q8 operate as an amplifier to a positive gate. When the blank gate is at +6.7v (burst time) Q9 becomes saturated, thus clamping the reference frequency to ground. When this same gate is at -2v, blank time, Q9 is biased off, allowing the reference frequency to appear at the base of Q19, where it fills in the blanks of the encoder video. The telemetry at the base of Q19 is as follows: (Compare with Figure 18).

Q10, activated by the Rb_{on} gate, clamps the reference frequency to ground during the fourth sequence.

The MTM (magnetometer) video is the next consideration. The fourth sequence consists of a 81.92-second analog burst attenuated 80 percent 16 times for .32 second each (channel 0 of each frame). This attenuation is accomplished by driving Q16 to saturation with the 0-all gate (Q15). Q17, activated by the Rb_{on} gate, clamps the MTM video to ground during the first three sequences.

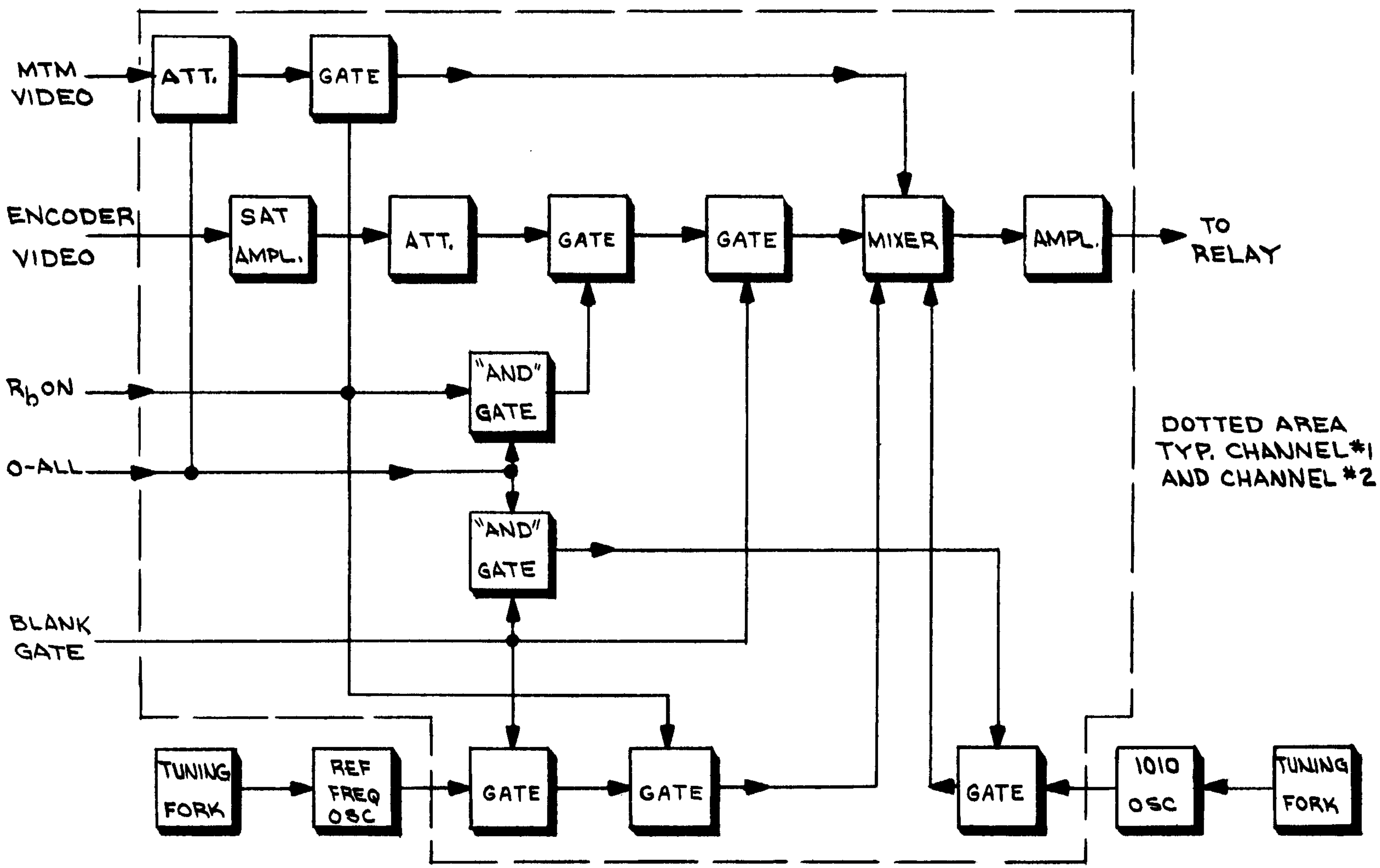

Figure 16 – Gated-Amplifier Signal Diagram

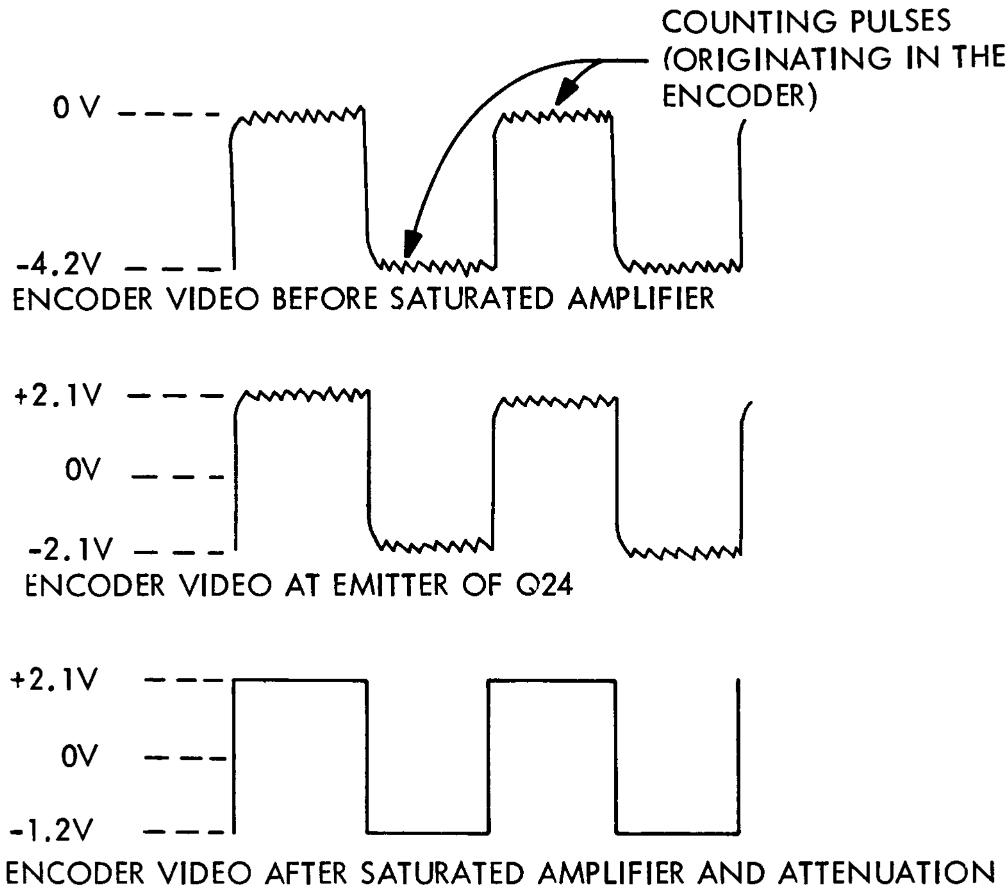

Figure 17 – Encoder Video Waveforms

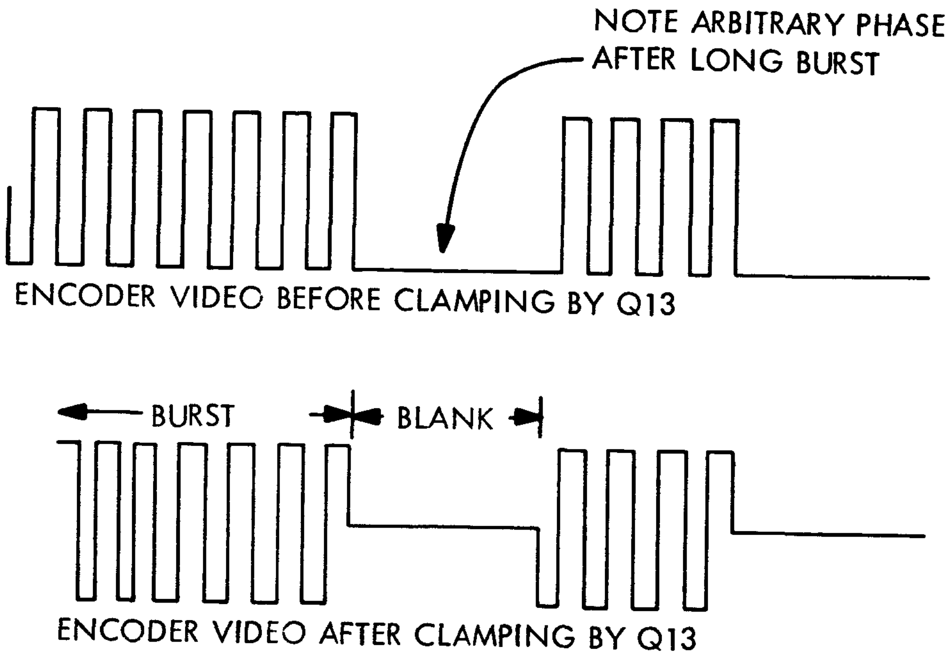

Figure 18 – Formation of Zero Reference Blank Time

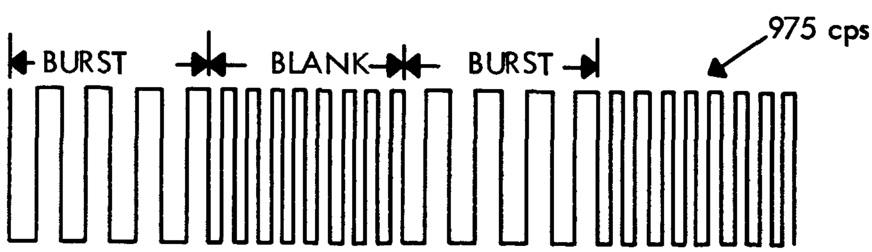

Figure 19 – Video With Blanks Filled In

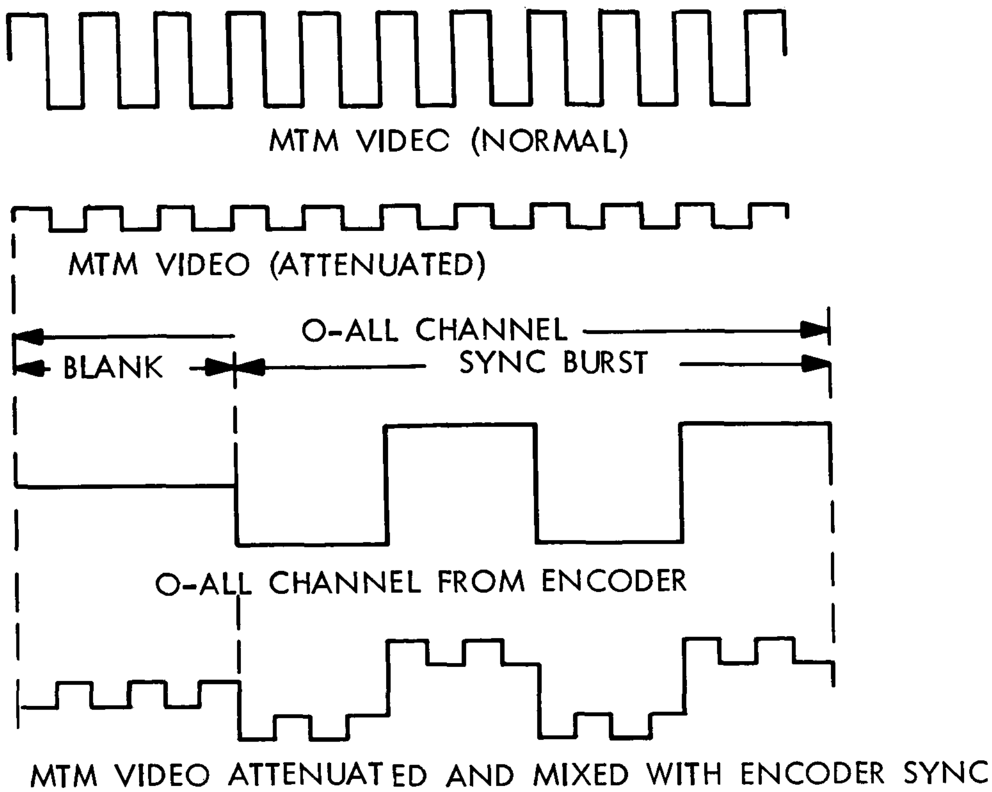

Figure 20 – Mixing of Magnetometer Video Encoder Sync Burst

Figure 20 shows the resulting waveforms when the MTM video and encoder sync are mixed during the fourth sequence. In addition to this, a 1010-cps fourth-sequence identification frequency is also mixed with the MTM (attenuated) video during the blank time of the 0-all channels. Figure 21 shows the formation of this waveform.

The 1010-cps frequency is mixed with the rest of the video when Q18 is biased off. Except for the 0-all channel of the fourth sequence, Q18 is biased on. The bias voltage required to turn it off is generated by the and gate, Q12, between the 0-all sync gate and the blank gate. Q19, the mixing point for all video, is a Class A amplifier which drives a pair of complementary emitter followers, Q20 and Q21.

The redundancy of the circuit is operated on a time-sharing basis. The two channels (Figure 14) drive the transmitter alternately. The switching is effected at the beginning of the fourth sequence. The transition of the Rb_{on} gate from +6.7v to -2v develops a negative

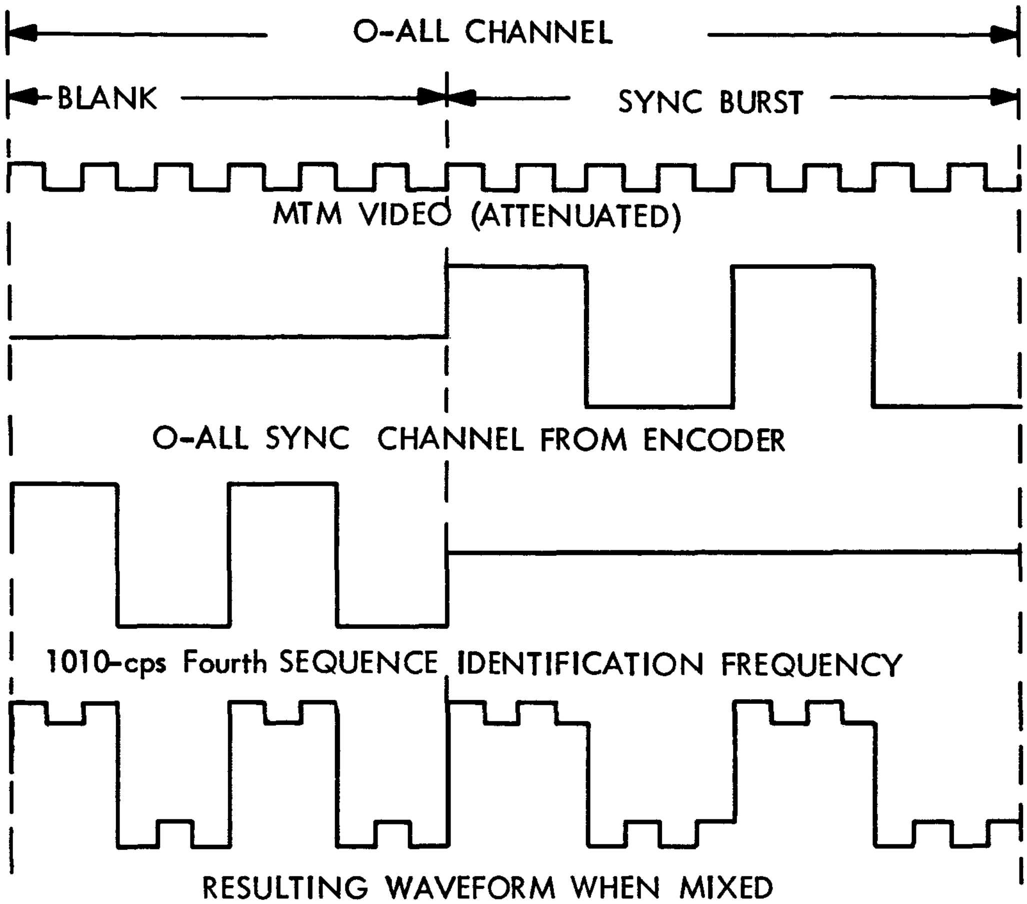

Figure 21 – Formation of 0-All Channel of Fourth Sequence

pulse at the base of Q55, saturating it momentarily. The positive pulse thus developed at its collector triggers the flip-flop, Q56 and Q57, via the steering diodes D3 and D4. If it is assumed that the flip-flop is in such a state that Q57 is saturated, Q58 will also be saturated due to the biasing of R120 and R115. With Q57 on, Q56 will be off, having about +8v at its collector. This voltage is sufficient to bias Q59 off via R124 and R135. In the above condition, the output of channel 2 will be driving the transmitter through Q58. The next triggering pulse from Q55 will reverse the above condition, switching in channel 1 via Q59.

2.5 Card 5 (Figures 24 and 53) (programmer functions only)

This card (IG5) contains the undervoltage relay and the electronics necessary to fire the squibs that activate the boom erection, yo-yo release, and magnetometer extension mechanisms. The timing sequence for orbital injection is:

Time (Seconds)	Event
T - 180	Start despin timers (from blockhouse, timer setting 1780 seconds)
T + 0	Liftoff
T +	MECO
T +	Stage 2 ignition
T + 180	Fairing separation
T +	SECO
T + 364	Spin-up
T + 370	Third-stage ignition (DAC timer starts)
T + 396	Third-stage burnout
T + 1600	Despin of spacecraft/stage 3 (±82 seconds spacecraft function)
T + 1870	Paddle erection and (DAC) ±187 seconds
T + 1872	Fluxgate erection
T + 1880	Separation (DAC)
T + 1880	Rb-vapor magnetometer extension

2.5.1 Despin timer (IG15, IG25, IG35, IG45) (Figures 54 and 55)

The despin timer is a redundant electronic clock activated from the blockhouse 180 seconds before liftoff. At the termination of its count, 1780 seconds later, its output drives redundant relays. Closure of the contacts of these relays fire the squibs that release the yo-yo despin mechanism.

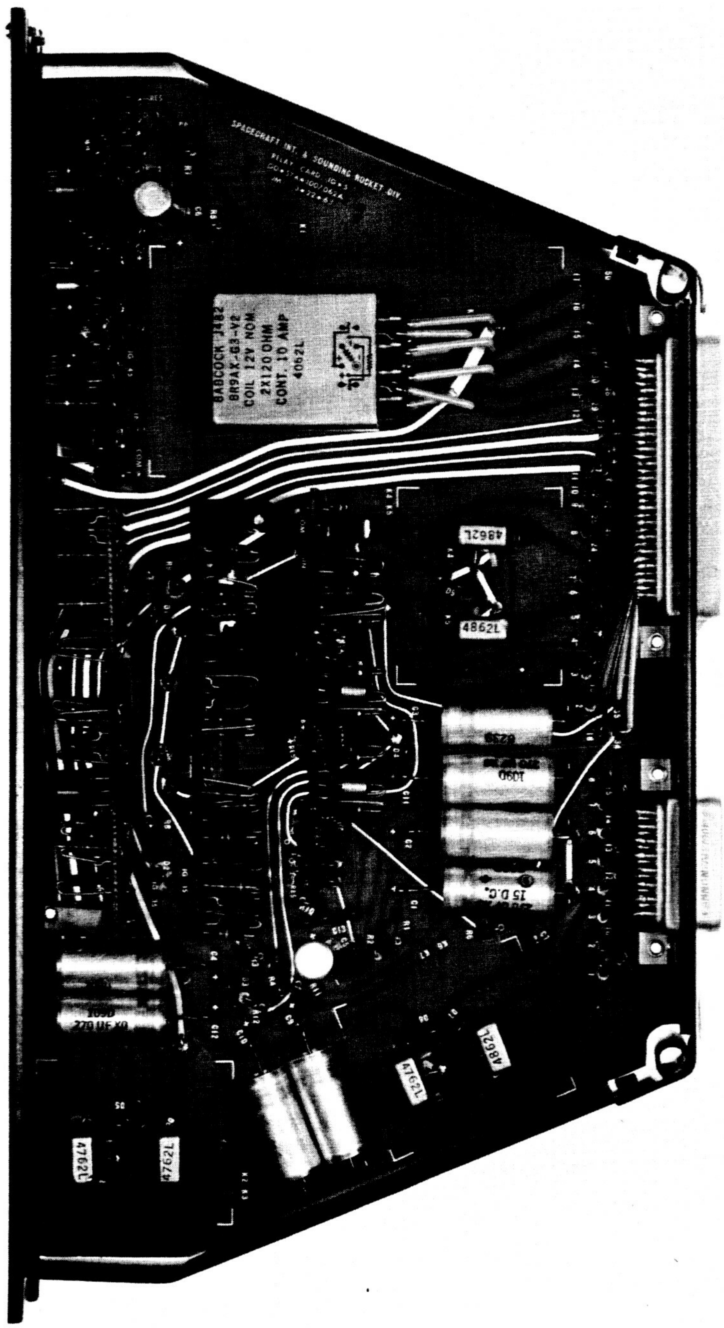

Figure 22 – IG5, Card 5, Relay Card (Top)

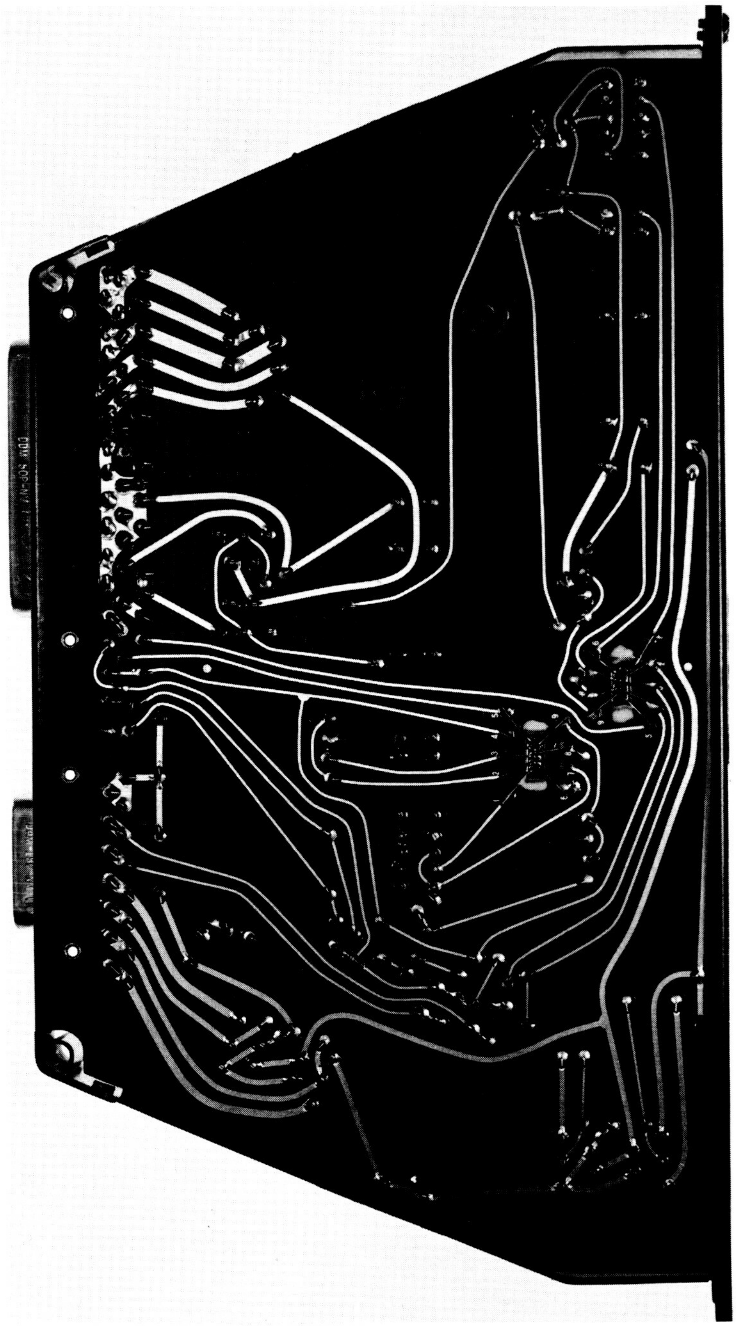

Figure 22 – IG 5, Card 5, Relay Card (Bottom)

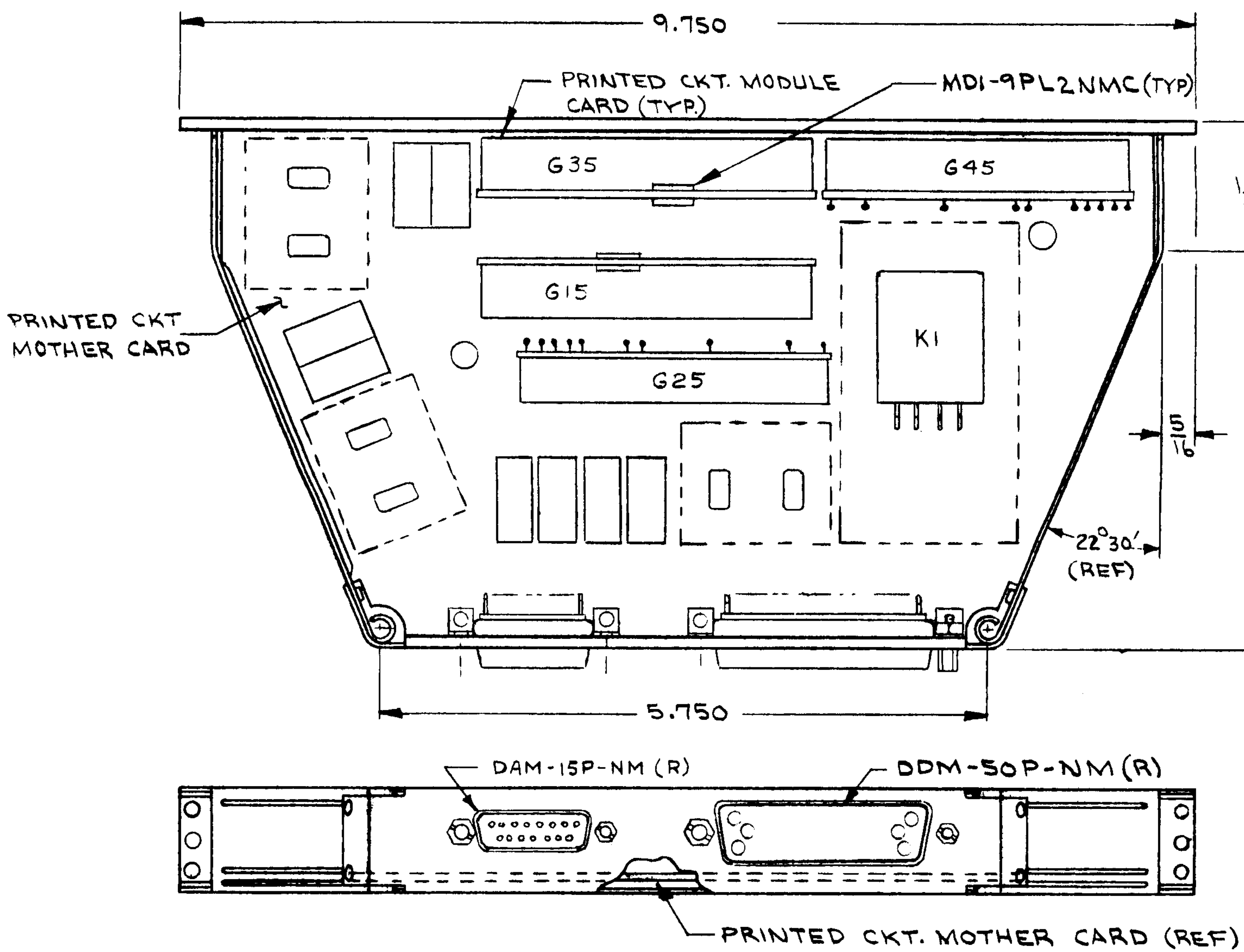

Figure 23 – Card 5

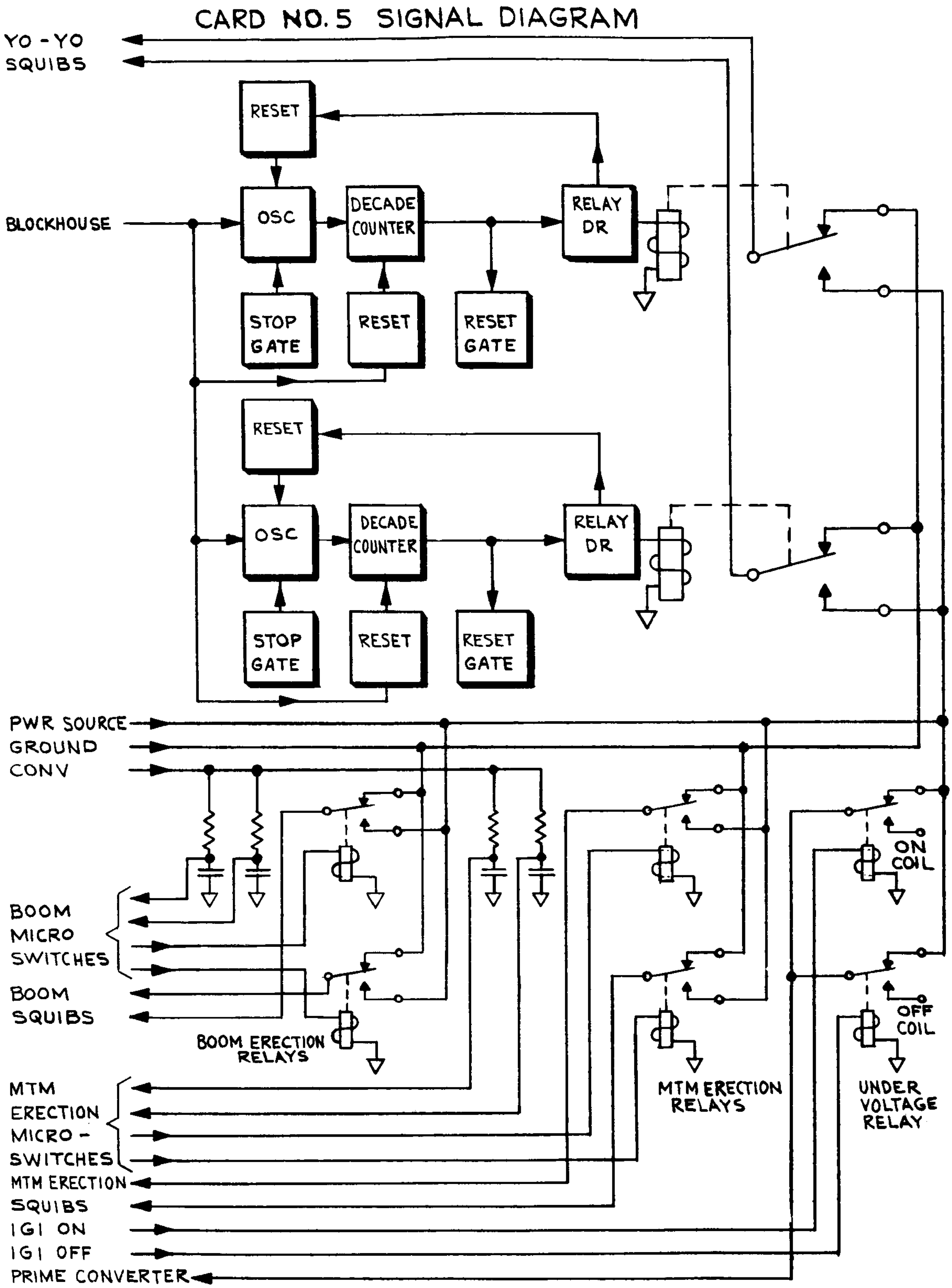

Figure 24 – Card 5, Signal Diagram

The despin timer has two major sections, the oscillator-relay driver and the magnetic-core counter. The oscillator-relay driver section of the timer (IG15 and IG35) (Figure 54) is held inactive by grounding pin 4 at the blockhouse through the umbilical cable. In this condition, the anode of Dl is at about +0.5v. This is not enough voltage on the emitter of Q2 to operate the unijunction oscillator (Q2, Cl, R2, R4, R5, R6, R7, and R8). R6 is used to temperature compensate the timing period (17.8 seconds) of the oscillator. Also, Q3 is biased off by R3 and Dl. With Q3 off there is no current drain by Q2. When the ground at pin 4 is released, the anode of Dl rises to B+, activating the unijunction oscillator Q2. This step in voltage is differentiated by C2, R15, and R16, forming a positive pulse at the gate of Q4. This pulse turns Q4 on, discharging C3 through its cathode load (R16, R17, R18, and the + reset coil of the magnetic-core counter). The discharge of C3 develops a positive pulse at the cathode of Q4. This pulse resets the magnetic-core counter and saturates Q5. Q5 clamps the false stop pulse from the counter to ground. (See section III. A. 2 for further explanation of false stop pulse.) After 1780 seconds, a pulse from the counter enters pin 1, turning Q6 on and discharging the two 270μ fd capacitors connected to pin 2 through the redundant relay coils. The pulse developed at the cathode of Q6 as a result of this discharge turns Ql on, removing B+ from the unijunction oscillator.

The magnetic-core counter used in this unit is identical to the one used in card 1, except that it has a divide-by-100 function instead of 10,000. (See 3.1.2 for explanation.)

2.5.2 Boom erection

Erection of the solar paddles causes two microswitches to close. Closure of these switches discharges Cl and C2 (Figure 53) through the coils of K2 and K3 respectively. The contacts of these relays fire the squibs that release the boom erection mechanism.

2.5.3 Magnetometer extension

Third-stage separation causes two microswitches to close. Closure of these switches discharge C9 and C10 through the coils of K6 and K7 respectively. The diodes D7 and D8 damp the inductive kick of the coils. The contacts of these relays fire the squibs that release the magnetometer extension mechanism.

2.5.4 Undervoltage relay

The undervoltage relay, K1, acts in response to signals from the undervoltage detector and recycle timer card 1). The contacts of this relay, connected in parallel, either make or break the connection between the batteries and the prime converter.

2.6 Card 6 (Figures 27 and 53)

The Miller timers card (IG6) houses two electrochemical timers to terminate operation of the satellite at the end of 1 year. Two timers are used for redundancy to ensure against a possible premature opening of either timer switch, which would reduce the life of the satellite. The timer switches are connected in parallel with each other and in series with the solar paddles and the payload batteries. At the end of 1 year, the solar paddles are disconnected from the batteries. This opening is monitored through telemetry, giving a check of the timing accuracy. The satellite will continue to operate on the batteries until they dissipate in approximately 2-1/2 hours under full load.

The timers, developed for GSFC by Miller Research Laboratories of Baltimore, Maryland, contain a U.S. Navy-developed electrochemical cell as the timing unit. The cell is filled with a lead fluoroborate electrolytic solution. Immersed in the solution is a lead pellet affixed to a silver wire that spring-loads a plunger at the end of the cell. The period of the timing function is determined by the deplating action of the polarizing current on the lead pellet plus the etching action of the current on the silver wire. The rupture of the silver wire releases the plunger, actuating a microswitch which disconnects the solar paddles from the batteries. The polarizing current required for any given time interval may be determined by the relation:

$$t \text{ (hours)} = \frac{270 \text{ milliamperes} - \text{hours}}{\text{polarizing current (ma)}}$$

The actual time interval will be t hours plus approximately 5 percent for the etching of the silver wire. For use as a 1-year timer ($t = 8760$ hours), the polarizing current required is 30.8 microamperes. This current is derived from the undervoltage detector card (IG1) by application of the regulated output from the undervoltage converter through the current-limiting resistors R3 and R4 (located on IG1).

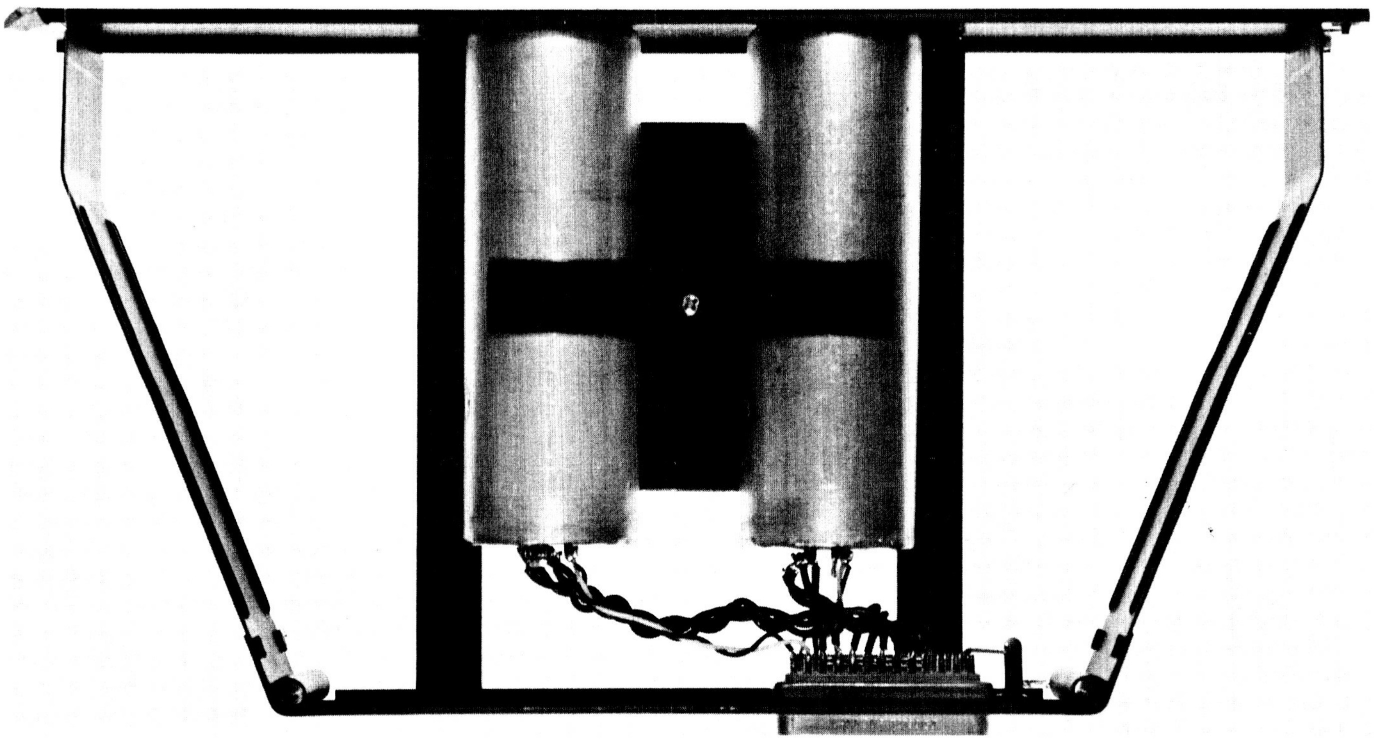

Figure 25 – IG6, Card 6, One Year Timer (Top)

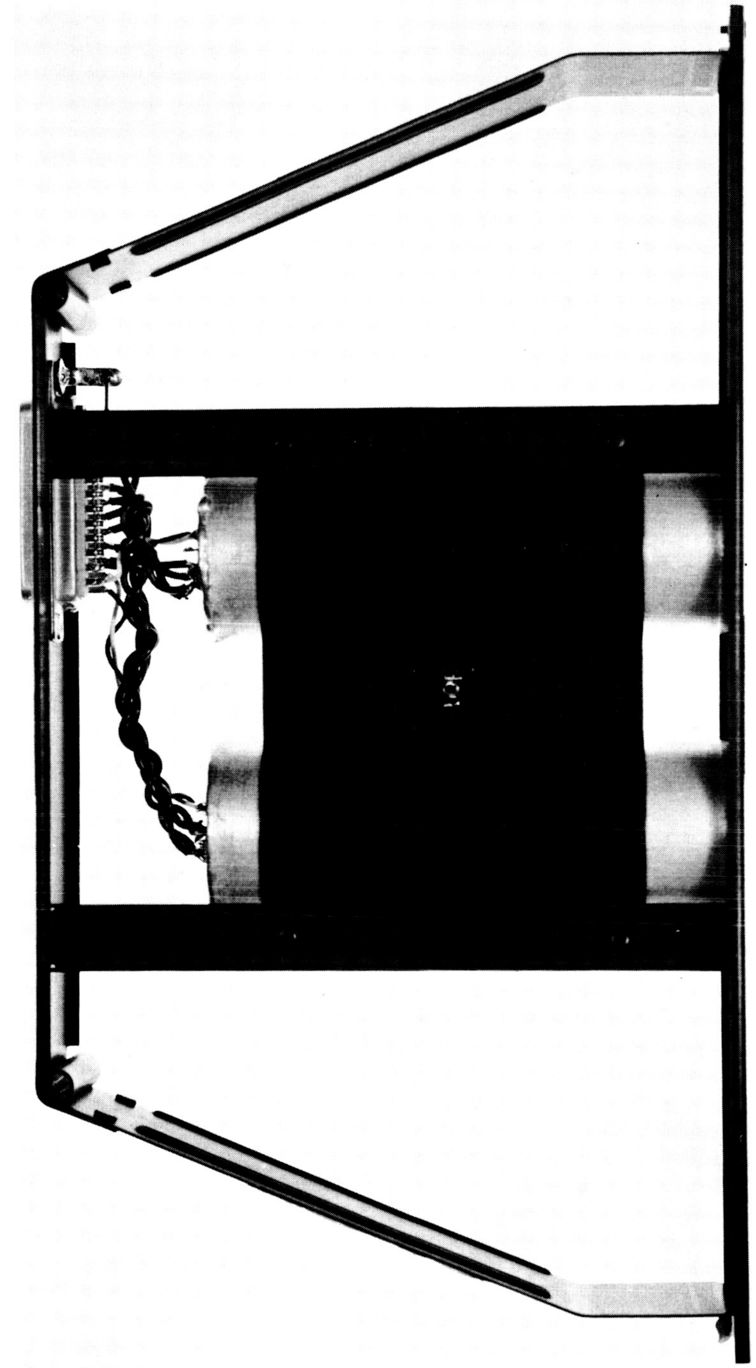

Figure 25 – IG6, Card 6, One Year Timer (Bottom)

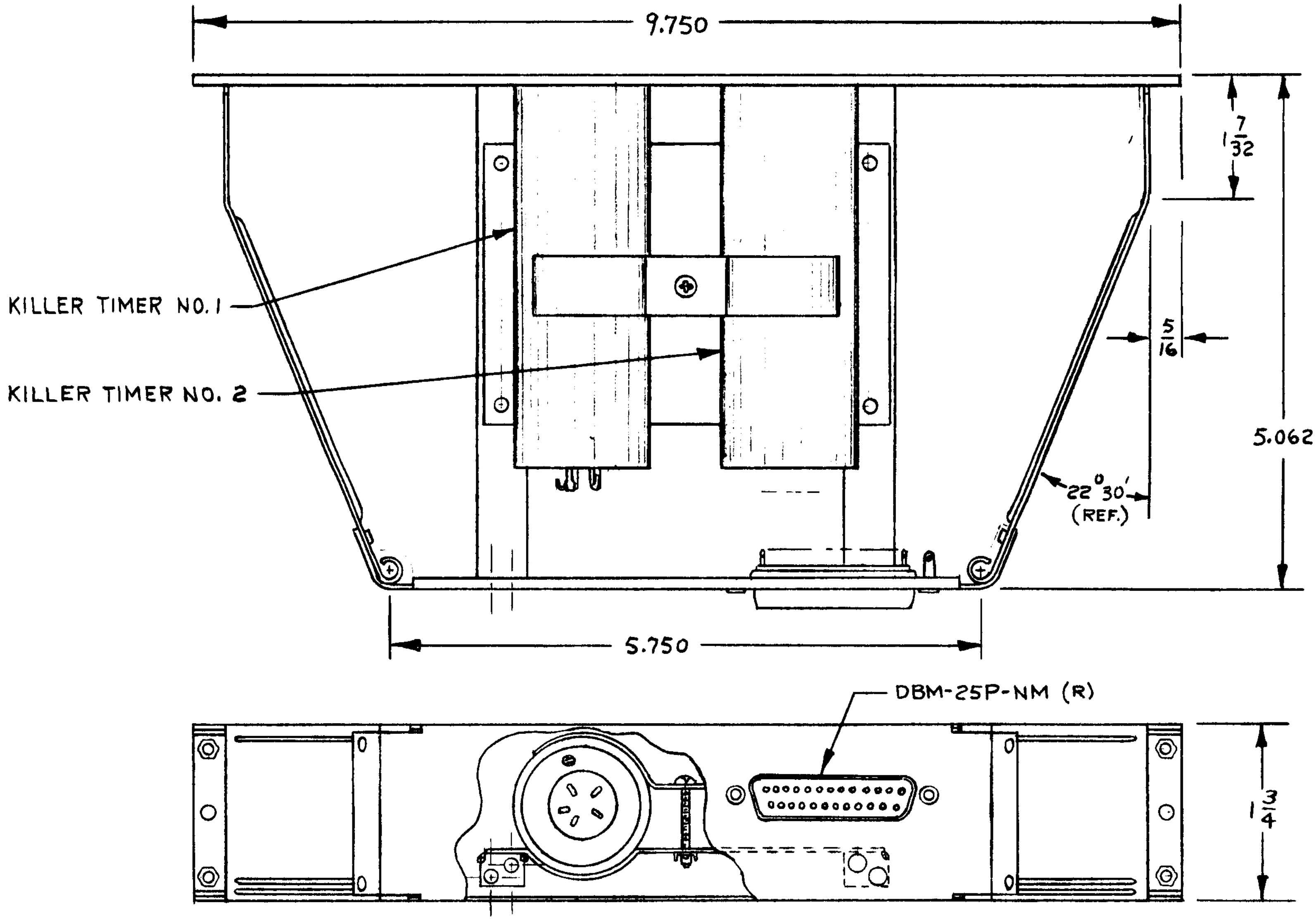

Figure 26—Card 6

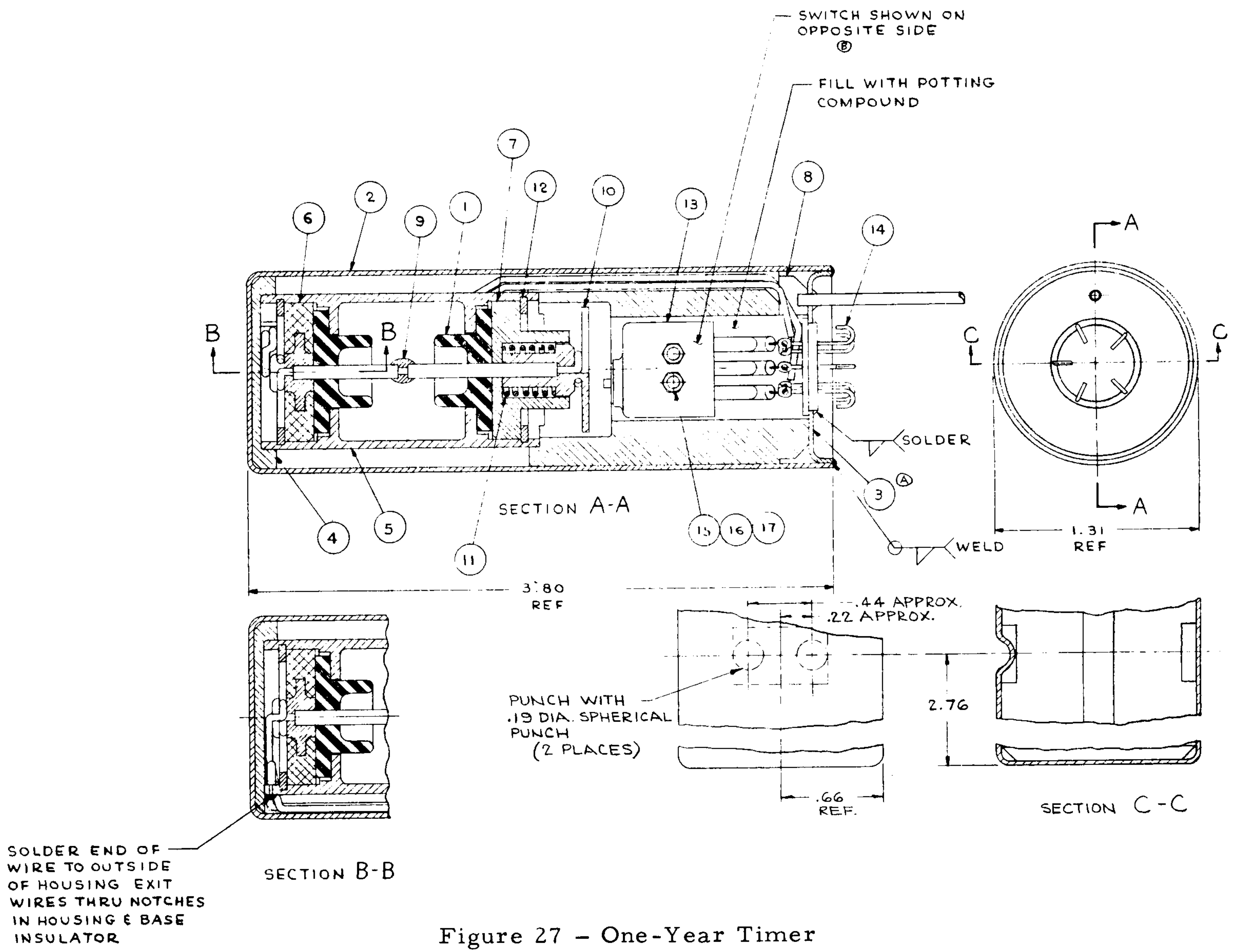

Figure 27 – One-Year Timer

3. Interfaces

3.1 Card 1

3.1.1 Input

a. Batteries - The current drain directly from the batteries due to monitoring of their voltage varies from $100\mu a$ to $160\mu a$ due to change in battery voltage.

b. Undervoltage converter - The current drain from this converter in the normal and undervoltage conditions is 3 ma and 10 ma respectively, at +12 volts.

c. Turn-on plug - The oscillator reset function of card 1 is available at this plug.

3.1.2 Output

a. Undervoltage relay - The relay is a 2PDT unit whose coils (on and off) are 150 ohms each. The off coil receives a pulse of +12v from the decade oscillator when an undervoltage condition occurs. This relay may also receive a positive pulse from the blockhouse through the umbilical cable.

b. One-year timers - The 1-year Miller timers are furnished with a current of $30.8\mu a$ directly from +12v within card 1. This current causes the timers to open the line between the solar cells and the batteries after a period of 1 year.

c. Payload test plug - The undervoltage time may be reduced from 8 hours to approximately 7 minutes by utilizing the speed-up function available at this plug. The rate of this oscillator may also be monitored at this plug.

3.2 Card 2

3.2.1 Input

a. Encoder - (1) Gas-cell thermal control (G-12 and G-72) - These units have emitter-follower inputs which present an impedance of approximately 1 megohm or greater to the Rb_{on} output of the encoder.

(2) Minus magnetometer calibrator (G-22) – Due to a blocking diode, the Rb_3 gate drives an essentially infinite impedance when it is +6. 7v. When the gate is at -2v, it sees an impedance of approximately 95 k ohms.

(3) Plug magnetometer calibrator (G-32) – When the Rb_1 gate is at +6. 7v, it sees an almost infinite impedance due to a blocking zener diode which is not conducting at this point. When the gate goes to -2v, however, zener action occurs and a 22 K ohms impedance is seen.

(4) Fluxgate calibrator-timer A and B (G-42 and 52) – The fluxgates A and B are ac-coupled to these units, thus a high input impedance results in the steady state at either +6. 7v or -2v. Only the transition time between these extremes is utilized, and here a very low impedance is presented.

(5) Lamp-starter gate (G-62) – This circuit is coupled to the encoder by means of an emitter-follower which reflects an impedance of 500 K ohms.

b. Programmer-converter – The maximum current drain by this card is 17 ma at +12v and 13 ma at -12v.

c. Rubidium vapor (Rb) Magnetometer – (1) Gas-cell thermal control (G-12) – Four 100 K ohms thermistors in parallel, located on the heating coil for the gas cell, provide the input to this thermal control circuitry. This input forms the grounded end of a voltage divider at the base of a transistor which actuates a Schmitt trigger.

d. Programmer card 3 – At the beginning of the fourth sequence, a positive voltage step is received from card 3 if the Rb lamp is not operating. This gate drives a grounded emitter-amplifier stage of 10 K ohms input impedance.

3.3.2 Output

a. As per outline – (1) Gas cell thermal control, (G-12 and G-7-2) – These units complete the circuit supplying power to two heating coils by grounding one end of each coil, the other end being connected to the battery line.

(2) Minus (G-22) magnetometer calibrators - This unit supplies a calibrating current to each of two coils. Coil 1 receives a current of 1.491 ma ±.1 percent. Coil 2 receives a current of 2.187 ma ±.1 percent, giving a current ratio of 1.466.

(3) Plus magnetometer calibrator (G-32) - This unit duplicates the function of the minus magnetometer calibrator, except that it supplies current to the coils in the reverse direction (positive).

(4) Lamp starter gate (G-62) - This unit supplies the gas cell with a +2v-to-zero volts gate for 5 seconds if the cell is not oscillating at the beginning of the fourth sequence. The supply impedance at zero volts is 7.5 K ohms.

b. Fluxgate calibrator coils - (1) Fluxgate A calibrator (G-42) - With the event of Fluxgate A sync from the encoder, this unit supplies a 500-millisecond +11.5v pulse through a 180-ohm resistor to the fluxgate experiment.

(2) Fluxgate B calibrator (G-52) - This unit is identical in its function to the foregoing, except that it is activated by encoder fluxgate B sync.

3.3 Card 3

3.3.1 Input

a. Rb outline - The photocell of this experiment is ac-coupled through a 39 μf capacitor to a common-emitter amplifier which presents an impedance of approximately 10 K ohms.

b. Programmer-converter - The total current drain to this unit is 20 ma at +12v and 7.5 ma at -12v.

3.3.2 Output

a. Outline - The H-1 current attenuator and driver amplifier within card 3 supplies a 1v rms signal to the phase-shift capacitor, also located within this card, which passes a current proportional to the frequency of the applied voltage. This current causes oscillation within the magnetometer and its electronics.

b. Programmer card 2 – If the above oscillatory condition exists, card 3 presents a signal of 11.5v at a 10 K ohm impedance to card 2. If it is not oscillating, this signal is zero volts.

c. Programmer card 4 – The magnetometer video, a 20-cycle to 10-kc 2.5v p-p square wave, is amplified in card 3 at 10 K ohm impedance and routed via coaxial cable to card 4.

3.4 Card 4

3.4.1 Input

a. Encoder – (1) Video – This signal is coupled to a 500 K ohm impedance.

(2) Rb on – This gate sees an impedance of approximately 1 megohm at both the +6.7v and -2v positions.

(3) 0- all sync – This gate drives an impedance of 450 K ohms at +6.7v and 250 K ohms -2v.

(4) Blank gate – When in the +6.7v position, this gate drives an impedance of 130 K ohms. At the -2v position, it drives an impedance of 750 K ohms.

b. Programmer card 3 – During sequences 1, 2, and 3 ("IMP PFM Encoder" prepared by H. D. White – Revision A, August 6, 1962), Card 4 presents an impedance of 100 K ohms to this card. During the fourth sequence this same impedance becomes approximately 200 K ohms, dropping to 120 K ohms during the zero channel of each frame within this sequence.

c. Programmer-converter – The maximum current requirements of this card are 14 ma at +12v and 7 ma at -12v.

3.4.2 Output

Card 4 provides a driving impedance of 10 K ohms or less to the transmitter.

3.5 Card 5 (programmer functions only)

3.5.1 Input

a. Undervoltage converter - Before lift-off, the despin timing electronics within this card will draw 5 ma at +12v. After separation, the drain will be 4 ma at the same voltage.

b. Programmer card 1 - The undervoltage control signal from card 1 is connected to the coils of the above-mentioned under-voltage relay.

c. Umbilical plug (at the payload shell) - When in place, this plug provides a short to ground from blockhouse which causes the despin timing electronics within card 5 to remain inactive. Removal of this short 60 seconds before liftoff initiates the despin timing cycle. The undervoltage relay control signal from the blockhouse also enters card 5 through this plug.

d. Fluxgate boom microswitch - The contacts of this switch provide a path for the discharge of a capacitor through the coil of a non-latching relay, the contacts of which provide a current path for the explosive squib bolts that release the fluxgate booms. This switch closes when the solar paddles are erected.

e. MTM extension microswitch - This switch has the same function as d. above, except that it is with reference to the MTM extension mechanism. It closes with the separation of the third stage from the payload.

3.5.2 Output

a. Despin squibs - The relay contacts within card 5 provide a means of connecting the payload battery to the despin squibs at the proper time.

b. Boom squibs - Card 5 provides the same function as a. above, except that it is with reference to the fluxgate boom squibs.

c. MTM extension squibs - Card 5 provides the same function as a. above, except that it is with reference to the MTM extension squibs.

d. Prime converter batteries – The input to this converter is connected to the batteries through the contacts of the undervoltage relay. The relay is a Babcock BR-9 2PDT latching type. The contacts are wired in parallel to increase its current-handling capacity.

3.6 Card 6

3.6.1 Input

a. Card 1 – Card 1 supplies a current of 30.8 microamperes to the Miller timers* within this card.

b. Solar paddles – The output of the solar paddles is connected to the batteries through a microswitch within the Miller timers.

3.6.2 Output

a. See 1.b. above.

---

*Developed by Miller Research Laboratories, Baltimore, Md.

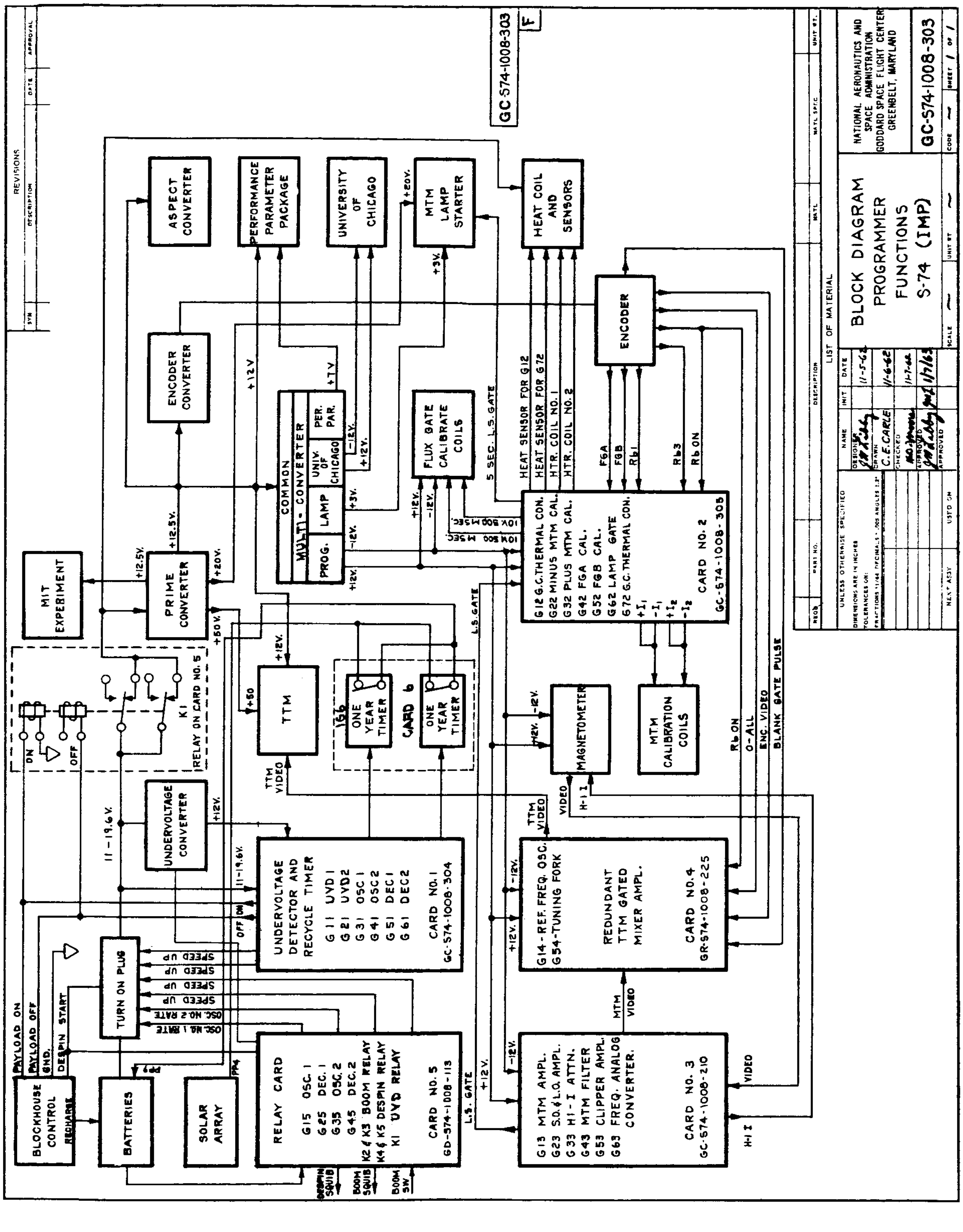
BLOCK DIAGRAM PROGRAMMER FUNCTIONS S-74 (IMP)
GC-574-1008-303
NATIONAL AERONAUTICS AND SPACE ADMINISTRATION
GODDARD SPACE FLIGHT CENTER
GREENBELT, MARYLAND
C.E. CARLE
ASPECT CONVERTER
PERFORMANCE PARAMETER PACKAGE
UNIVERSITY OF CHICAGO
MTM LAMP STARTER
HEAT COIL AND SENSORS
ENCODER
ENCODER CONVERTER
MULTI - CONVERTER
COMMON
PROG.
LAMP
UNIV. OF CHICAGO
PER. PAR.
FLUX GATE CALIBRATE COILS
MIT EXPERIMENT
PRIME CONVERTER
TTM
ONE YEAR TIMER
CARD 6
MAGNETOMETER
MTM CALIBRATION COILS
K1 RELAY ON CARD NO. 5
UNDERVOLTAGE CONVERTER
UNDERVOLTAGE DETECTOR AND RECYCLE TIMER
G11 UVD1
G21 UVD2
G31 OSC1
G41 OSC2
G51 DEC1
G61 DEC2
CARD NO.1
GC-574-1008-304
G12 G.C. THERMAL CON.
G22 MINUS MTM CAL.
G32 PLUS MTM CAL.
G42 FGA CAL.
G52 FGB CAL.
G62 LAMP GATE
G72 G.C. THERMAL CON.
CARD NO. 2
GC-574-1008-305
G14 - REF. FREQ. OSC.
G54 - TUNING FORK
REDUNDANT TTM GATED MIXER AMPL.
CARD NO. 4
GR-574-1008-225
G13 MTM AMPL.
G23 S.O. & L.O. AMPL.
G33 HI-I ATTN.
G43 MTM FILTER
G53 CLIPPER AMPL.
G63 FREQ. ANALOG CONVERTER.
CARD NO. 3
GC-574-1008-210
RELAY CARD
G15 OSC.1
G25 DEC.1
G35 OSC.2
G45 DEC.2
K2 & K3 BOOM RELAY
K4 & K5 DESPIN RELAY
K1 UVD RELAY
CARD NO. 5
GD-574-1008-113
TURN ON PLUG
BLOCKHOUSE CONTROL
BATTERIES
SOLAR ARRAY
PAYLOAD ON
PAYLOAD OFF
GND.
DESPIN START
RECHARGE
SPEED UP
OSC. NO. 2 RATE
OSC. NO. 1 RATE
HEAT SENSOR FOR G12
HEAT SENSOR FOR G72
HTR. COIL NO. 1
HTR. COIL NO. 2
5 SEC. L.S. GATE
L.S. GATE
FGA
FGB
Rb1
Rb3
Rb ON
0-ALL
ENC. VIDEO
BLANK GATE PULSE
TTM VIDEO
MTM VIDEO
VIDEO
H-I
DESPIN SQUIB
BOOM SQUIB
BOOM SW.
11 - 19.6 V.
+12V.
-12V.
+12.5V.
+20V.
+50V.
+3V.
+7V.

Figure 28

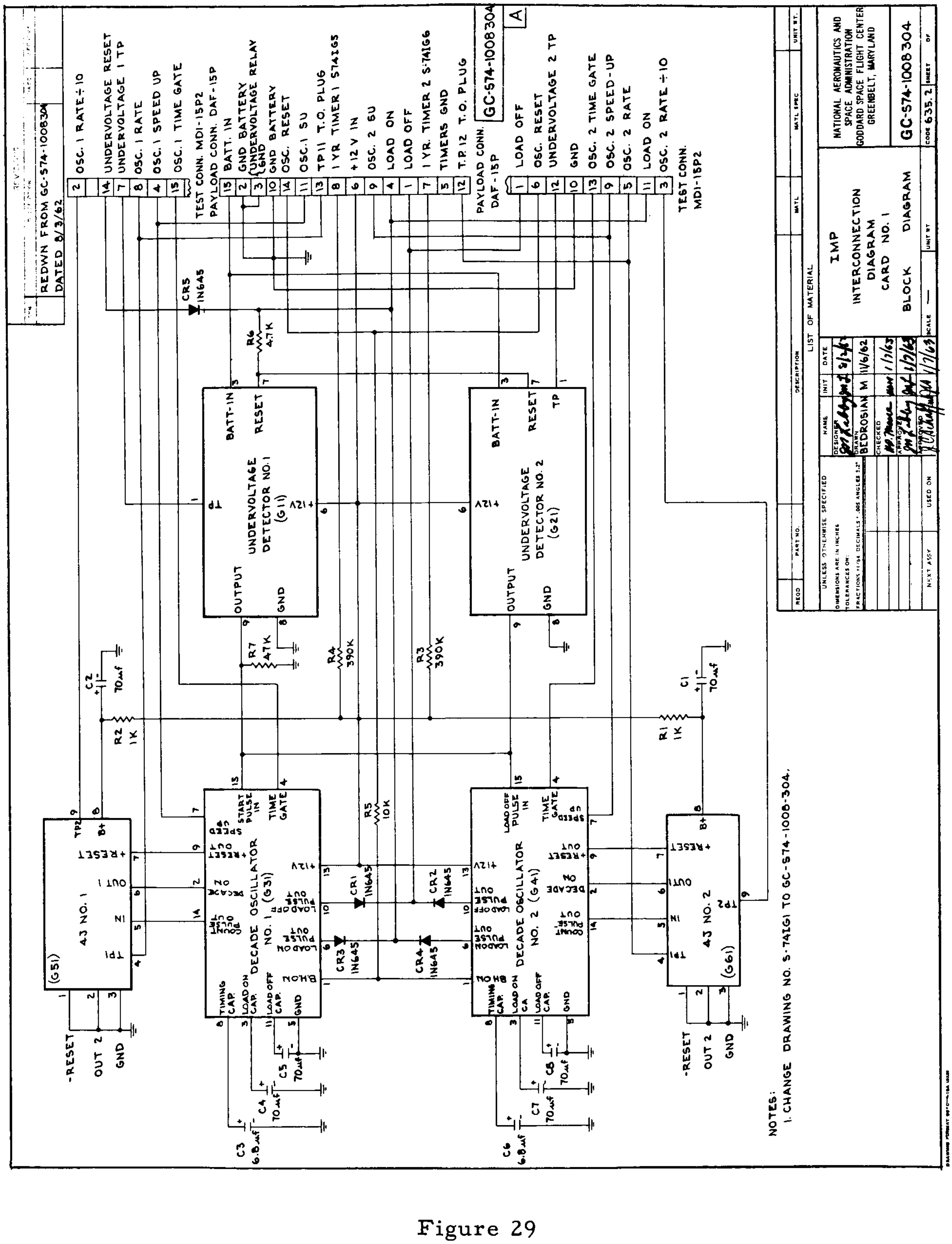

REDWN FROM GC-574-1008304
DATED 8/3/62
GC-574-1008304
A
UNDERVOLTAGE DETECTOR NO. 1 (G11)
UNDERVOLTAGE DETECTOR NO. 2 (G21)
DECADE OSCILLATOR NO. 1 (G31)
DECADE OSCILLATOR NO. 2 (G41)
4-3 NO. 1 (G51)
4-3 NO. 2 (G61)
TEST CONN. MDI-15P2
PAYLOAD CONN. DAF-15P
NOTES:
1. CHANGE DRAWING NO. S-741G1 TO GC-574-1008-304.
LIST OF MATERIAL
NATIONAL AERONAUTICS AND SPACE ADMINISTRATION
GODDARD SPACE FLIGHT CENTER
GREENBELT, MARYLAND
IMP
INTERCONNECTION
DIAGRAM
CARD NO. 1
BLOCK DIAGRAM
GC-574-1008304
BEDROSIAN
11/6/62

Figure 29

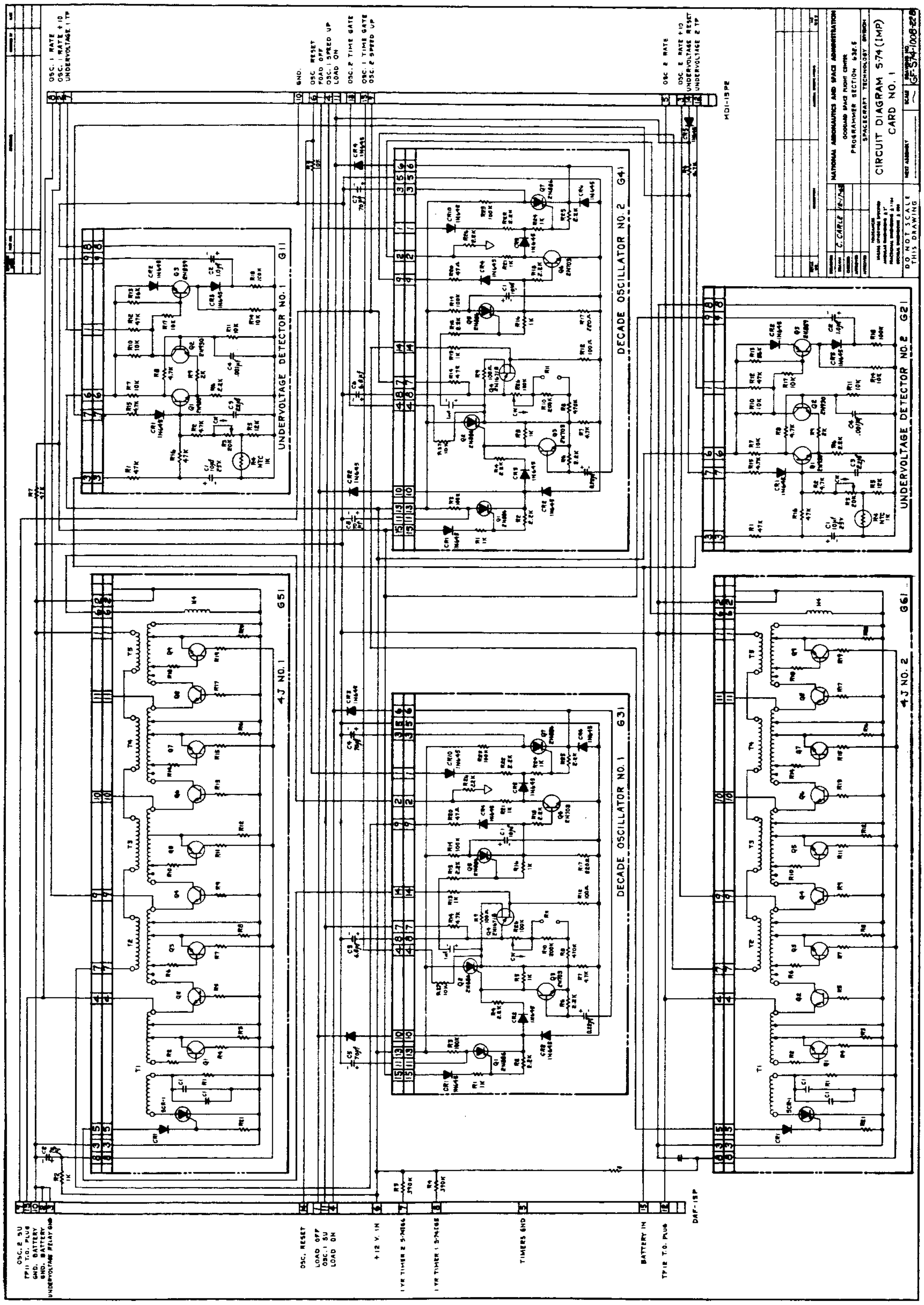
UNDERVOLTAGE DETECTOR NO. 1
G11
DECADE OSCILLATOR NO. 2
G41
UNDERVOLTAGE DETECTOR NO. 2
G21
4J NO. 1
G51
DECADE OSCILLATOR NO. 1
G31
4J NO. 2
G61
CIRCUIT DIAGRAM 5.74 (IMP)
CARD NO. 1

Figure 30

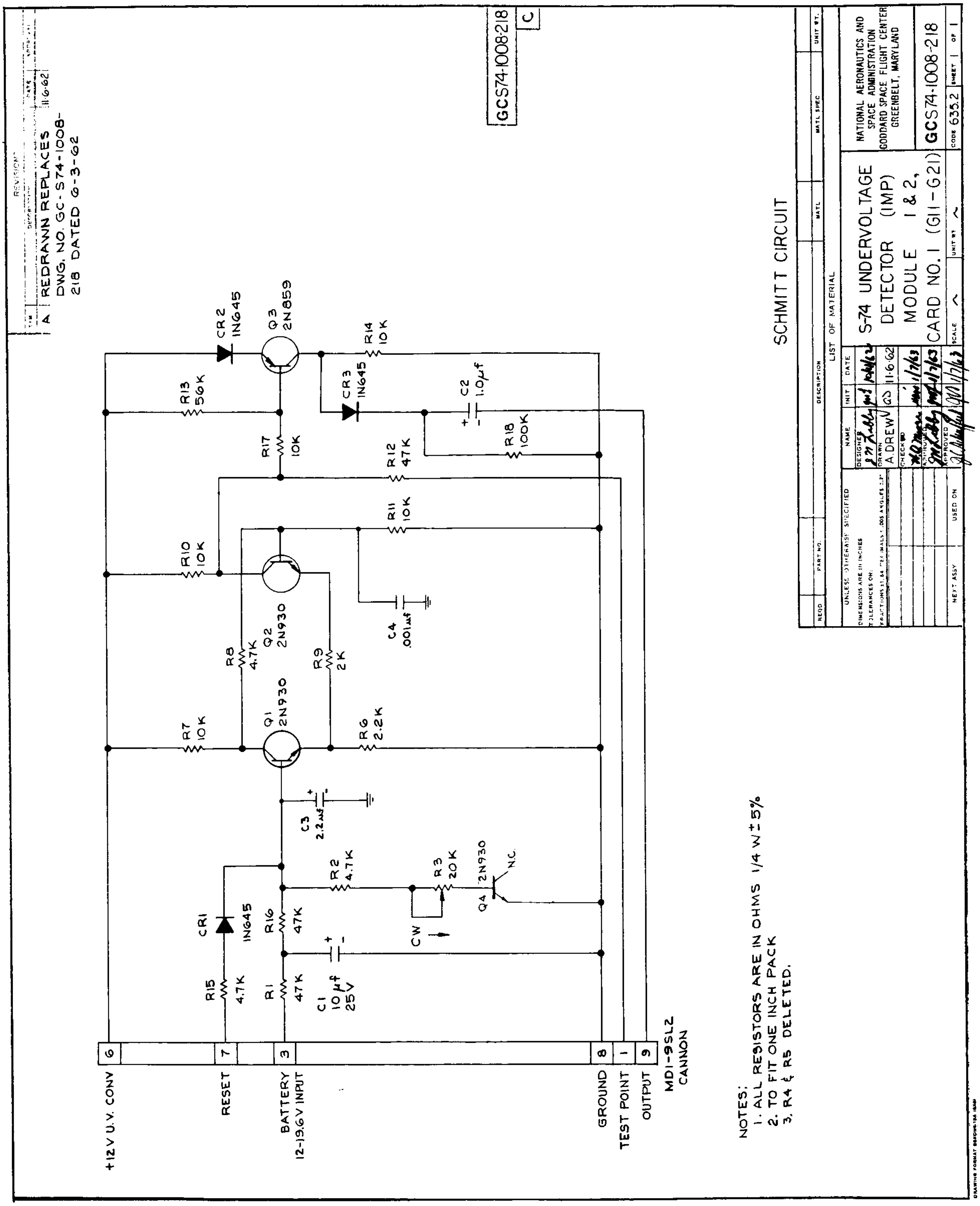
REVISIONS
A
REDRAWN REPLACES DWG. NO. GC-S74-1008-218 DATED 6-3-62
11-6-62
GCS74-1008-218
C
+12V U.V. CONV
RESET
BATTERY 12-19.6V INPUT
GROUND
TEST POINT
OUTPUT
MDI-9SL2 CANNON
R15 4.7K
CR1 1N645
R1 47K
R16 47K
C1 10 μf 25V
R2 4.7K
R3 20K
CW
Q4 2N930
N.C.
C3 2.2 μf
R7 10K
Q1 2N930
R6 2.2K
R8 4.7K
Q2 2N930
R9 2K
C4 .001 μf
R10 10K
R11 10K
R12 47K
R17 10K
R13 56K
CR2 1N645
Q3 2N859
R14 10K
CR3 1N645
C2 1.0 μf
R18 100K
NOTES:
1. ALL RESISTORS ARE IN OHMS 1/4 W ± 5%
2. TO FIT ONE INCH PACK
3. R4 & R5 DELETED.
SCHMITT CIRCUIT
LIST OF MATERIAL
ADREW
11-6-62
S-74 UNDERVOLTAGE DETECTOR (IMP) MODULE 1 & 2, CARD NO. 1 (G11-G21)
NATIONAL AERONAUTICS AND SPACE ADMINISTRATION
GODDARD SPACE FLIGHT CENTER
GREENBELT, MARYLAND
GCS74-1008-218
635.2

Figure 31

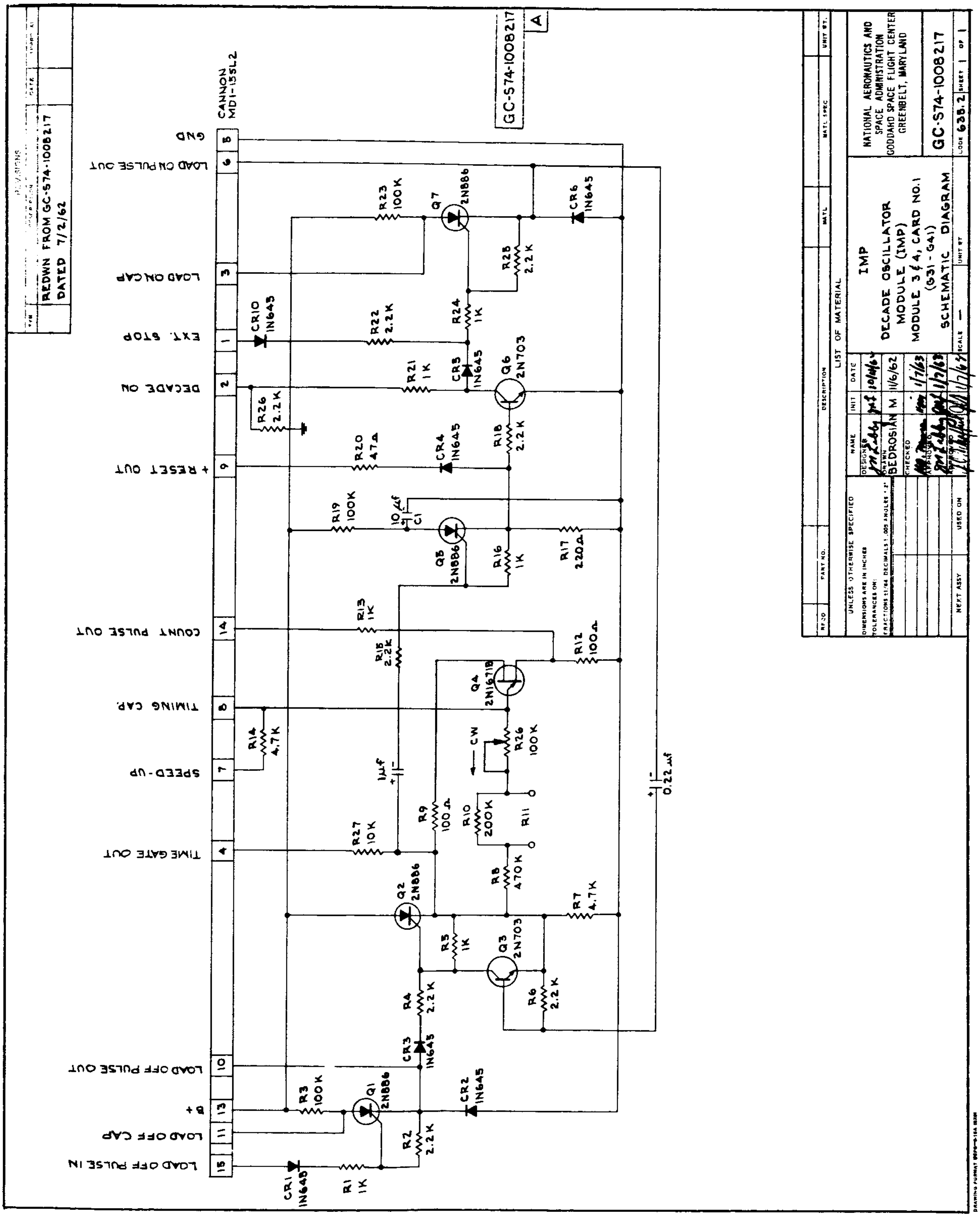
REDWN FROM GC-S74-1008217
DATED 7/2/62
CANNON MD1-15SL2
GC-S74-1008217
A
GND
LOAD ON PULSE OUT
LOAD ON CAP
EXT. STOP
DECADE ON
+RESET OUT
COUNT PULSE OUT
TIMING CAP.
SPEED-UP
TIME GATE OUT
LOAD OFF PULSE OUT
+B
LOAD OFF CAP
LOAD OFF PULSE IN
NATIONAL AERONAUTICS AND SPACE ADMINISTRATION
GODDARD SPACE FLIGHT CENTER
GREENBELT, MARYLAND
IMP
DECADE OSCILLATOR
MODULE (IMP)
MODULE 3 & 4, CARD NO. 1
(G31-G41)
SCHEMATIC DIAGRAM
GC-S74-1008217
BEDROSIAN
11/6/62

Figure 32

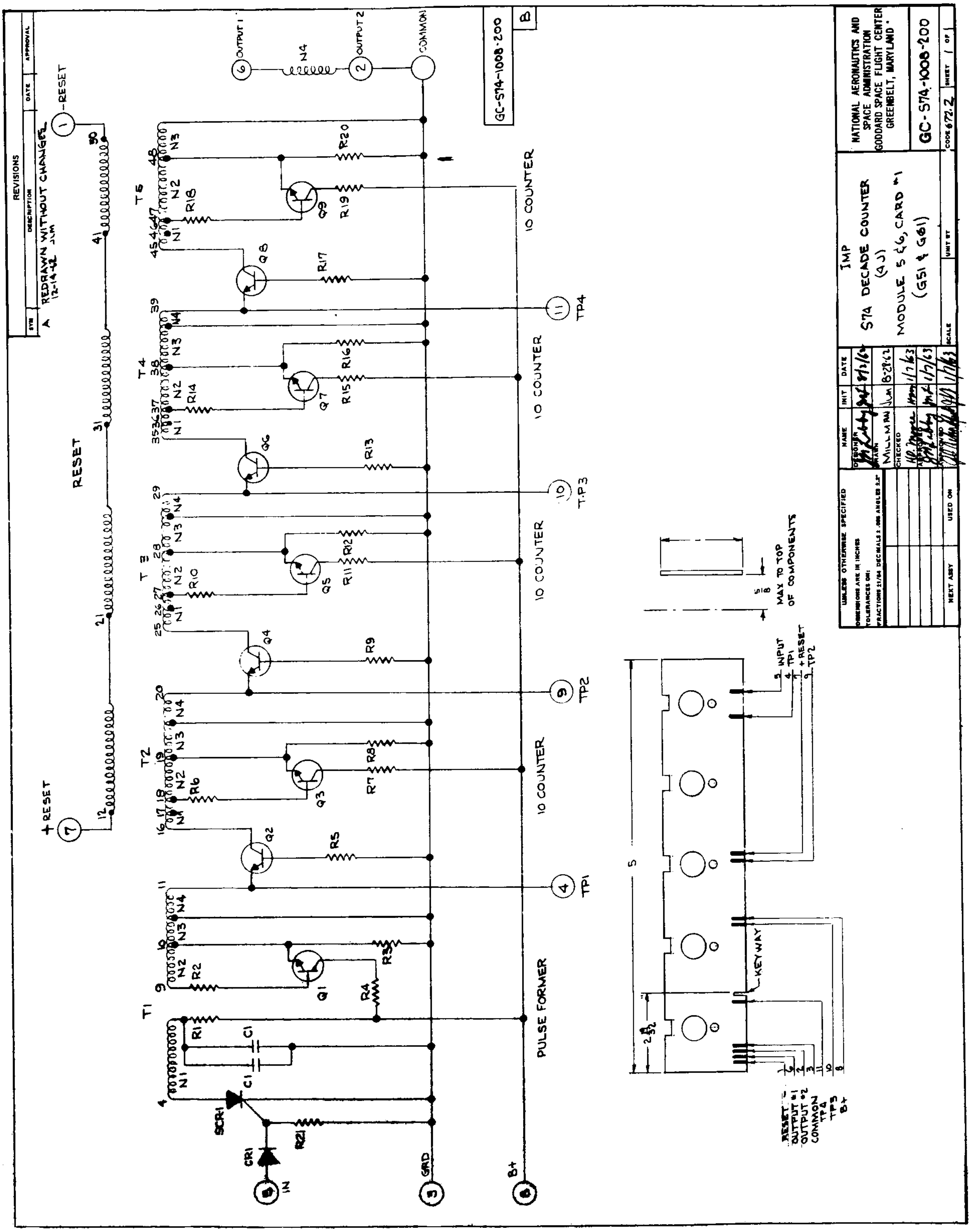

NATIONAL AERONAUTICS AND SPACE ADMINISTRATION
GODDARD SPACE FLIGHT CENTER
GREENBELT, MARYLAND
IMP
S7A DECADE COUNTER
(4J)
MODULE 5 & 6, CARD #1
(G51 & G61)
GC-574-1008-200
REVISIONS
REDRAWN WITHOUT CHANGES
PULSE FORMER
RESET
+RESET
-RESET
10 COUNTER
OUTPUT 1
OUTPUT 2
COMMON
KEYWAY
MAX TO TOP OF COMPONENTS

Figure 33

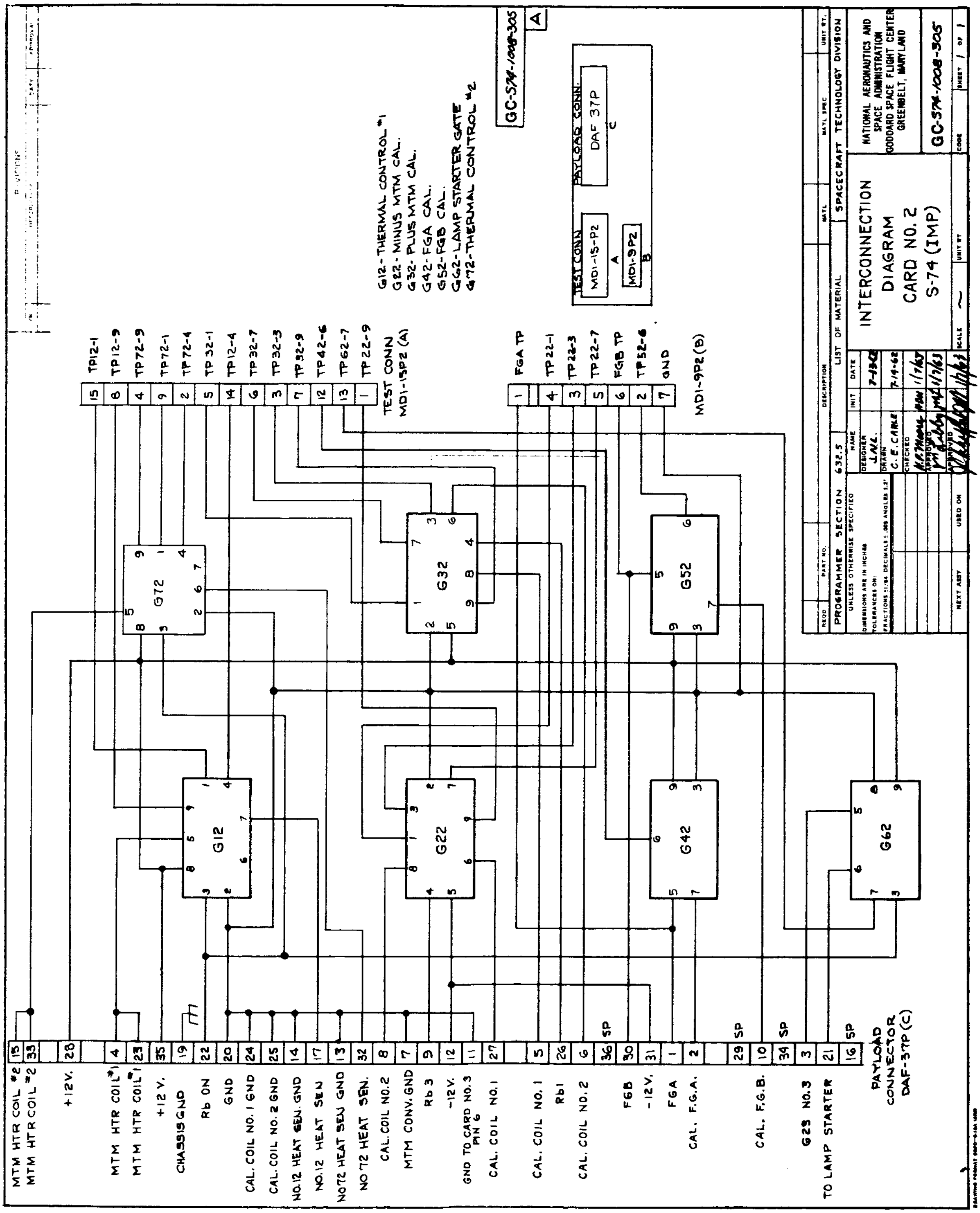
G12 - THERMAL CONTROL #1
G22 - MINUS MTM CAL.
G32 - PLUS MTM CAL.
G42 - FGA CAL.
G52 - FGB CAL.
G62 - LAMP STARTER GATE
G72 - THERMAL CONTROL #2
TEST CONN
MD1-15-P2
PAYLOAD CONN
DAF 37P
MD1-9P2
GC-S74-1008-305
TEST CONN MD1-15P2 (A)
MD1-9P2 (B)
PAYLOAD CONNECTOR DAF-37P (C)
MTM HTR COIL #2
+12V.
MTM CONV. GND
GND
TO LAMP STARTER
PROGRAMMER SECTION
SPACECRAFT TECHNOLOGY DIVISION
INTERCONNECTION DIAGRAM
CARD NO. 2
S-74 (IMP)
NATIONAL AERONAUTICS AND SPACE ADMINISTRATION
GODDARD SPACE FLIGHT CENTER
GREENBELT, MARYLAND

Figure 34

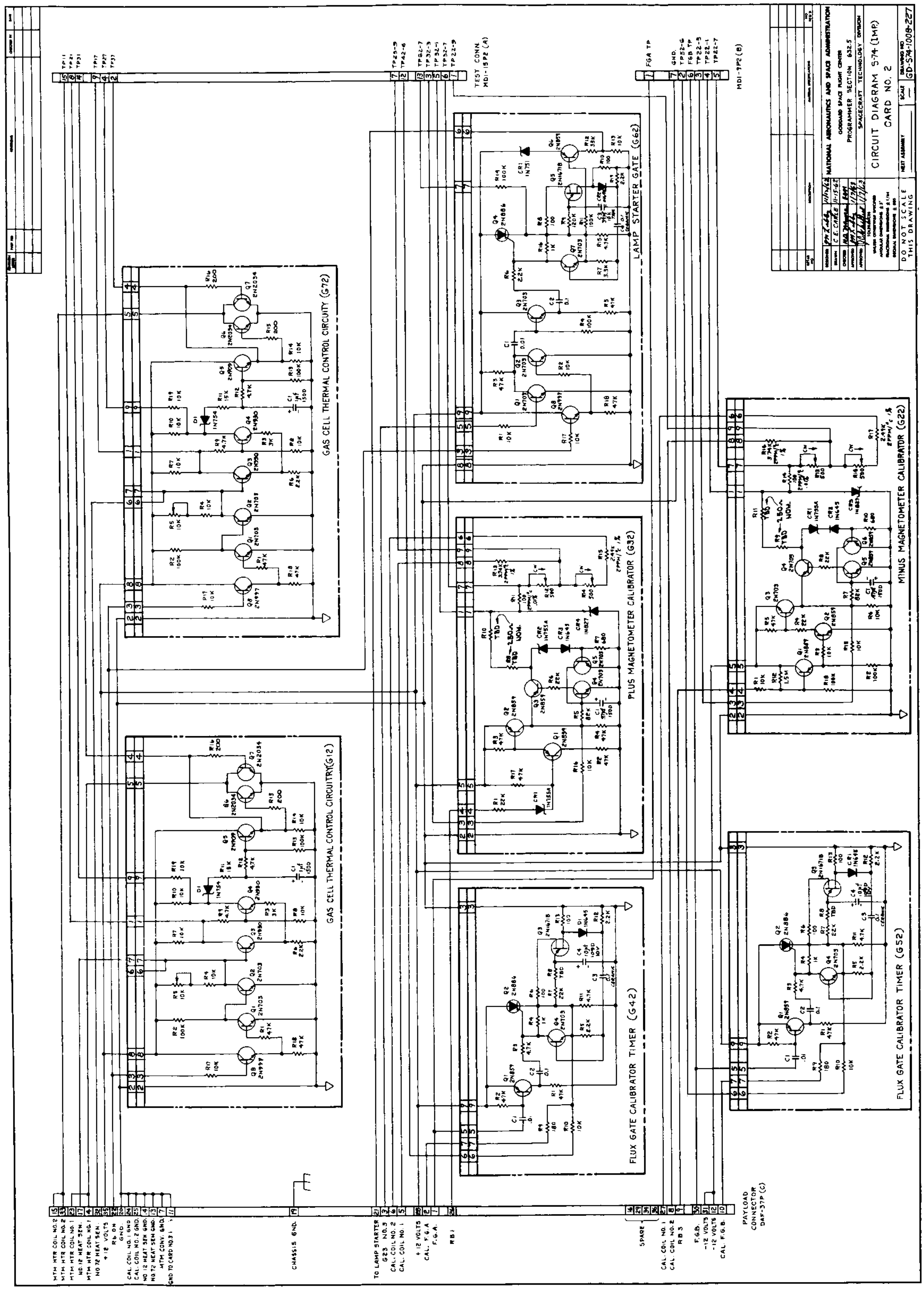
GAS CELL THERMAL CONTROL CIRCUITRY (G72)
GAS CELL THERMAL CONTROL CIRCUITRY (G12)
LAMP STARTER GATE (G62)
PLUS MAGNETOMETER CALIBRATOR (G32)
MINUS MAGNETOMETER CALIBRATOR (G22)
FLUX GATE CALIBRATOR TIMER (G42)
FLUX GATE CALIBRATOR TIMER (G52)
TEST CONN MDI-15P2 (A)
MDI-9P2 (B)
PAYLOAD CONNECTOR DAF-37P (C)
CIRCUIT DIAGRAM S-74 (IMP) CARD NO. 2
DO NOT SCALE THIS DRAWING
CHASSIS GND.

Figure 35

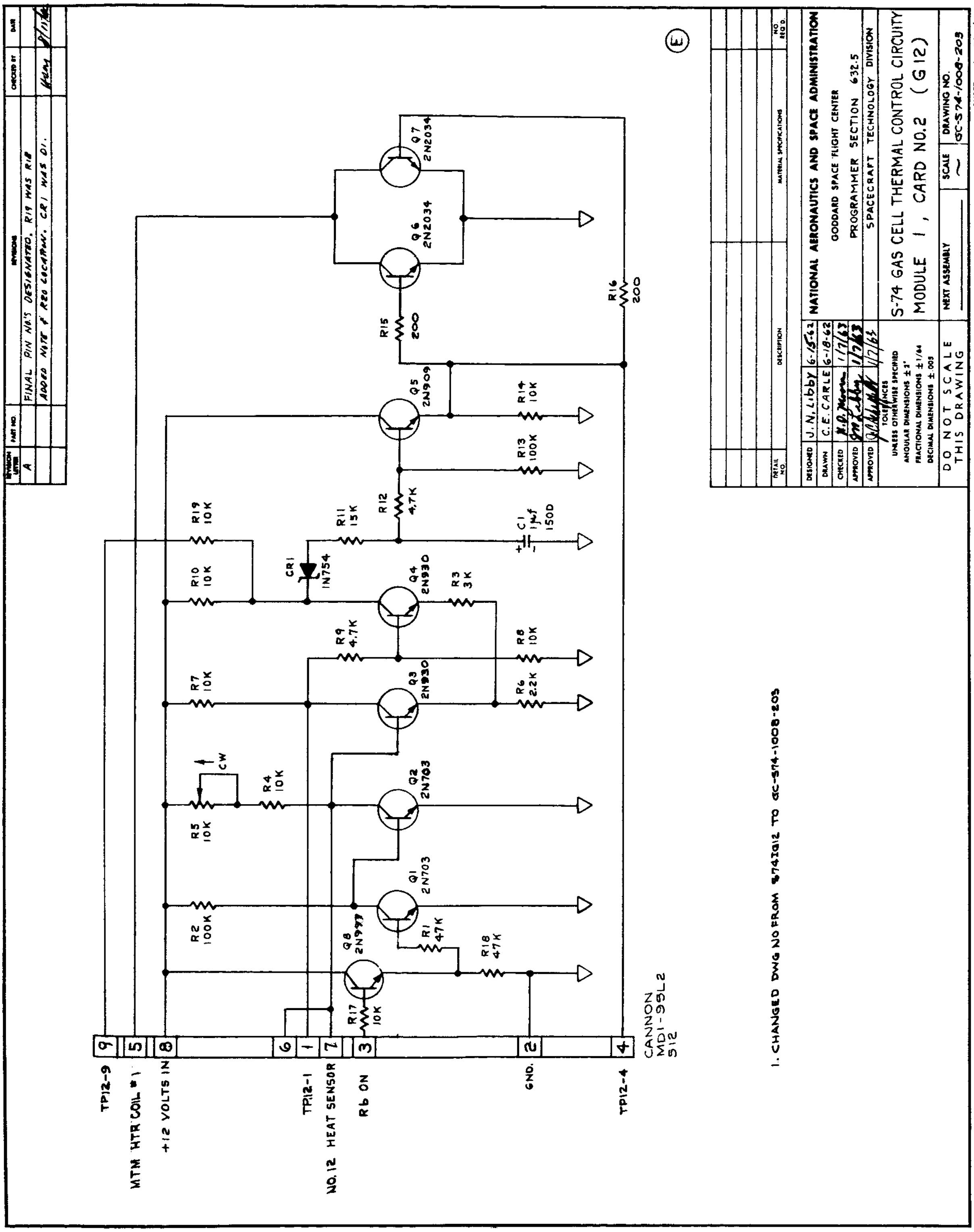

NATIONAL AERONAUTICS AND SPACE ADMINISTRATION
GODDARD SPACE FLIGHT CENTER
PROGRAMMER SECTION 632.5
SPACECRAFT TECHNOLOGY DIVISION
S-74 GAS CELL THERMAL CONTROL CIRCUITY
MODULE 1, CARD NO.2 (G12)
DESIGNED J. N. Libby 6-15-62
DRAWN C. E. CARLE 6-18-62
DO NOT SCALE THIS DRAWING
SHEET 1 OF 1
FINAL PIN NO'S DESIGNATED. R19 WAS R18
ADDED NOTE & REO LOCATION. CR1 WAS D1.
1. CHANGED DWG NO FROM S74G12 TO GC-574-1008-205
CANNON MD1-99L2 S12
TP12-9
MTM HTR COIL #1
+12 VOLTS IN
TP12-1
NO.12 HEAT SENSOR
Rb ON
GND.
TP12-4
Q1 2N703
Q2 2N703
Q3 2N930
Q4 2N930
Q5 2N909
Q6 2N2034
Q7 2N2034
Q8 2N997
CR1 1N754
C1 1μf 150D
R1 47K
R2 100K
R3 3K
R4 10K
R5 10K
R6 2.2K
R7 10K
R8 10K
R9 4.7K
R10 10K
R11 15K
R12 4.7K
R13 100K
R14 10K
R15 200
R16 200
R17 10K
R18 47K
R19 10K
CW

Figure 36

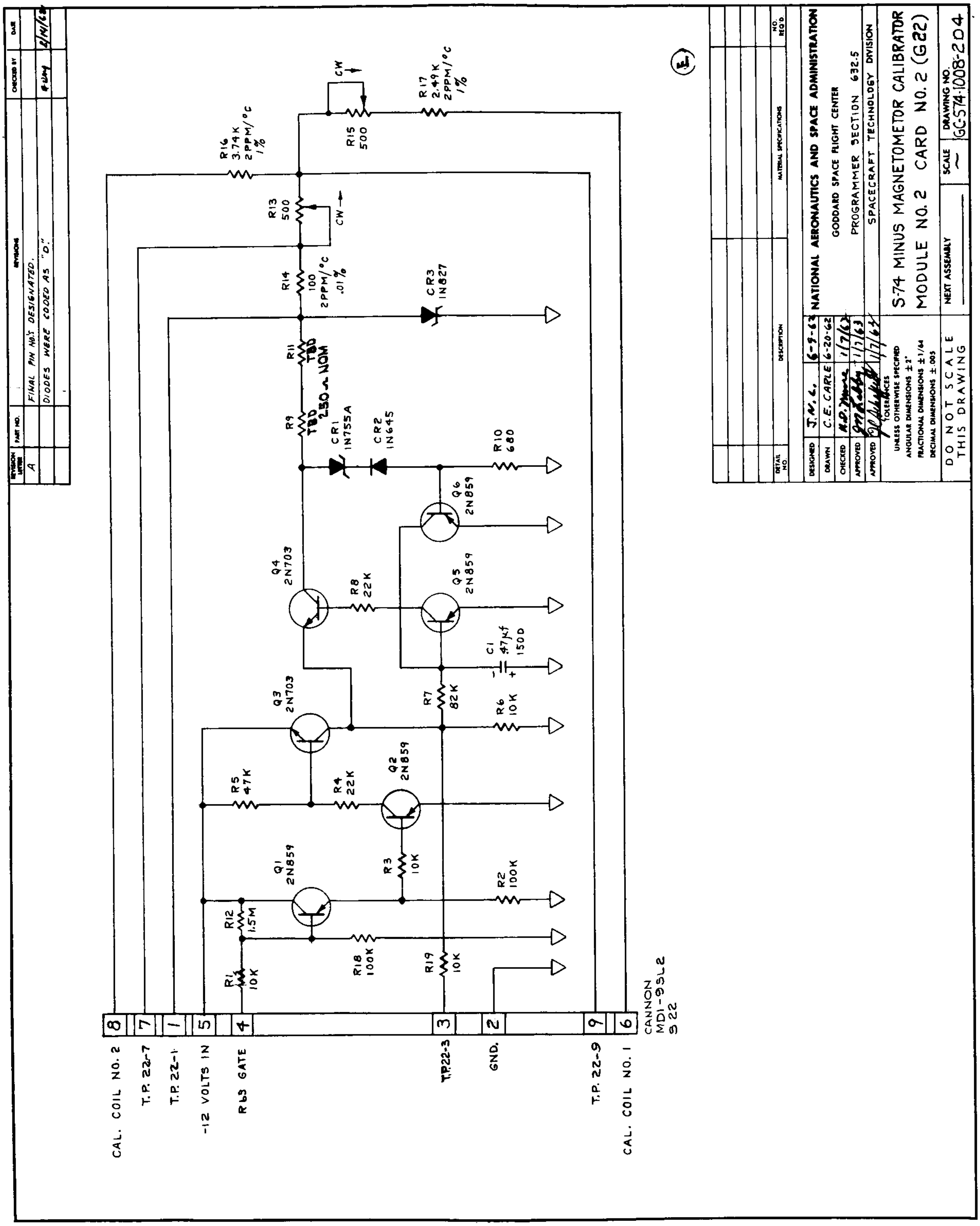
NATIONAL AERONAUTICS AND SPACE ADMINISTRATION
GODDARD SPACE FLIGHT CENTER
PROGRAMMER SECTION 632.5
SPACECRAFT TECHNOLOGY DIVISION
S-74 MINUS MAGNETOMETER CALIBRATOR
MODULE NO. 2 CARD NO. 2 (G22)
DO NOT SCALE THIS DRAWING
CAL. COIL NO. 2
T.P. 22-7
T.P. 22-1
-12 VOLTS IN
GND.
T.P. 22-9
CAL. COIL NO. 1
CANNON MD1-9SL2

Figure 37

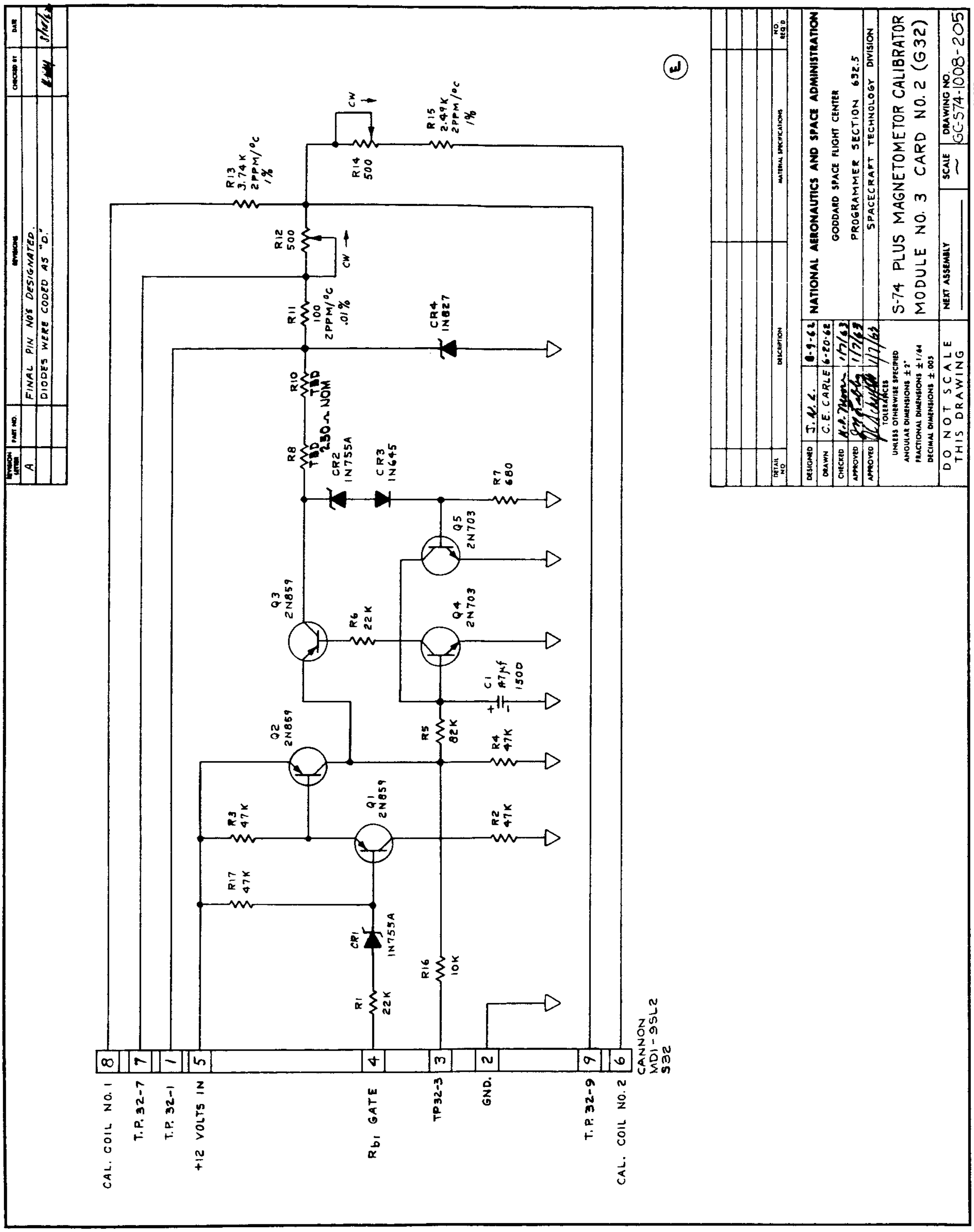
NATIONAL AERONAUTICS AND SPACE ADMINISTRATION
GODDARD SPACE FLIGHT CENTER
PROGRAMMER SECTION 632.5
SPACECRAFT TECHNOLOGY DIVISION
S-74 PLUS MAGNETOMETER CALIBRATOR
MODULE NO. 3 CARD NO. 2 (G32)
DRAWING NO. GC-574-1008-205
DO NOT SCALE THIS DRAWING
FINAL PIN NO'S DESIGNATED.
DIODES WERE CODED AS "D."
CAL. COIL NO. 1
T.P. 32-7
T.P. 32-1
+12 VOLTS IN
R_{b1} GATE
TP32-3
GND.
T.P. 32-9
CAL. COIL NO. 2
CANNON MDI-9SL2 S32

Figure 38

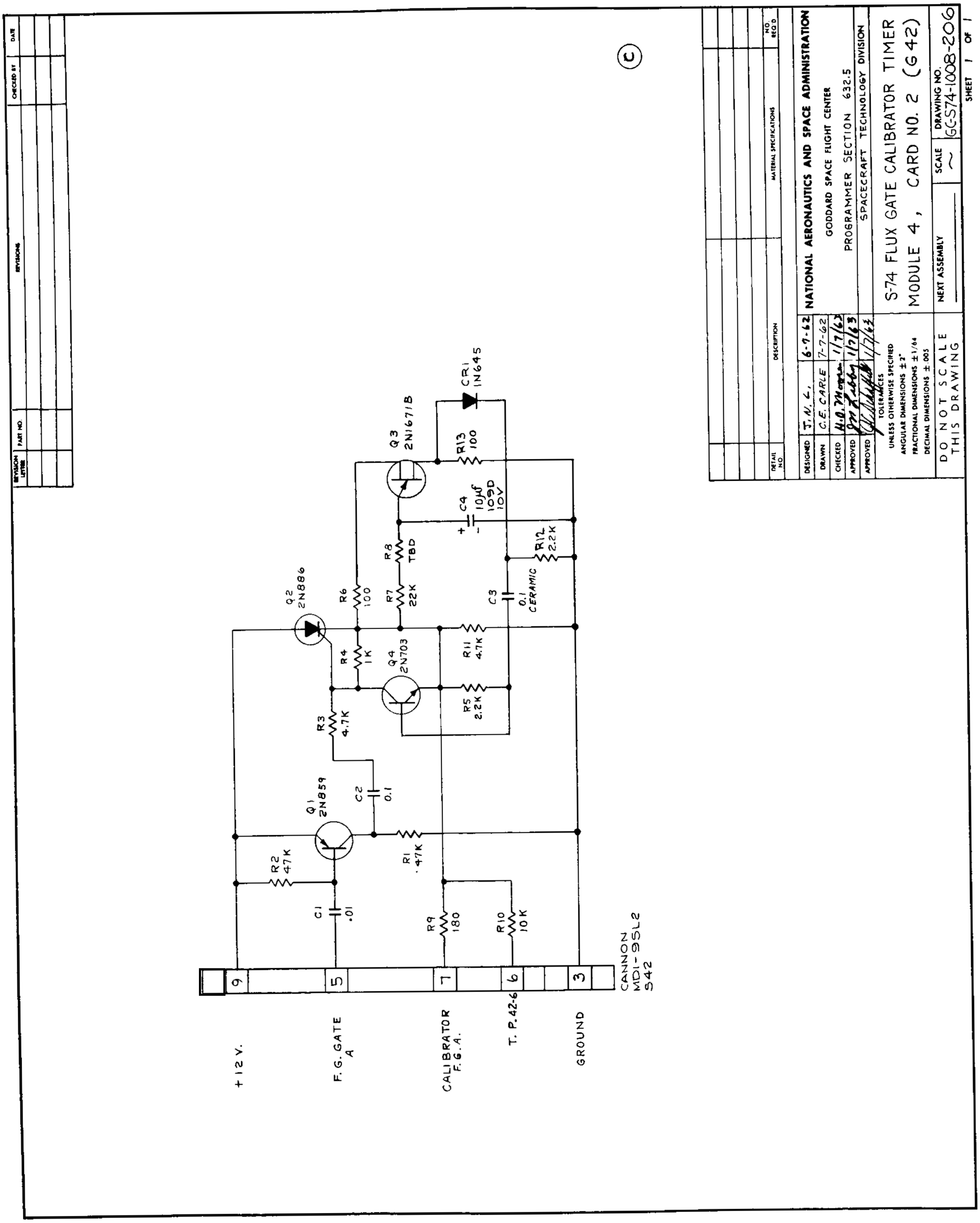
NATIONAL AERONAUTICS AND SPACE ADMINISTRATION
GODDARD SPACE FLIGHT CENTER
PROGRAMMER SECTION 632.5
SPACECRAFT TECHNOLOGY DIVISION
S-74 FLUX GATE CALIBRATOR TIMER
MODULE 4, CARD NO. 2 (G42)
DRAWING NO. GC-S74-1008-206
SHEET 1 OF 1
DO NOT SCALE THIS DRAWING
DESIGNED J. N. L. 6-7-62
DRAWN C.E. CARLE 7-7-62
+12 V.
F. G. GATE A
CALIBRATOR F. G. A.
T. P. 42-6
GROUND
CANNON MDI-9SL2 S42
Q1 2N859
Q2 2N886
Q3 2N1671B
Q4 2N703
CR1 1N645
C1 .01
C2 0.1
C3 0.1 CERAMIC
C4 10µf 109D 10V
R1 47K
R2 47K
R3 4.7K
R4 1K
R5 2.2K
R6 100
R7 22K
R8 TBD
R9 180
R10 10K
R11 4.7K
R12 2.2K
R13 100

Figure 39

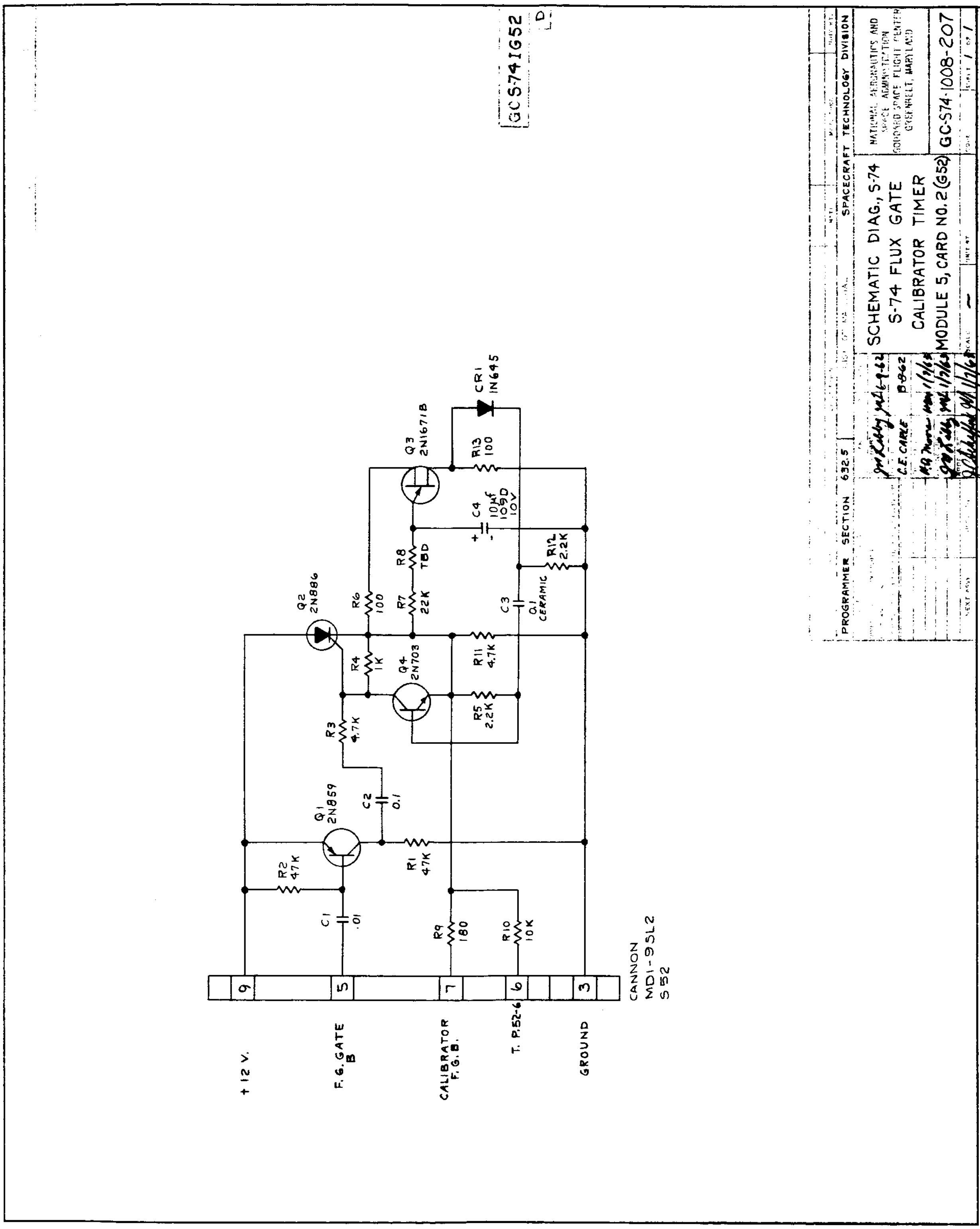
GC-S74-IG52
SCHEMATIC DIAG., S-74
S-74 FLUX GATE
CALIBRATOR TIMER
MODULE 5, CARD NO. 2 (G52)
GC-S74-1008-207
SPACECRAFT TECHNOLOGY DIVISION
PROGRAMMER SECTION 632.5
NATIONAL AERONAUTICS AND SPACE ADMINISTRATION
GODDARD SPACE FLIGHT CENTER
GREENBELT, MARYLAND
+12 V.
F. G. GATE B
CALIBRATOR F.G.B.
T. P.52-6
GROUND
CANNON
MDI-9SL2
S52
Q1 2N859
Q2 2N886
Q3 2N1671B
Q4 2N703
CR1 IN645
R1 47K
R2 47K
R3 4.7K
R4 1K
R5 2.2K
R6 100
R7 22K
R8 TBD
R9 180
R10 10K
R11 4.7K
R12 2.2K
R13 100
C1 .01
C2 0.1
C3 0.1 CERAMIC
C4 10μf 109D 10V

Figure 40

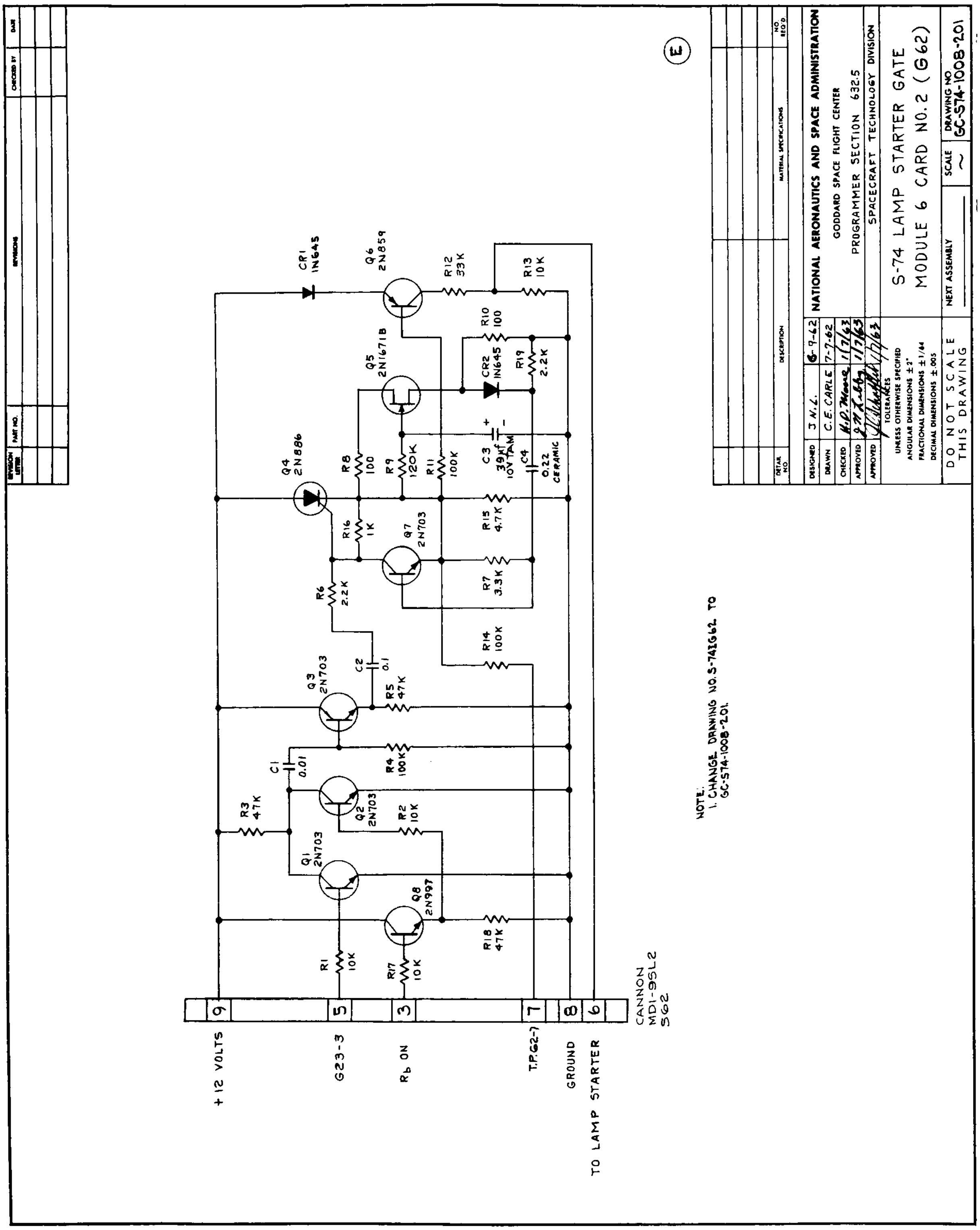
NATIONAL AERONAUTICS AND SPACE ADMINISTRATION
GODDARD SPACE FLIGHT CENTER
PROGRAMMER SECTION 632.5
SPACECRAFT TECHNOLOGY DIVISION
S-74 LAMP STARTER GATE
MODULE 6 CARD NO. 2 (G62)
DRAWING NO GC-S74-1008-201
DO NOT SCALE THIS DRAWING
+12 VOLTS
G23-3
Rb ON
T.P.G2-7
GROUND
TO LAMP STARTER
CANNON MDI-9SL2 SG2
NOTE:
1. CHANGE DRAWING NO. S-74IG62 TO GC-S74-1008-201.
Q1 2N703
Q2 2N703
Q3 2N703
Q4 2N886
Q5 2N1671B
Q6 2N859
Q7 2N703
Q8 2N997
CR1 1N645
CR2 1N645
C1 0.01
C2 0.1
C3 39μf 10V TAM
C4 0.22 CERAMIC

Figure 41

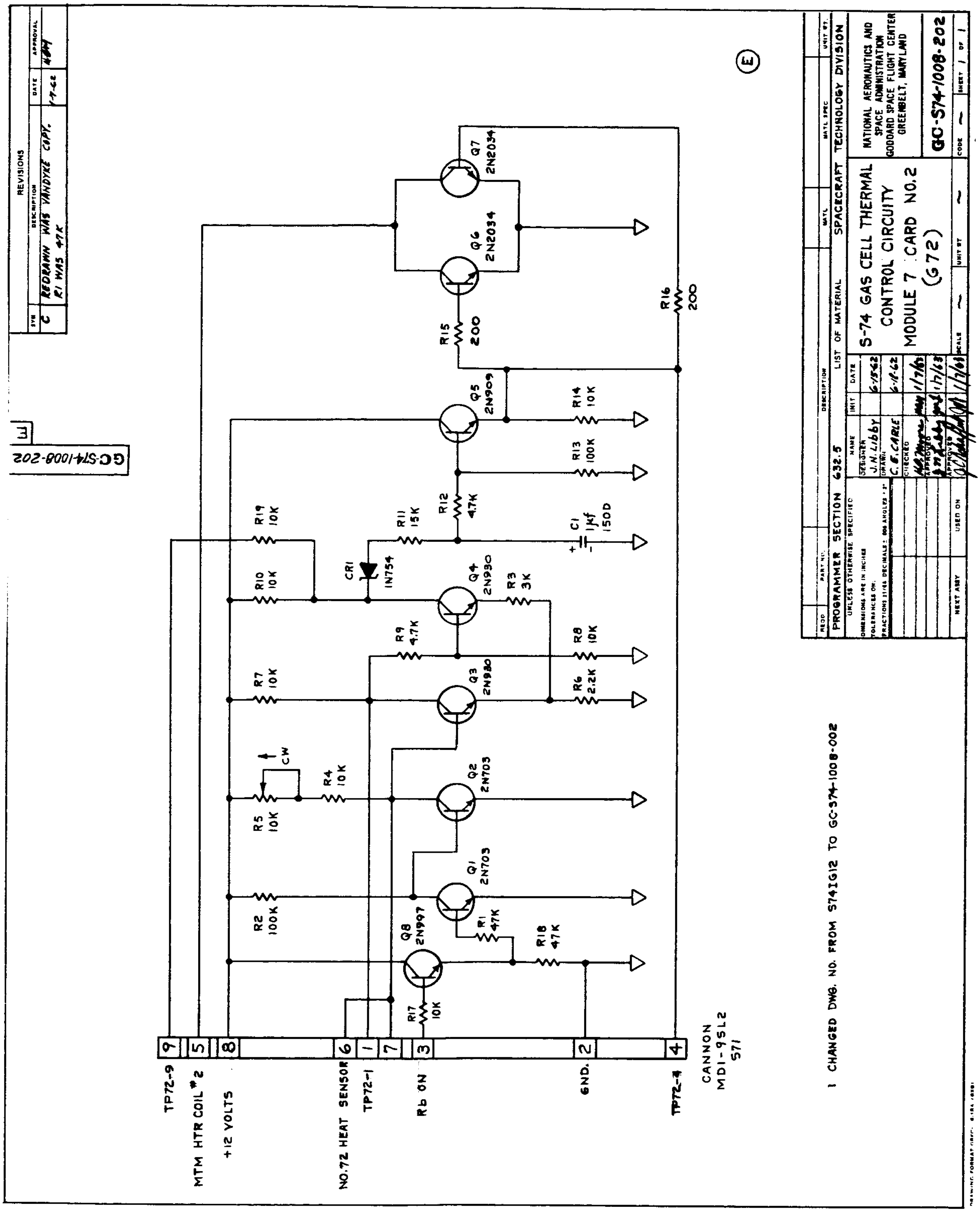

S-74 GAS CELL THERMAL
CONTROL CIRCUITY
MODULE 7 CARD NO.2
(G72)
SPACECRAFT TECHNOLOGY DIVISION
NATIONAL AERONAUTICS AND SPACE ADMINISTRATION GODDARD SPACE FLIGHT CENTER GREENBELT, MARYLAND
GC-S74-1008-202
PROGRAMMER SECTION 632.5
1 CHANGED DWG. NO. FROM S741G12 TO GC-S74-1008-002
CANNON MDI-9SL2 571
TP72-9
MTM HTR COIL #2
+12 VOLTS
NO.72 HEAT SENSOR
TP72-1
Rb ON
GND.
TP72-4

Figure 42

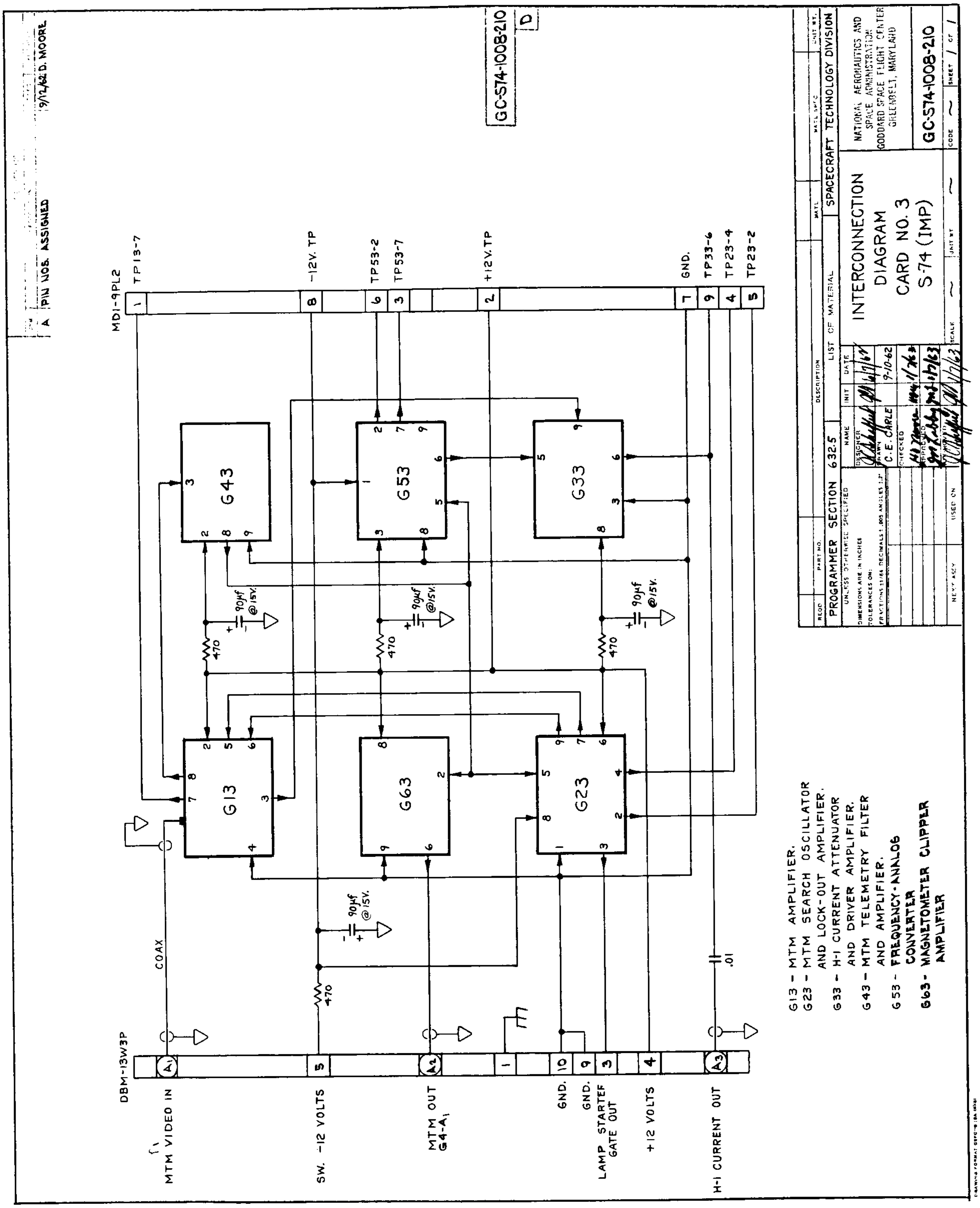
INTERCONNECTION DIAGRAM CARD NO. 3 S-74 (IMP)
GC-S74-1008-210
SPACECRAFT TECHNOLOGY DIVISION
NATIONAL AERONAUTICS AND SPACE ADMINISTRATION GODDARD SPACE FLIGHT CENTER GREENBELT, MARYLAND
PROGRAMMER SECTION 632.5
C.E. CARLE 9-10-62
PIN NOS. ASSIGNED
9/12/62 D. MOORE
MDI-9PL2
DBM-13W3P
TP13-7
-12V. TP
TP53-2
TP53-7
+12V. TP
GND.
TP33-6
TP23-4
TP23-2
MTM VIDEO IN
SW. -12 VOLTS
MTM OUT G4-A1
GND.
GND.
LAMP STARTER GATE OUT
+12 VOLTS
H-I CURRENT OUT
COAX
G13
G23
G33
G43
G53
G63
90µf @15V.
470
.01
G13 - MTM AMPLIFIER.
G23 - MTM SEARCH OSCILLATOR AND LOCK-OUT AMPLIFIER.
G33 - H-I CURRENT ATTENUATOR AND DRIVER AMPLIFIER.
G43 - MTM TELEMETRY FILTER AND AMPLIFIER.
G53 - FREQUENCY-ANALOG CONVERTER
G63 - MAGNETOMETER CLIPPER AMPLIFIER

Figure 43

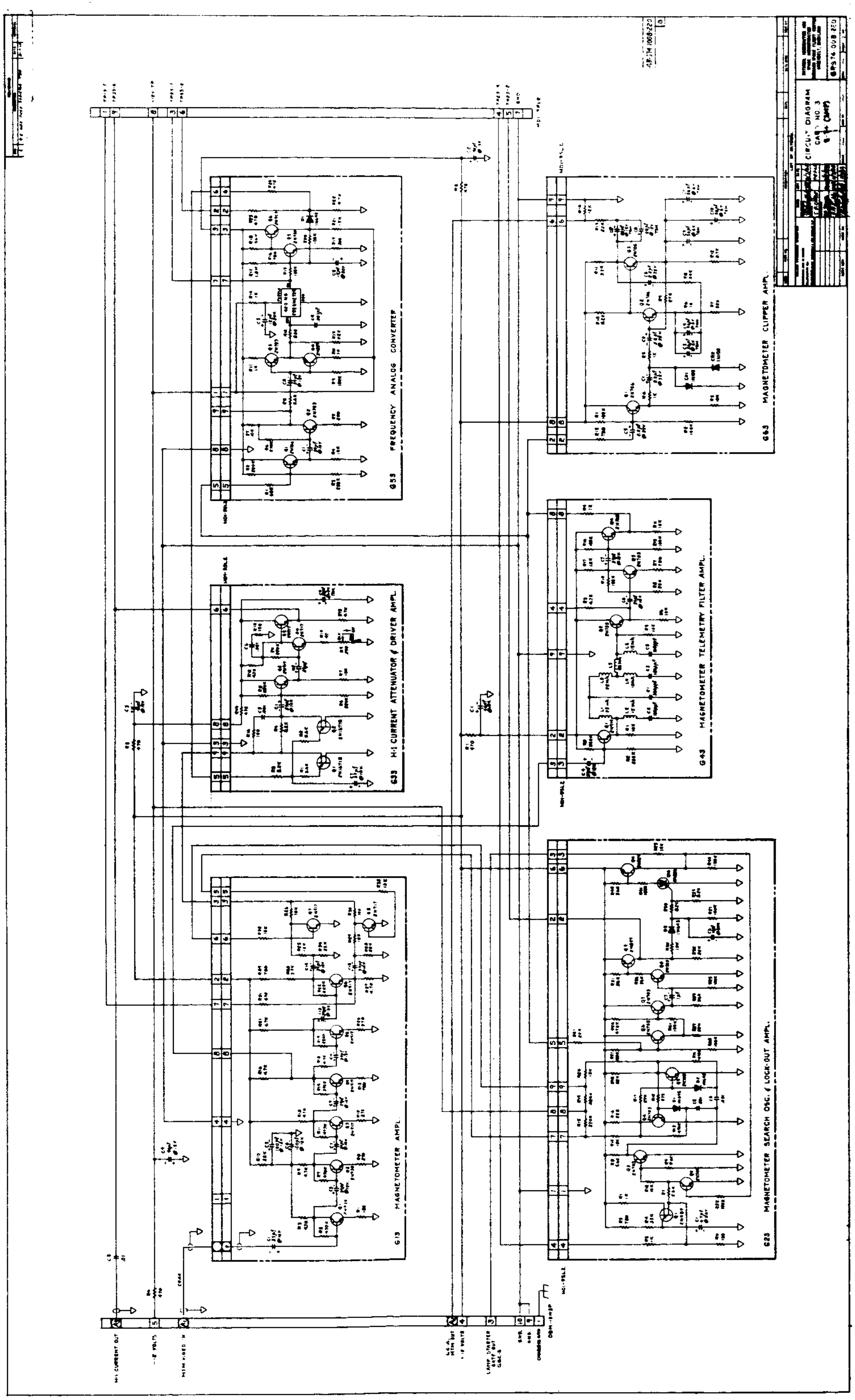

Figure 44

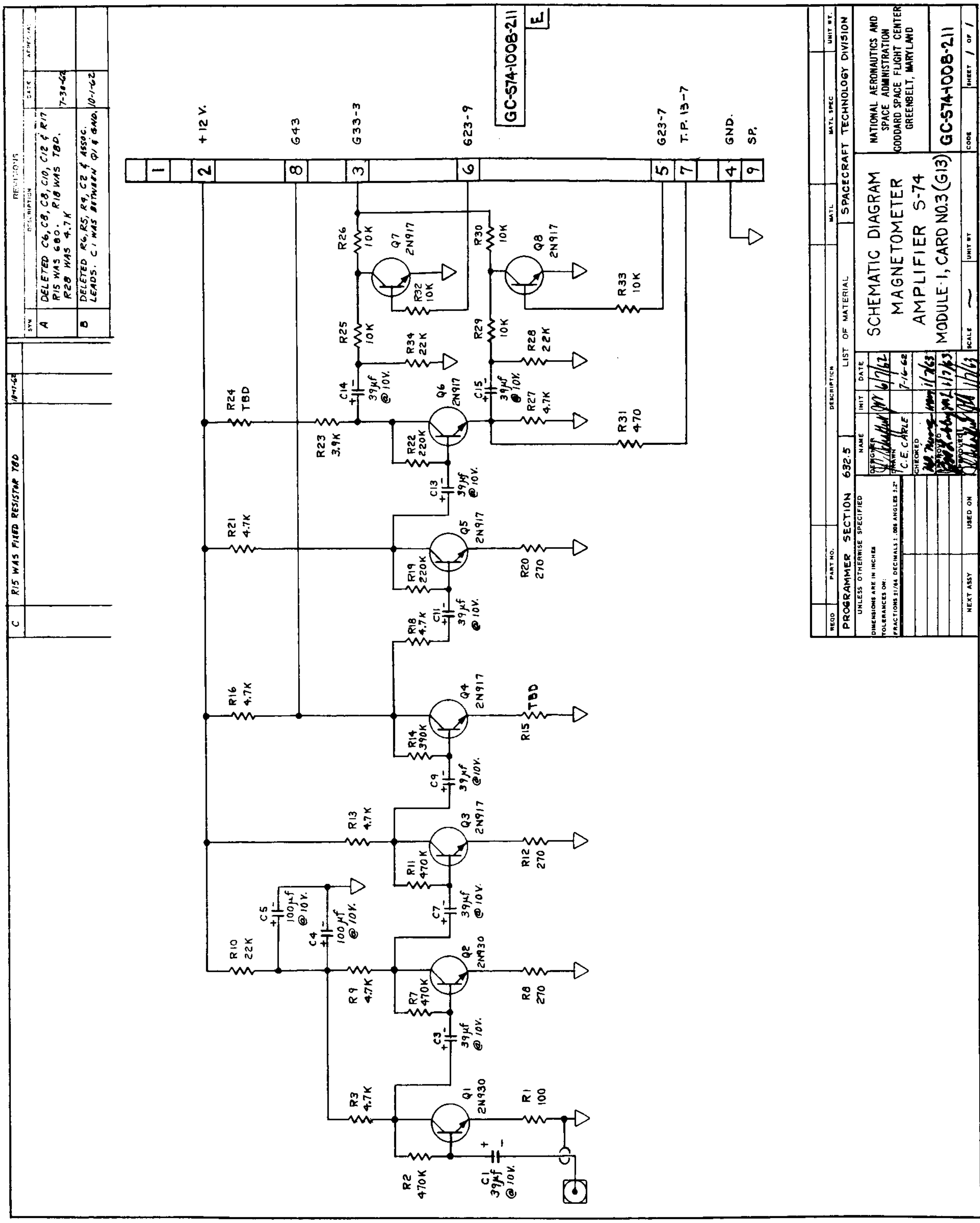
GC-574-1008-211
SCHEMATIC DIAGRAM
MAGNETOMETER
AMPLIFIER S-74
MODULE·1, CARD NO.3 (G13)
NATIONAL AERONAUTICS AND SPACE ADMINISTRATION
GODDARD SPACE FLIGHT CENTER
GREENBELT, MARYLAND
SPACECRAFT TECHNOLOGY DIVISION
PROGRAMMER SECTION 632.5
C.E. CAPLE
+12 V.
G43
G33-3
G23-9
G23-7
T.P. 13-7
GND.
SP.

Figure 45

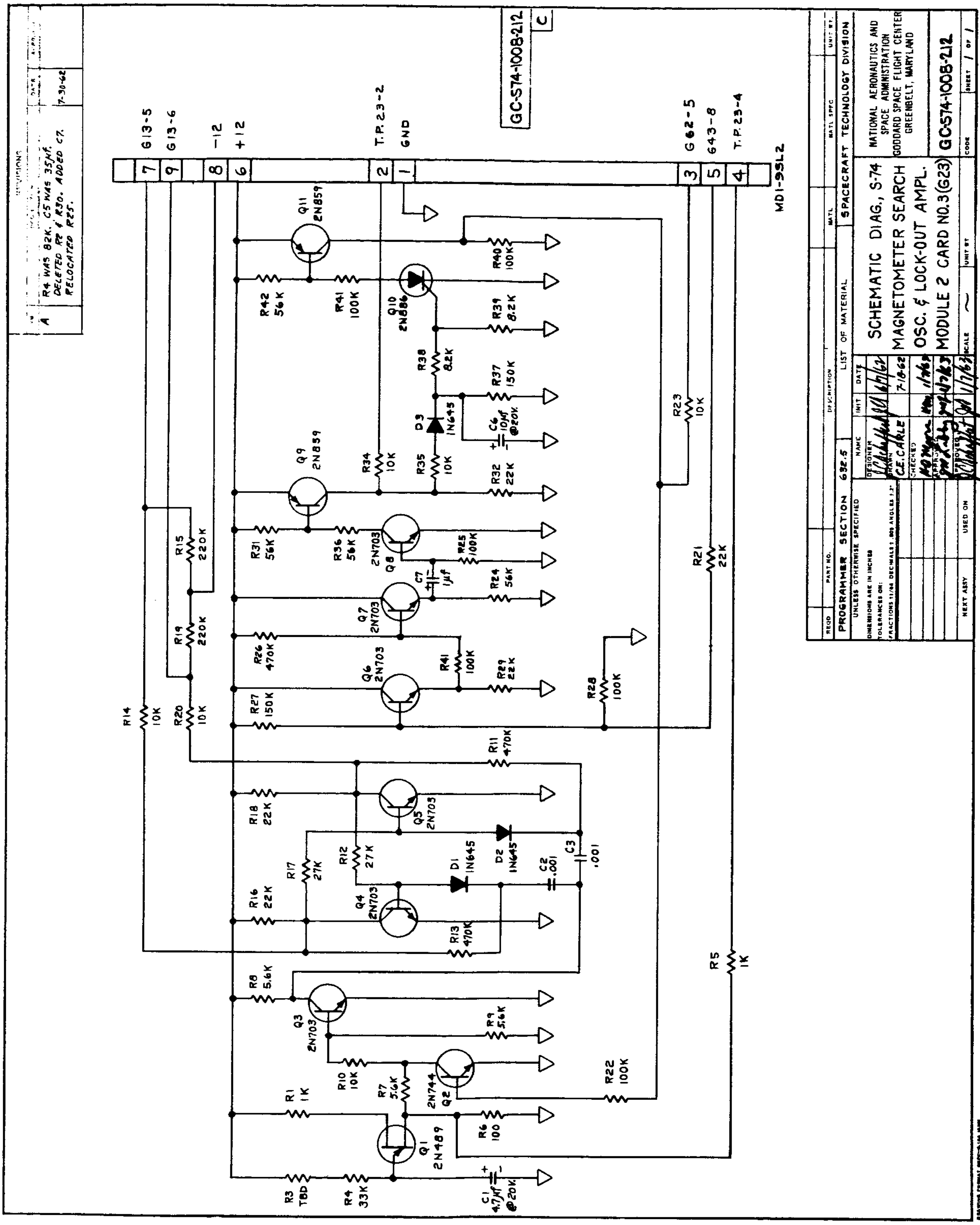
GC-S74-1008-212
SCHEMATIC DIAG., S-74
MAGNETOMETER SEARCH
OSC. & LOCK-OUT AMPL.
MODULE 2 CARD NO.3 (G23)
NATIONAL AERONAUTICS AND SPACE ADMINISTRATION
GODDARD SPACE FLIGHT CENTER
GREENBELT, MARYLAND
SPACECRAFT TECHNOLOGY DIVISION
MD1-95L2

Figure 46

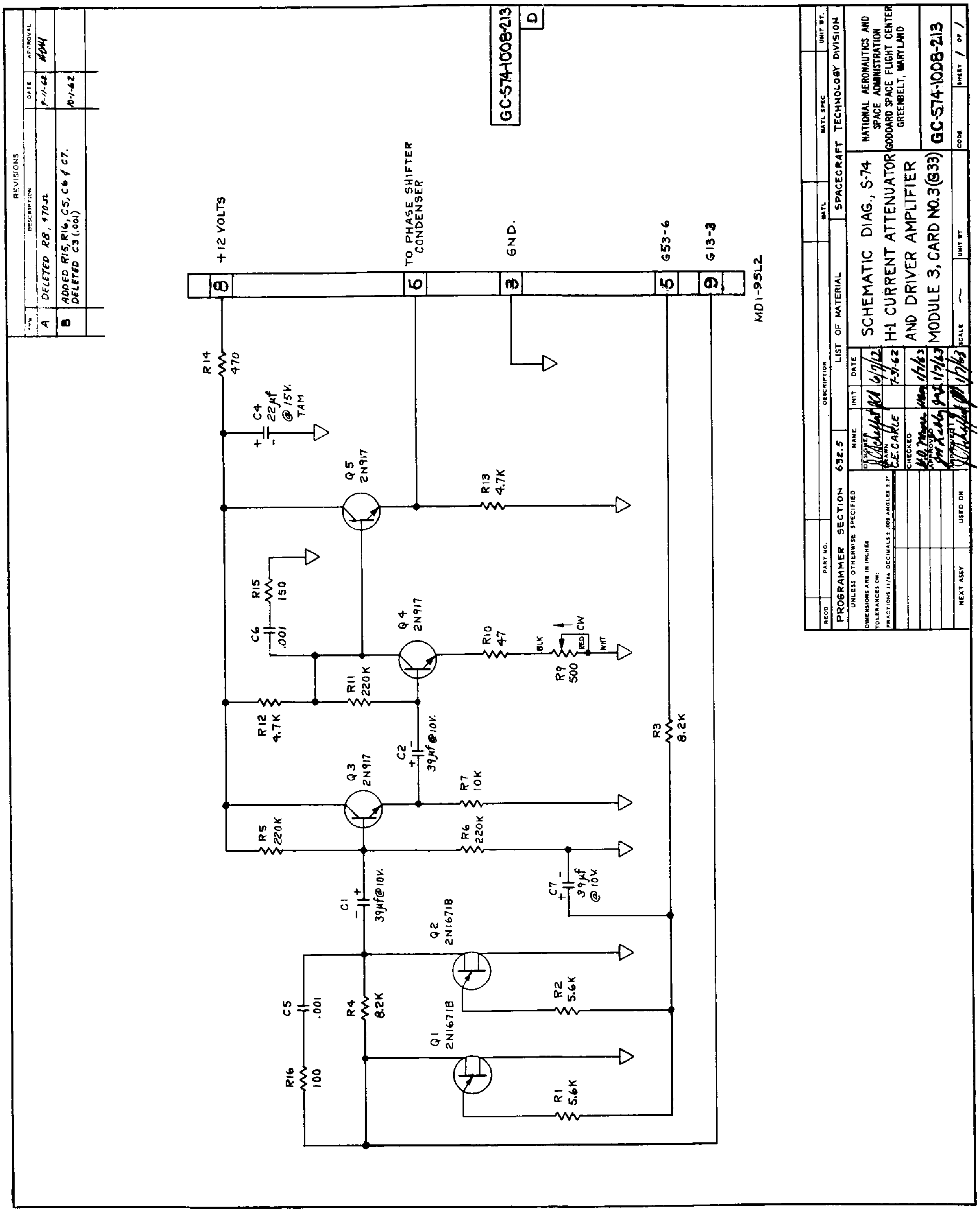
REVISIONS
A DELETED R8, 470Ω
B ADDED R15, R16, C5, C6 & C7. DELETED C3 (.001)
GC-574-1008-213
D
+12 VOLTS
TO PHASE SHIFTER CONDENSER
GND.
G53-6
G13-3
MD1-95L2
R14 470
C4 22µf @15V. TAM
Q5 2N917
R13 4.7K
R15 150
C6 .001
Q4 2N917
R10 47
R9 500
CW
R11 220K
R12 4.7K
C2 39µf @10V.
Q3 2N917
R7 10K
R5 220K
R6 220K
R3 8.2K
C1 39µf @10V.
C7 39µf @10V.
Q2 2N1671B
C5 .001
R4 8.2K
R2 5.6K
Q1 2N1671B
R16 100
R1 5.6K
SPACECRAFT TECHNOLOGY DIVISION
PROGRAMMER SECTION 632.5
SCHEMATIC DIAG., S-74
H-1 CURRENT ATTENUATOR AND DRIVER AMPLIFIER
MODULE 3, CARD NO.3 (S33)
NATIONAL AERONAUTICS AND SPACE ADMINISTRATION
GODDARD SPACE FLIGHT CENTER
GREENBELT, MARYLAND
GC-574-1008-213

Figure 47

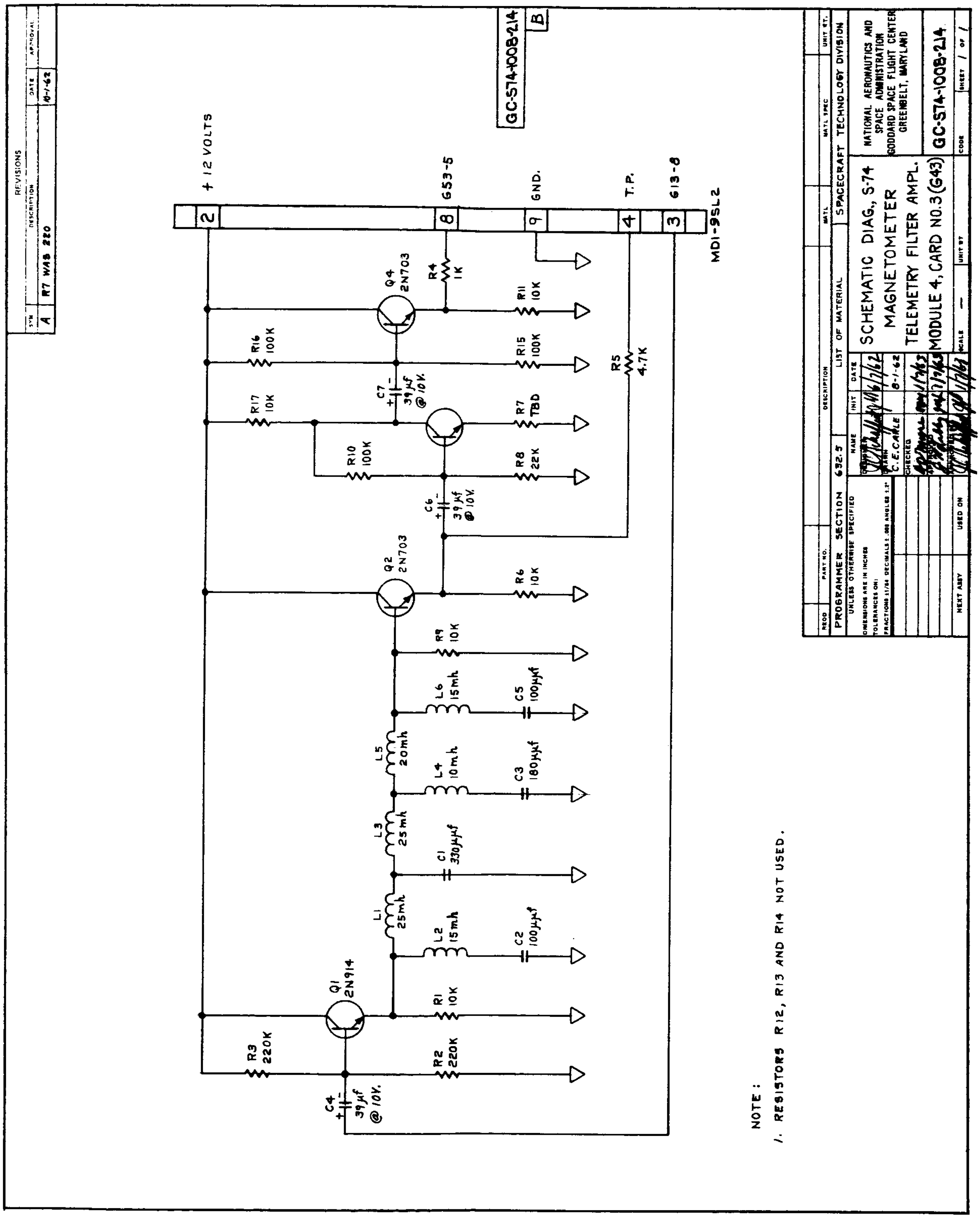
GC-S74-1008-214
REVISIONS
A R7 WAS 220 10-1-62
+12 VOLTS
G53-5
GND.
T.P.
G13-8
MDI-9SL2
Q1 2N914
Q2 2N703
Q4 2N703
R1 10K
R2 220K
R3 220K
R4 1K
R5 4.7K
R6 10K
R7 TBD
R8 22K
R9 10K
R10 100K
R11 10K
R15 100K
R16 100K
R17 10K
L1 25mh
L2 15mh
L3 25mh
L4 10mh
L5 20mh
L6 15mh
C1 330μμf
C2 100μμf
C3 180μμf
C5 100μμf
C4 39μf @10V.
C6 39μf @10V.
C7 39μf @10V.
NOTE:
1. RESISTORS R12, R13 AND R14 NOT USED.
PROGRAMMER SECTION 632.5
SPACECRAFT TECHNOLOGY DIVISION
SCHEMATIC DIAG., S-74 MAGNETOMETER TELEMETRY FILTER AMPL. MODULE 4, CARD NO.3 (G43)
NATIONAL AERONAUTICS AND SPACE ADMINISTRATION GODDARD SPACE FLIGHT CENTER GREENBELT, MARYLAND
C. E. CARLE 8-1-62
GC-S74-1008-214
SHEET 1 OF 1

Figure 48

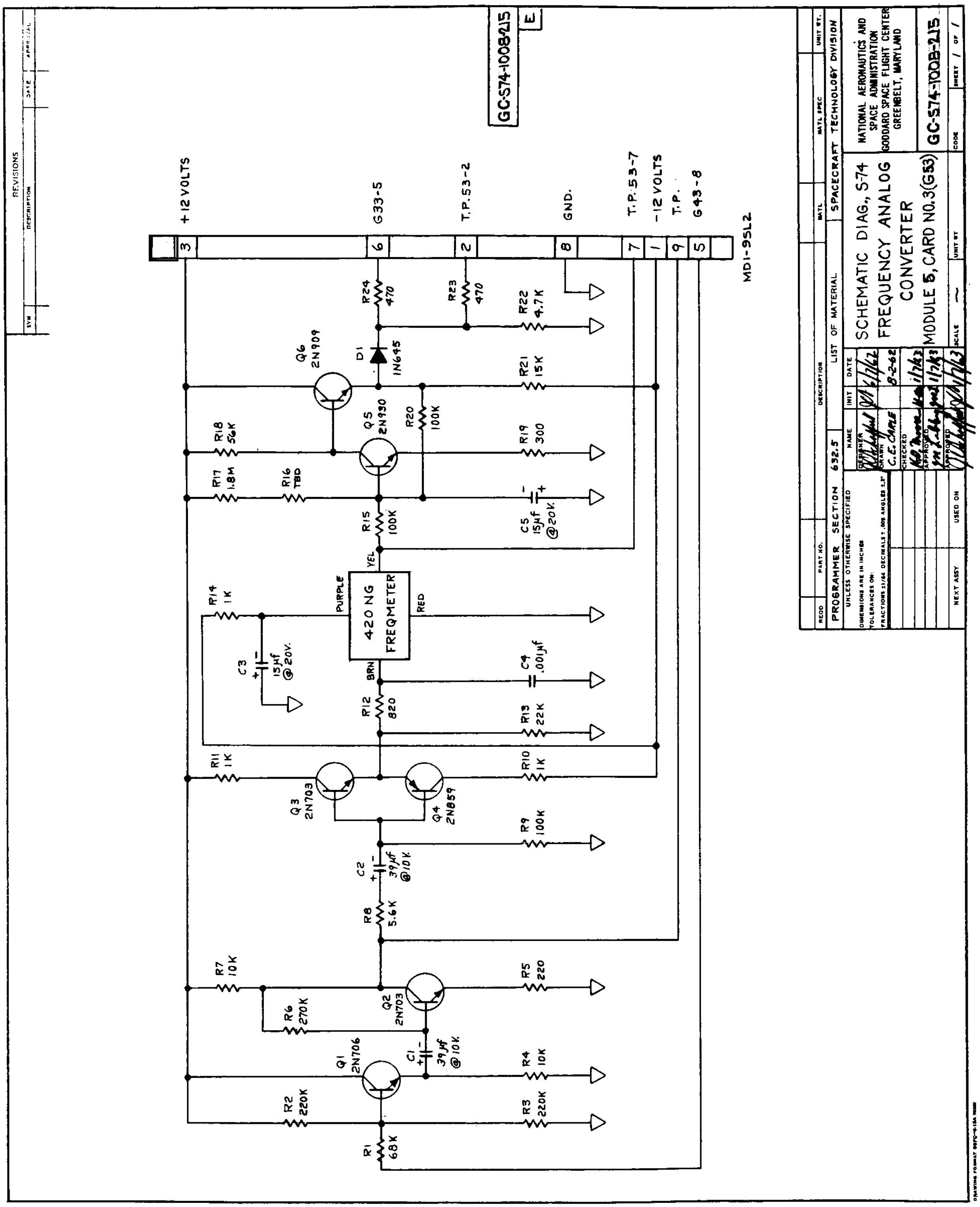
+12 VOLTS
G33-5
T.P. 53-2
GND.
T.P. 53-7
-12 VOLTS
T.P.
G43-8
MDI-95L2
420 NG FREQMETER
SCHEMATIC DIAG., S-74
FREQUENCY ANALOG
CONVERTER
MODULE 5, CARD NO.3(G53)
NATIONAL AERONAUTICS AND SPACE ADMINISTRATION
GODDARD SPACE FLIGHT CENTER
GREENBELT, MARYLAND
SPACECRAFT TECHNOLOGY DIVISION
PROGRAMMER SECTION 632.5
GC-S74-100B-215

Figure 49

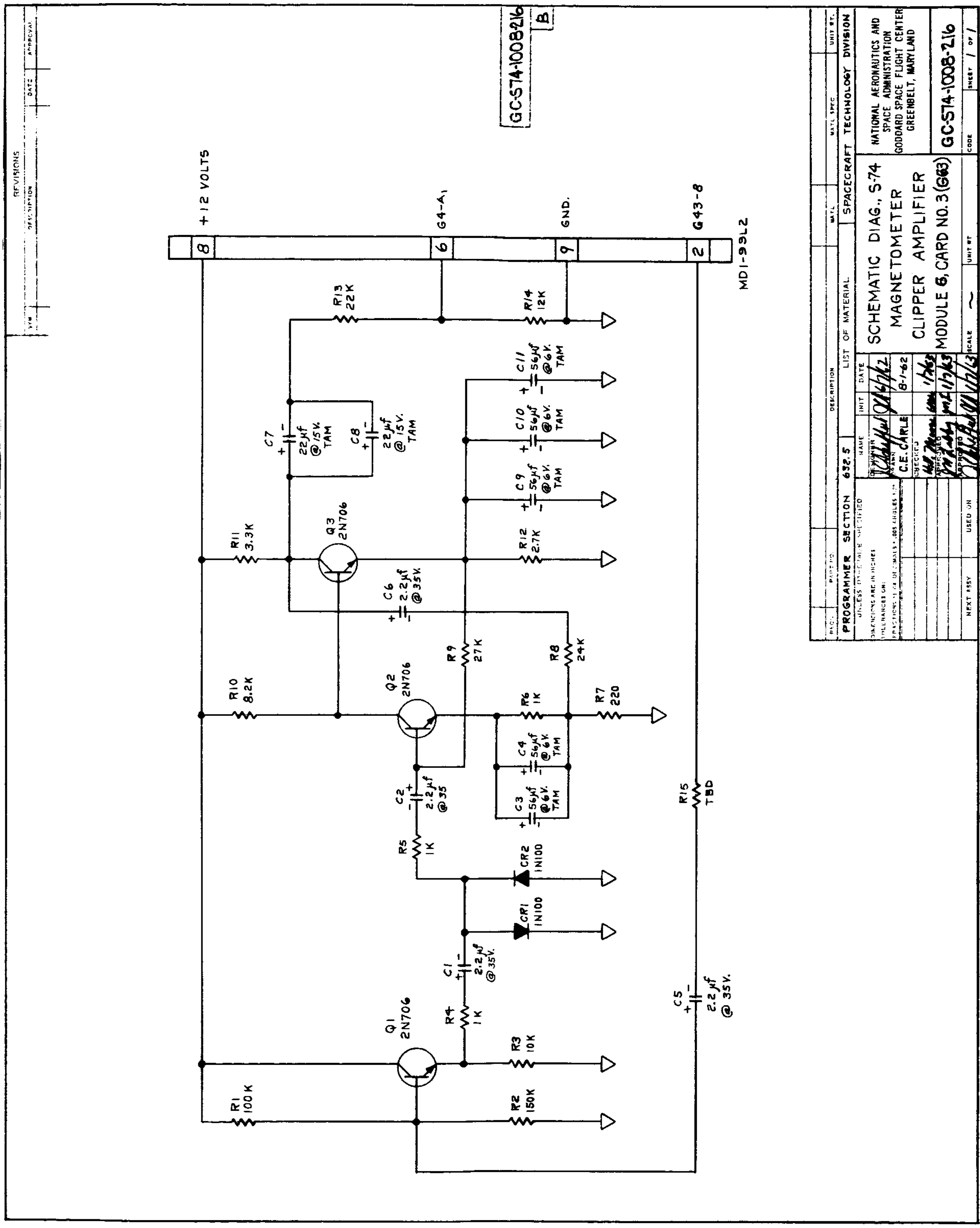
GC-574-1008-216
B
REVISIONS
+12 VOLTS
G4-A1
GND.
G43-8
MD1-99L2
R13 22K
R14 12K
C7 22μf @15V. TAM
C8 22μf @15V. TAM
C11 56μf @6V. TAM
C10 56μf @6V. TAM
C9 56μf @6V. TAM
R11 3.3K
Q3 2N706
R12 2.7K
C6 2.2μf @35V.
R9 27K
R8 24K
R10 8.2K
Q2 2N706
R6 1K
R7 220
C4 56μf @6V. TAM
C3 56μf @6V. TAM
C2 2.2μf @35
R5 1K
CR2 1N100
CR1 1N100
R15 TBD
C1 2.2μf @35V.
R4 1K
Q1 2N706
C5 2.2μf @35V.
R3 10K
R1 100K
R2 150K
SPACECRAFT TECHNOLOGY DIVISION
NATIONAL AERONAUTICS AND SPACE ADMINISTRATION
GODDARD SPACE FLIGHT CENTER
GREENBELT, MARYLAND
PROGRAMMER SECTION 632.5
C.E.CARLE
8-1-62
SCHEMATIC DIAG., S-74
MAGNETOMETER
CLIPPER AMPLIFIER
MODULE 6, CARD NO. 3 (G63)
GC-574-1008-216
SHEET 1 OF 1

Figure 50

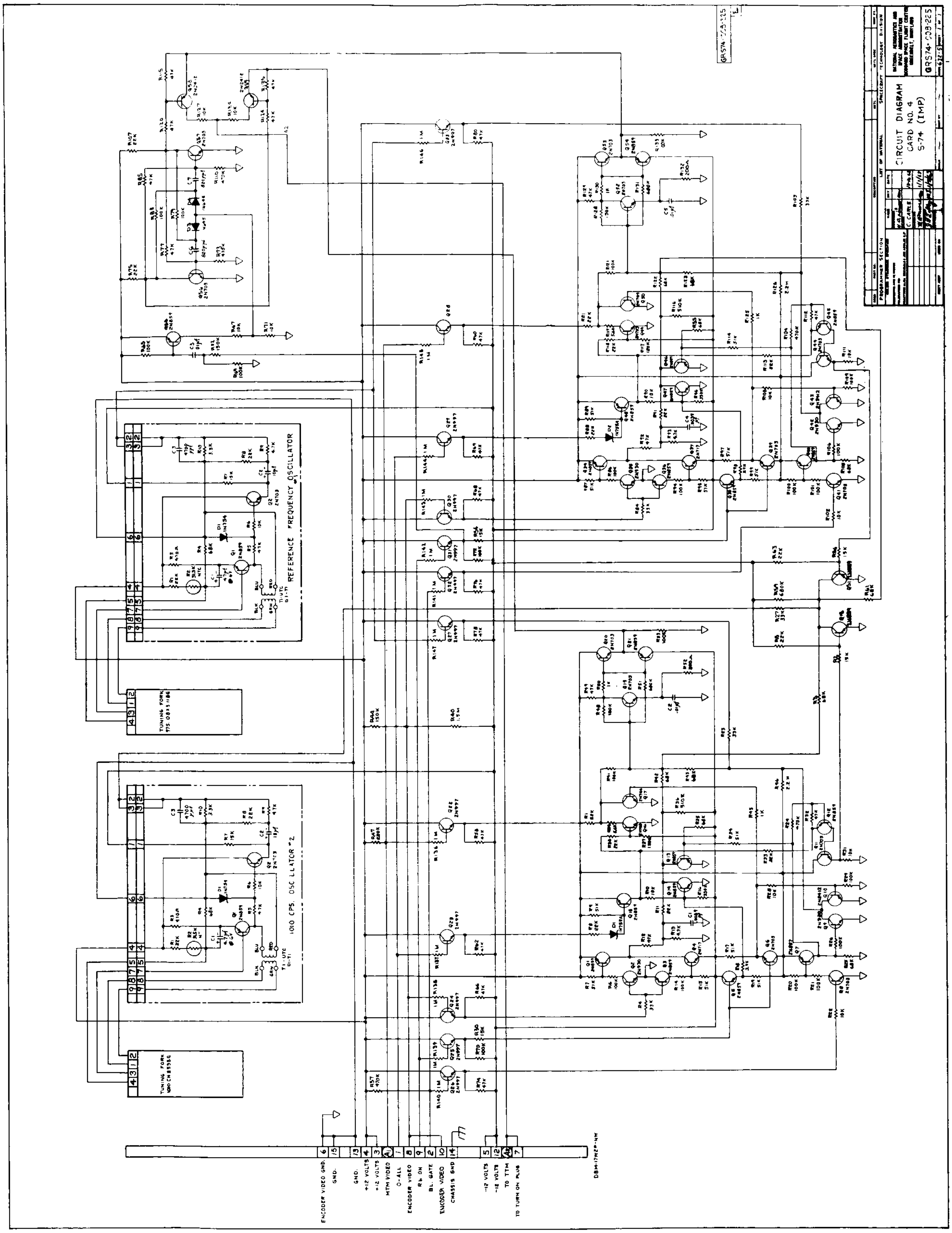
CIRCUIT DIAGRAM
CARD NO. 4
S-74 (IMP)
REFERENCE FREQUENCY OSCILLATOR

Figure 51

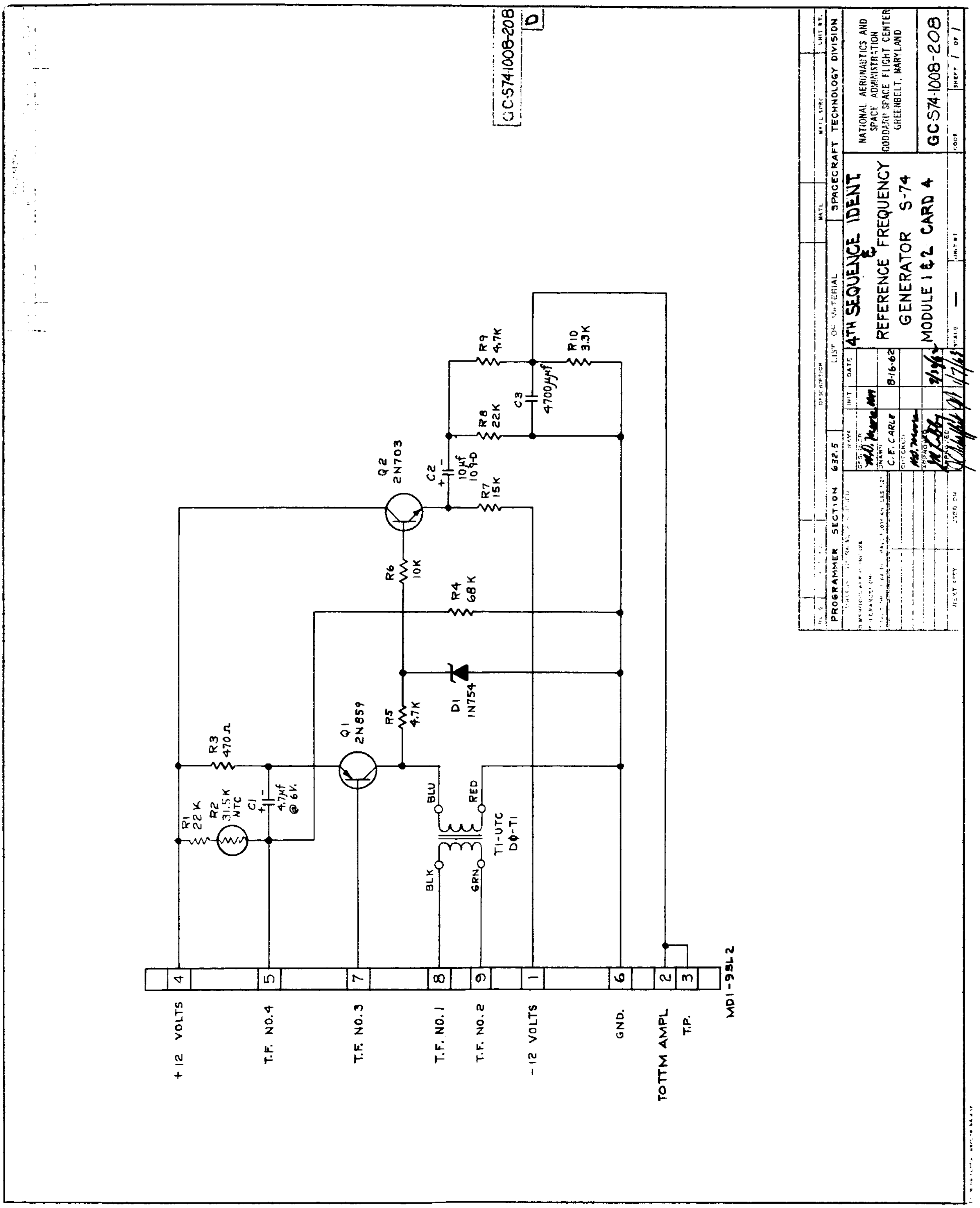
GC-S74-1008-208
D
4TH SEQUENCE & IDENT
REFERENCE FREQUENCY
GENERATOR S-74
MODULE 1 & 2 CARD 4
NATIONAL AERONAUTICS AND SPACE ADMINISTRATION
GODDARD SPACE FLIGHT CENTER
GREENBELT, MARYLAND
SPACECRAFT TECHNOLOGY DIVISION
PROGRAMMER SECTION 632.5
C.E. CARLE
8-16-62
GC-S74-1008-208
+12 VOLTS
T.F. NO.4
T.F. NO.3
T.F. NO.1
T.F. NO.2
-12 VOLTS
GND.
TOTTM AMPL
T.P.
MDI-95L2
R1 22K
R2 31.5K NTC
C1 4.7μf @ 6V.
R3 470Ω
Q1 2N859
R5 4.7K
D1 1N754
R4 68K
R6 10K
Q2 2N703
R7 15K
C2 10μf 10V-D
R8 22K
C3 4700μμf
R9 4.7K
R10 3.3K
T1-UTC DO-T1
BLU
RED
BLK
GRN

Figure 52

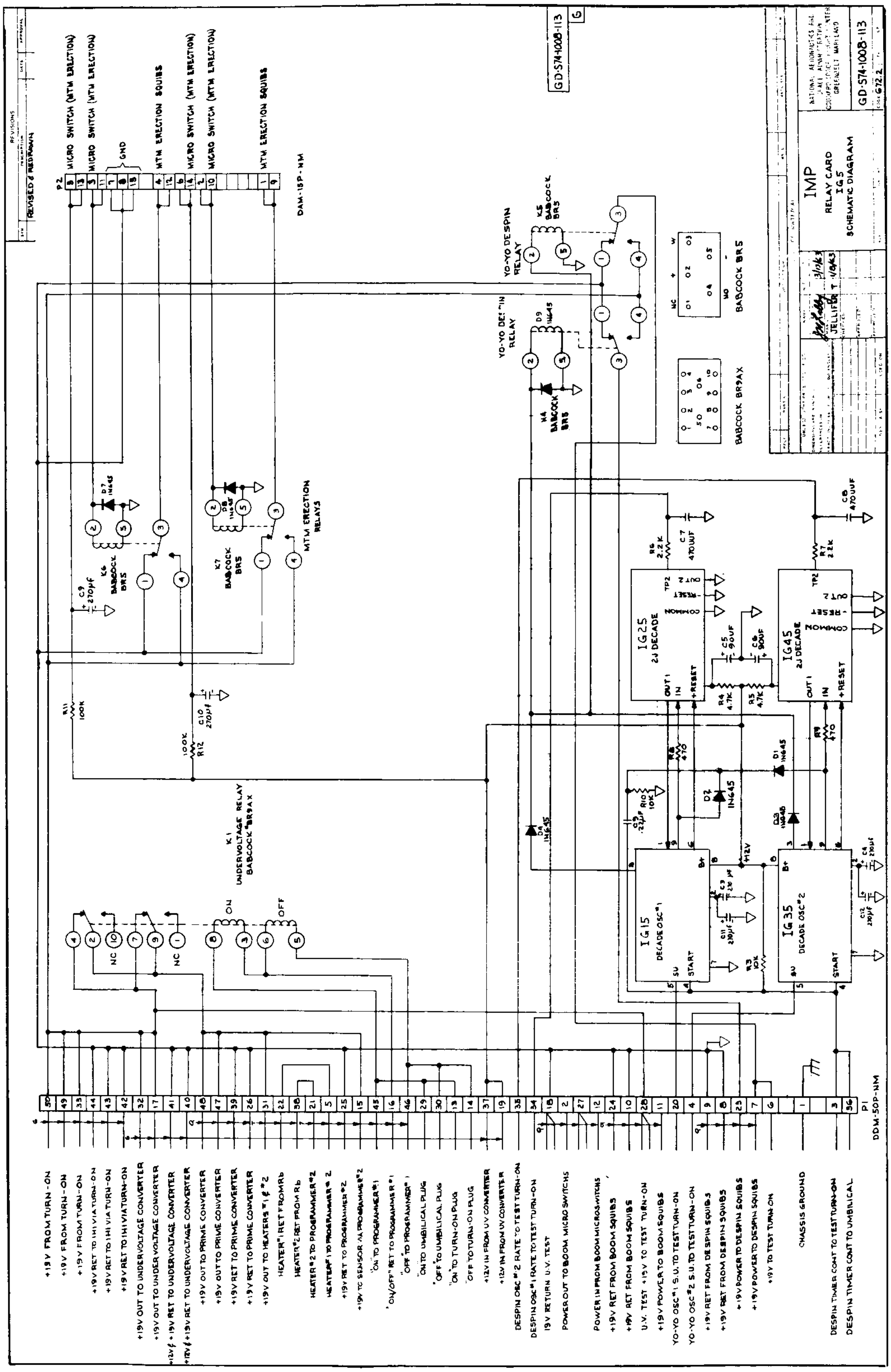

Figure 53

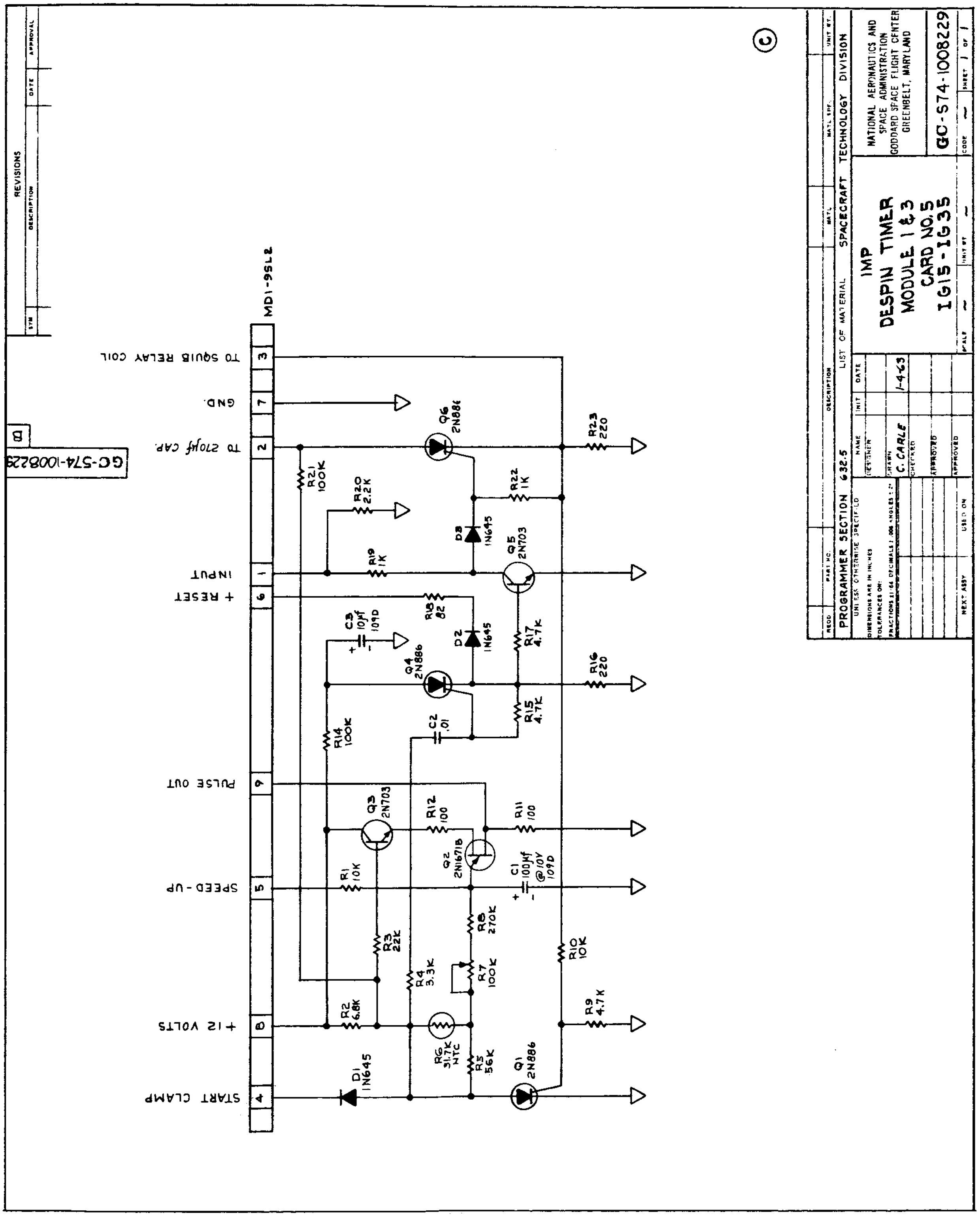
IMP
DESPIN TIMER
MODULE 1 & 3
CARD NO.5
IG15 - IG35
GC-S74-1008229
NATIONAL AERONAUTICS AND SPACE ADMINISTRATION
GODDARD SPACE FLIGHT CENTER
GREENBELT, MARYLAND
SPACECRAFT TECHNOLOGY DIVISION
PROGRAMMER SECTION 632.5
C. CARLE
1-4-63
REVISIONS
MD1-9SL2
TO SQUIB RELAY COIL
GND.
TO 210μf CAP.
INPUT
+ RESET
PULSE OUT
SPEED-UP
+12 VOLTS
START CLAMP

Figure 54

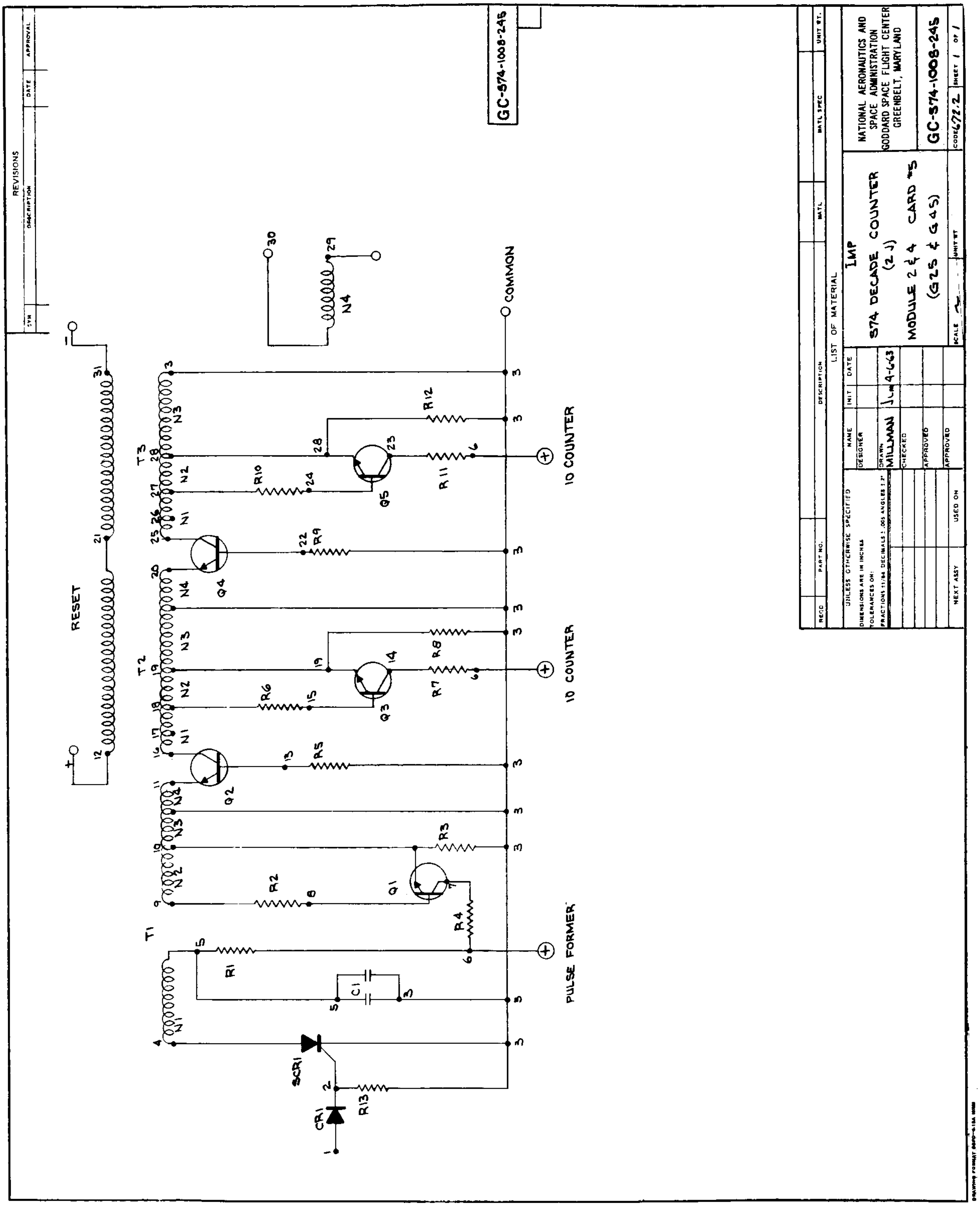
GC-574-1008-245
REVISIONS
RESET
COMMON
10 COUNTER
10 COUNTER
PULSE FORMER
LIST OF MATERIAL
IMP
574 DECADE COUNTER
(2 J)
MODULE 2 & 4 CARD #5
(G25 & G45)
NATIONAL AERONAUTICS AND SPACE ADMINISTRATION
GODDARD SPACE FLIGHT CENTER
GREENBELT, MARYLAND
MILLMAN
GC-574-1008-245

Figure 55

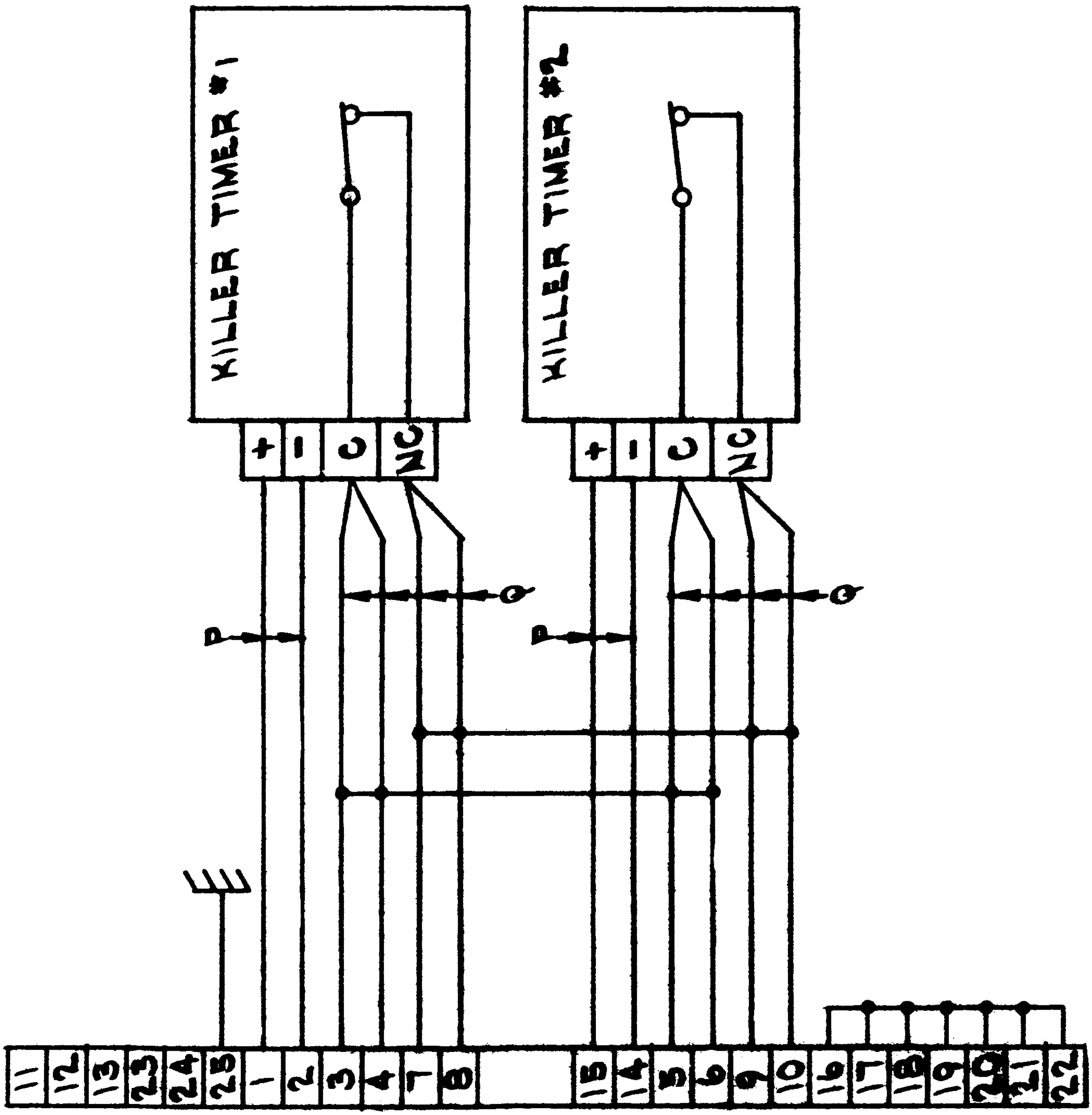

Figure 56

ERRATA

JUNE 27, 1963

GSFC Document X-632-63-111

IMP PROGRAMMER

Page	Line	Change
11	-	G42 and G52 output pulse width from .25 sec. to .5 sec.
16	FGA & FGB	250 Msec. gate gen. to 500 Msec gate gen.
25	*	See H.D. White, etc., to See IMP PFM Encoder, revision A, August 6, 1962, by H. D. White.
27	Fig.12	tuning fork no. 975.0BX3110BG to no. 975CN259SG
32	28	"is as follows:" to "is shown in figure 19."
33	Fig.16	"TO RELAY" to "TO GATE"
38 thru 54		Disregard all information concerning Fluxgate Boom Erection circuitry as it is no longer a programmer function.
49	7	"Undervoltage converter" to "Undervoltage regulator"
49	9	"+12 volts" to "+10.1 volts"
49	19	"+12V" to "+10.1V"
50	28	"3.3.2 Output" to "3.2.2 Output"
50	29	"As per outline-" to "Rubidium Vapor (Rb) Magnetometer-"
51	21	"Rb outline" to "Rubidium Vapor (Rb) Magnetometer"
51	27	"Outline-" to "Rubidium Vapor (Rb) Magnetometer-"
52	9 thru 23	Input impedance of Card 4 to all signals is now in excess of .5 Megohms.
53	3	"Undervoltage converter" to "Undervoltage regulator"

The Undervoltage Converter (S74IP8) has been replaced by a redundant Undervoltage Regulator (S74IG7) which is supplied by the Programmers Section.